The Role of Hippo Signalling in Cell Fate Decisions in Mouse Embryonic Stem Cells and Pre-Implantation Development

Brimson, Christopher

Award date:
2016

Awarding institution:
University of Bath

The Role of Hippo Signalling in Cell Fate Decisions in Mouse Embryonic Stem Cells and Pre-implantation Development

Christopher A. Brimson

A thesis submitted for the degree of Doctor of Philosophy

University of Bath

Department of Biology & Biochemistry

January 2016

Acknowledgements

Firstly I would like to thank my parents for their constant love and support.

I would like to thank Silvia Muñoz Descalzo and Professor David Tosh for their advice, guidance and discussion. This work would not be possible without them. I would also like to thank Professor Melanie Welham and Makoto Furutani-Seiki.

I would like to thank:

My brother James, for inspiration and leading me into science.

Elena Corujo Simon for helping me to find happiness.

Jack Brown, Vicki Wright and Julia Tratt

James Corbett, Leonard Griffiths, Stephen Weston, Nelly Wung, Zoe Burke, Mike Storm, Abdullah Alaqel.

Sean Porazinski, Huw Davies, Huija Wang

Finally I would like to thank the University of Bath for funding.

“It is a far, far better thing that I do, than I have ever done; it is a far, far better rest that I go to than I have ever known”

A Tale of Two Cities

Abstract

The Hippo signalling pathway is a conserved kinase cascade involved in the regulation of tissue growth and organ size. Activation of the Hippo pathway through multiple upstream inputs results in phosphorylation and inactivation of the transcriptional co-activator, Yes associated protein (Yap). While the role of Yap as an oncogene and an effector of the Hippo pathway is well established, its role in cellular differentiation is less well known. In this present work I have utilised quantitative immunofluorescence analysis to examine the expression of Yap in the differentiation of mouse embryonic stem cells (mESCs). I show that differentiation of mESCs is accompanied by an initial increase in nuclear Yap expression. Furthermore, I show that this increase in nuclear Yap expression is associated with differentiation towards the primitive endoderm lineage (PrE). Moreover, small molecule inhibition of Yap was able to decrease the proportion of cells differentiating towards PrE.

Following on from these *in vitro* studies, I examine the expression of Yap *in vivo* in the corresponding differentiation event in mouse pre-implantation embryos. I show that increased nuclear Yap expression is associated with expression of the PrE-specific transcription factor Gata6 during specification and eventual sorting of the PrE. Culturing embryos in the presence of small molecule inhibitors of Yap resulted in decreased expression of Gata6 and a reduction in trophectoderm cell number. These studies demonstrate that Yap is involved in the process of cellular differentiation and is associated with specification of the PrE lineage.

Finally I attempt to create an inducible knockout of Yap in mESCs using a serial targeting strategy, with the intention of creating a model system in which to examine the role of Yap in mESCs.

Abbreviations

4OHT	4-hydroxy-tamoxifen
Amot	Angiomotin
aPKC	atypical protein kinase C
AU	Arbitrary Units
BSA	Bovine serum albumin
Cas9	CRISPR associated protein 9
Cdx2	Caudal type homeobox-2
CK1	Casein kinase 1
Cre-ERT^2	Fusion protein of Cre and the Estrogen receptor
CRISPR	Clustered regularly-interspaced short palindromic repeats
DMSO	Dimethyl-sulfoxide
Dobu	Dobutamine
Dox	Doxycycline
E	Embryonic Day
Epi	Epiblast
EUCOMM	European conditional mouse mutagenesis project
Fgf	Fibroblast growth factor
Fgfr	Fibroblast growth factor receptor
Flp	Flipase
GEF	Guanine exchange factor
Gp130	Glycoprotein 130
HDR	Homology directed repair
Hek293	Human embryonic kidney 293 cells
Hpo	Hippo kinase
ICM	Inner cell Mass
iPSCs	Induced pluripotent stem cells
JAK	Janus associated tyrosine kinases
KOMP	Knock out mouse project

KOSR	Knockout serum replacement
Lats 1/2	Large tumour suppressor homologue
LIF	Leukaemia inhibitory factor
LIFR	Leukaemia inhibitory factor receptor
Lrp2	Low density Lipoprotein Receptor-Related protein2
LRPCR	Long range PCR
MAPK	Mitogen activated protein kinase
Mats	Mob as tumour suppressor
mESCs	Mouse embryonic stem cells
MINS	Modular interactive nuclear segmentation (Image analysis)
MSCs	Mesenchymal stem cells
Mst1/2	Mammalian Sterile like kinase 1/2
Neo	Neomycin (G418)
Nf2	Neurofibromin 2
NHEJ	Non homologous end joining
Oct4	Octamer-binding transcription 4 (also POU5F1)
PBS	Phosphate buffered saline
PCR	Polymerase chain reaction
PD	PD0325901 (MEK Inhibitor)
Pdgfrα	Platelet derived growth factor α
PrE	Primitive Endoderm
Puro	Puromycin
pYap	Yap phosphorylated at Serine 112
Rh5	Rhodopsin 5
Rh6	Rhodopsin 6
ROCK	Rho-Kinase
RT-PCR	Reverse transcriptase PCR
Sav	Salvador
SFK	SRC family kinase

siRNA	Small interfering RNA
SL	Serum and LIF
SOCS5/6	Suppressor of cytokine signalling 5/6
Sox2	SRY-Box 2
Sox7	SRY-Box 7
STAT3	Signal transducer and activator of transcription 3
TALENs	Transcription activator-like effector nucleases
TE	Trophectoderm
Verte	Verteporfin
Wts	Wts kinase
WWTR1	Taz
Yap	Yes associated protein
YapE08	Yap targeted knockout first mESC clone
YapS112A	Mutation of Yap Serine 112 for Alanine
Yki	Yorkie
β-TRCP	β-transducin repeat-containing protein

Table of Contents

Table of Figures

Table of tables

Chapter 1: Introduction

1.1 The Hippo signalling pathway

The *Drosophila* Hippo signalling pathway

The Hippo pathway was first discovered in genetic mosaic screens of *Drosophila* in a search for mutations that resulted in tissue overgrowth. These screens revealed a kinase cascade comprising of Hippo kinase (Hpo), Warts kinase (Wts) and the scaffolding proteins Salvador (Sav) and Mob as tumour suppressor (Mats) (Harvey, Pfleger & Hariharan, 2003; Justice *et al.*, 1995; Xu *et al.*, 1995; Tapon *et al.*, 2002; Lai *et al.*, 2005). In this kinase cascade, the Hpo-Sav kinase complex phosphorylates and activates the Wts-Mats kinase complex (Wu *et al.*, 2003; Wei, Shimizu & Lai, 2007). The Wts-Mats kinase complex subsequently phosphorylates the transcriptional co-activator Yorkie (Yki) resulting in its retention in the cytoplasm (Figure 1.1) (Huang *et al.*, 2005; Dong *et al.*, 2007). When in the nucleus, Yki interacts with the transcription factor Scalloped, activating target genes associated with the promotion of proliferation and inhibition of apoptosis (Zhang *et al.*, 2008). Deletion of Yki diminishes the overgrowth phenotype seen in Hpo, Wts and Sav mutants thus indicating Yki as the effector of Hippo signalling (Huang *et al.*, 2005).

Hippo signalling is conserved in mammals

The Hippo signalling pathway is highly conserved in mammals. The mammalian homologs of Hpo, Wts, Sav and Mats are Mammalian sterile like kinase 1/2 (Mst1/2), Large tumour suppressor homologue 1/2 (Lats1/2), Salvador (Sav1) and Mob kinase activator 1A/B (Mob1/2), respectively (Callus, Verhagen & Vaux, 2006; Praskova, Xia & Avruch, 2008; Chan *et al.*, 2005). As in *Drosophila*, these proteins form a kinase cascade, which upon activation, phosphorylates and inactivates the mammalian homologs of Yki, Yes-associated protein (Yap) and Taz (also known as Wwtr1), preventing their interaction with the Scalloped homologs Tead1-4 (Figure 1.1) (Dong *et al.*, 2007; Lei *et al.*, 2008). The physiological relevance of the conservation of Hippo signalling was demonstrated by transgenic over expression of Yap in mice resulting in

an increase in size of the liver, ultimately leading to hepatocellular carcinoma (Dong *et al.*, 2007; Camargo *et al.*, 2007). These studies identified Yap as one of the main effectors of the Hippo pathway.

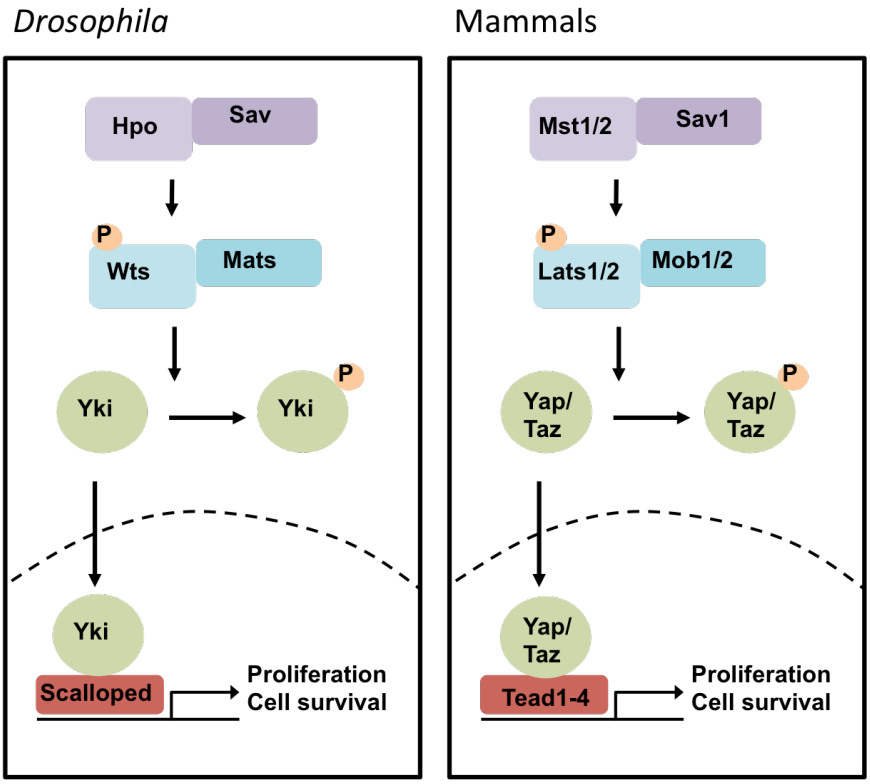

Figure 1.1. Conservation of the Hippo kinase cascade in *Drosophila* and mammals. The corresponding proteins in Drosophila and mammals are represented in the same colours. In the nucleus Yki/Yap/Taz acts as a transcriptional co-activator, binding to Scalloped/Tead transcription factors and activating target gene expression. Upon activation of the Hippo kinase cascade Yki/Yap/Taz is phosphorylated and subsequently sequestered in the cytoplasm.

Yes associated protein (Yap)

Yap was first identified in the chicken as a 65kDa protein, which interacts with the non-receptor tyrosine kinase c-Yes (Sudol, 1994). Anti-idiotypic antibodies were generated against the N-Terminal of the Yes protein in order to discover novel interacting proteins, leading to the discovery of Yap binding to c-Yes via an SH3 binding domain (Sudol, 1994). cDNA derived from chicken Yap was subsequently used as a probe to screen human and mouse cDNA libraries, leading to the discovery of human and mouse Yap (Sudol *et al.*, 1995a). Analysis of the comparison between the analogous Yap proteins revealed a protein module containing two tryptophan residues, and was therefore named the WW domain (Sudol *et*

al., 1995b). WW domains mediate protein-protein binding via interaction with PPxY motifs.

Structural analyses of Yap revealed subsequent protein interaction domains (Figure 1.2), including a coiled coil domain and a PDZ binding motif, allowing Yap to interact with proteins containing a PDZ domain (Mohler *et al.*, 1999; Oka & Sudol, 2009). PDZ domains are ≈90 amino acid protein-interaction domains that are often found in trans-membrane or cytoskeletal associated proteins (Reviewed in Ye & Zhang, 2013).

A transcriptional activation domain was mapped to the C-terminus of Yap, and fusion of Yap to the DNA binding domain of Gal4 is able to activate transcription at levels comparable to the potent transcriptional activator VP16 (Yagi *et al.*, 1999). As Yap does not contain a DNA binding domain, it is recruited to DNA through association with transcription factors. Yap has been shown to interact, via WW its domains, with multiple DNA binding transcription factors, for example the Runt family member Runx2 and the p53 family member p73 (Yagi *et al.*, 1999; Strano, 2001). However, in an unbiased screen for target transcription factors of Yap, the Tead family of transcription factors were identified as the prominent target (Zhao *et al.*, 2008). Yap interacts with Tead via a Tead-binding domain (Li *et al.*, 2010). Furthermore, the cell growth and oncogenic properties of Yap were diminished upon knockdown of Tead, suggesting that Tead transcription factors are essential mediators of Hippo signalling.

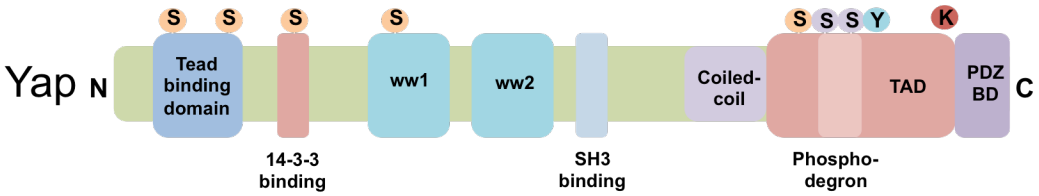

Figure 1.2. Yap contains multiple regulatory domains. Schematic representing the known multiple interaction domains of Yap and residues targeted post-translational modification. The five serine residues phosphorylated by Lats are shown in yellow. The two serine residues phosphorylated by CK1 are shown in lilac. The tyrosine residue phosphorylated by Src/Yes is shown in blue. The lysine residue targeted for methylation by Set7 is shown in red. TAD is Transcriptional activation domain. PDZ-BD is PDZ binding domain. (Figure adapted from Piccolo, Dupont & Cordenonsi, 2014).

Regulation of Yap activity by the Hippo pathway

Yap can be directly phosphorylated on serine residues in five conserved HxRxxS motifs by the Hippo pathway kinase Lats (Figure 1.2). Phosphorylation of YAP S127 (Yap S112 in mouse) by Lats results in the generation of a 14-3-3 binding site (Figure 1.2) (Zhao *et al.*, 2007; Hao *et al.*, 2007). Subsequent binding of Yap to 14-3-3 proteins results in Yap being sequestered in the cytoplasm, thus unable to translocate to the nucleus to activate target gene expression (Zhao *et al.*, 2007; Hao *et al.*, 2007). Phosphorylation of YAP S397 (Yap S381 in mouse) by Lats primes Yap for subsequent phosphorylation by Casein Kinase 1 (CK1), resulting in the generation of a 'phosphodegron', a motif that is recognised by β-transducin repeat-containing protein (β-TRCP) (Zhao *et al.*, 2010). β-TRCP is an adaptor for SCF E3 ubiquitin ligases, which subsequently poly-ubiquitinates Yap, leading to its destruction by the proteasome (Zhao *et al.*, 2010). Lats is thus able to regulate Yap activity spatially and temporally, through subcellular localization and protein stability respectively. Activation of the Hippo pathway therefore suppresses gene activation whilst inactivation of the pathway results in target gene expression.

Upstream regulators of the Hippo Pathway

Whilst the regulation of Yap activity by the Hippo signalling kinase cascade is relatively well understood, the upstream regulators of Hippo signalling are only recently beginning to be defined.

G-Protein-Coupled receptor signalling

G-Protein-coupled receptors are a large family of receptors that sense extracellular molecules and relay signals through associated G proteins. Upon binding of a ligand, the receptor acts as a guanine nuclear exchange factor (GEF), activating an associated G protein, which can then dissociate from the receptor and affect intracellular signalling (Reviewed in Wettschureck & Offermanns, 2005). Ligands such as lysophosphatidic acid and sphingosine-1-phosphate, that signal through receptors coupled to Gα12/13 or Gαq/11, have been found to inhibit Lats kinase, resulting in translocation of Yap to the nucleus and activation of target gene expression (Yu *et al.*, 2012; Miller *et al.*, 2012). However, ligands that signal through $G\alpha_s$ coupled receptors, such as adrenaline and glucagon can increase phosphorylation of Yap by Lats, thus decreasing nuclear Yap activity (Yu *et al.*, 2012).

Mechanical cues, cell shape and the actin cytoskeleton

Yap subcellular localization has been linked to mechanical cues. Culturing cells on a rigid surface that allows cells to spread results in nuclear localization of Yap and subsequent proliferation (Dupont *et al.*, 2011). Conversely, culture of cells on a compliant surface that does not favour cell spreading results in cytoplasmic localization of Yap and subsequent growth arrest (Dupont *et al.*, 2011). These changes in the subcellular localization of Yap appear to be regulated by cell shape. Disruption of F-actin stress fibres results in increased phosphorylation and subsequent cytoplasmic localization of Yap (Wada *et al.*, 2011; Sansores-Garcia *et al.*, 2011). The spectrin cytoskeleton has also been found to influence the subcellular localisation of Yap (Fletcher *et al.*, 2015; Deng *et al.*, 2015). Inhibition of myosin or Rho-kinase (ROCK), a Rho-GTPase effector important in generation of actin-myosin induced cellular tension also leads to increased cytoplasmic localization of Yap (Wada *et al.*, 2011; Dupont *et al.*, 2011). Mechanical cues therefore appear to be important in regulation of the subcellular localization of Yap, however the exact mechanisms by which actin affects the Hippo kinase cascade is unknown.

Cell adhesion & polarity

A fundamental hallmark of non-transformed cells in culture is cell-contact inhibition, such that upon reaching confluence, cells will cease to proliferate (Eagle, Levine & Koprowski, 1968). Cell contact mediated adhesion at high cellular density has been shown to result in activation of Hippo signalling, resulting in phosphorylation and subsequent cytoplasmic retention of Yap (Zhao *et al.*, 2007). Furthermore overexpression of Yap confers cells with the ability to overcome cell-contact inhibition (Zhao *et al.*, 2007). This suggests that cell-cell contacts are important for regulation of Hippo signalling.

Cell-cell contacts are also important for the establishment of epithelial apical-basal polarity. Apical-basal polarity is maintained by the action of protein complexes, which localize to specific positions along the apical-basal axis. These protein complexes include the Crumbs complex, the Par/atypical Protein kinase C (aPKC) module, the Scribble module and the adherens junctions (Reviewed in Dow & Humbert, 2007). The Hippo pathway has been linked to many of these protein complexes.

The Crumbs polarity complex associates with tight-junction complexes localised to the apical domain of polarized epithelial cells (Roh, 2003). Depletion of Crumbs components CRB3 or PALS results in decreased phosphorylation of Yap and increased nuclear Yap expression (Varelas *et al.*, 2010). Angiomotin (Amot), another protein which associates with the Crumbs complex, has also been shown to interact with Yap resulting in increased phosphorylation and cytoplasmic retention (Zhao *et al.*, 2011). In a similar manner to the Crumbs complex, Scribble promotes phosphorylation and cytoplasmic retention of Yap (Chen *et al.*, 2012).

Disruption of the adherens junction components α-catenin and E-cadherin results in inactivation of the Hippo signalling pathway leading to Yap mediated cell proliferation (Schlegelmilch *et al.*, 2011; Kim *et al.*, 2011). The tumour suppressor neurofibromin 2 (Nf2) has been shown to be upstream of the Hippo kinases, localized in close proximity to

adherens junctions where it may promote the appropriate protein scaffolds for activation of Lats (Moroishi *et al.*, 2015).

It is clear that multiple upstream inputs feed into the Hippo signalling pathway, including extracellular molecules, mechanical cues and information from cell polarity and adhesion.

Yap in development and cell fate choice

Despite its role as an oncogene (Overholtzer *et al.*, 2006; Zender *et al.*, 2006; Steinhardt *et al.*, 2008), Yap has also been found to be important in a number of cell fate decisions. Mesenchymal stem cells (MSCs) can differentiate into adipocytes or osteoblasts, depending on the stiffness of the culture conditions. On stiff surfaces MSCs will differentiate towards osteoblasts, whilst on soft surfaces MSCs will differentiate towards adipocytes (Engler *et al.*, 2006). This was found to be linked to Hippo signalling, in that on stiff surfaces, Hippo signalling was inactivated, such that Yap could translocate to the nucleus (Dupont *et al.*, 2011). More importantly, ectopic expression of Yap in MSCs cultured on soft surfaces resulted in differentiation towards osteoblasts (Dupont *et al.*, 2011). This suggests that the mechanical regulation of Hippo signalling influences cell fate through regulation of Yap activity.

Yap is important in mouse development, and *Yap*$^{-/-}$ mice die shortly after implantation at embryonic day (E) 8.5, exhibiting defects in yolk sac vasculogenesis and a shortened body axis (Morin-Kensicki *et al.*, 2006).

1.2 Pre-implantation mouse development

The first two cell fate choices in the mouse embryo result in the specification of embryonic and extra-embryonic tissues (Figure 1.3). Specification of the first extra-embryonic lineage, the trophectoderm (TE) is important for formation of the placenta. The second extra-embryonic lineage gives rise to the primitive endoderm (PrE) which will form the parietal and visceral endoderm, as well as contributing to the embryonic gut (Kwon, Viotti & Hadjantonakis, 2008). Specification of the epiblast (Epi) from the inner cell mass (ICM) will give rise to the embryo proper

(reviewed in Schrode *et al.*, 2013). Early blastomeres from the 2-cell to 8-cell stages are totipotent, in that they can contribute to all lineages of the developing embryo, and following subsequent spatial segregation and cell lineage specification, blastomeres gradually lose their totipotency (Figure 1.3).

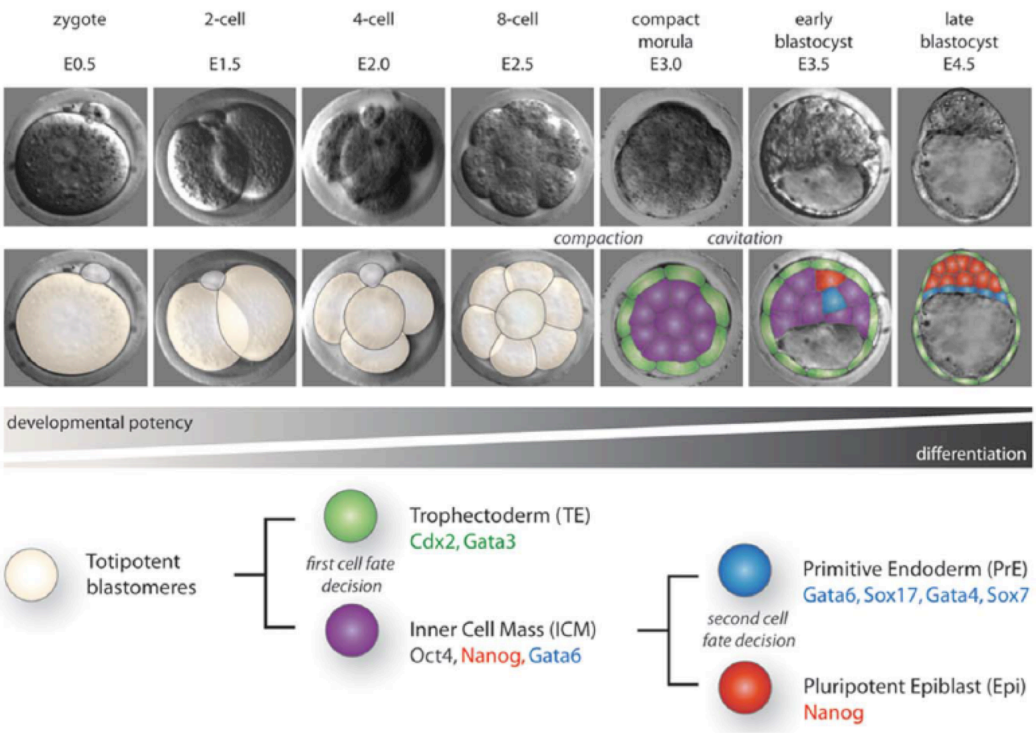

Figure 1.3. Overview of mouse pre-implantation development. Schematic of pre-implantation development leading to formation of the blastocyst. E= embryonic day. (Figure from Schrode *et al.*, 2013).

Specification of the TE and ICM

The first cell fate decision, resulting in the specification of TE and the ICM, occurs following compaction of the embryo at the 8-cell stage, around embryonic day 3 of development (E3.0). Prior to compaction blastomeres are loosely connected and morphologically identifiable. Upon compaction, cell-cell contact adhesion increases through the adhesion molecule E-cadherin and subsequently each blastomere becomes polarized along the apical-basal axis. Subsequent cell divisions give rise to blastomeres that occupy an inner or outer position within the embryo, with outer cells remaining polarized and inner cells becoming apolar. By the 32-cell stage (E3.5), the outer cells will form the TE and the inner cells will form the ICM (Figure 1.3).

The outer and inner cells also differ in their expression levels of lineage specific transcription factors (Guo *et al.*, 2010). Cell fates are controlled by differential activity of lineage specific transcription factors. Specifically, caudal type homeobox-2 (Cdx2) is required for TE, while Nanog and Oct4 specify the ICM lineage (Niwa *et al.*, 2005; Ralston & Rossant, 2008; Strumpf *et al.*, 2005; Nichols *et al.*, 1998; Schöler *et al.*, 1989). Initially at the 8-cell stage Cdx2 is expressed heterogeneously in all blastomeres but by the 32-cell stage, becomes restricted to the outer cells that will form the TE (Dietrich & Hiiragi, 2007). This restricted expression of Cdx2 is required to repress the ICM lineage specific marker Oct4 (Niwa *et al.*, 2005; Ralston & Rossant, 2008; Strumpf *et al.*, 2005). Cdx2 expression has been shown to be regulated by the transcription factor Tead4 (Nishioka *et al.*, 2008; Yagi *et al.*, 2007). *Tead4*$^{-/-}$ embryos display significantly reduced Cdx2 and Gata3 expression and all their cells express markers of ICM (Ralston *et al.*, 2010; Nishioka *et al.*, 2008; Yagi *et al.*, 2007). Tead4 has also been shown to directly regulate an enhancer of *Cdx2* (Rayon *et al.*, 2014). However Tead4 is expressed in the nucleus in all blastomeres (Nishioka *et al.*, 2008), which presents the question of how the restricted expression of Cdx2 in outer cells occurs.

The current model suggests that the key mechanism underlying this phenomenon is differential regulation of Yap by the Hippo signalling pathway (Figure 1.4). Inner cells have increased Hippo signalling, resulting in phosphorylation and cytoplasmic retention of Yap (Nishioka *et al.*, 2009). In outer, polarized cells, Hippo signalling is inactivated, leading to the nuclear localisation of Yap. In the nucleus Yap binds Tead4 and promotes Cdx2 expression, thereby promoting TE cell fate (Nishioka *et al.*, 2009).

The differential activation of Hippo signalling in inner and outer cells is believed to be regulated by a combination of cell-cell adhesion and the polarity of the cell (Hirate *et al.*, 2013). Disruption of the aPKC polarity complex activates Hippo signalling resulting in cytoplasmic Yap in all blastomeres at the 32-cell stage (Hirate *et al.*, 2013). However, in dissociated embryos, this activation of the Hippo pathway was not seen,

suggesting a requirement in cell-cell adhesion for activation of the Hippo pathway (Hirate *et al.*, 2013). The spatial regulation of Yap by the Hippo pathway is therefore important for the specification of TE and ICM cell fates.

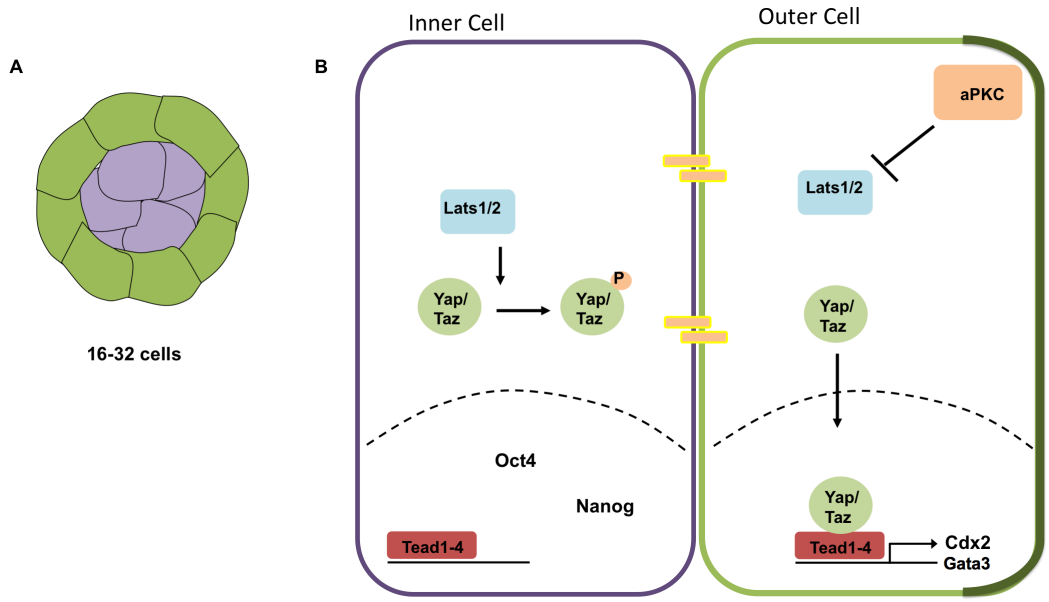

Figure 1.4. Specification of trophectoderm lineage via differential activity of the Hippo pathway. (**A**) Schematic of compact morula with inner cells highlighted in purple and outer cells highlighted in green. (**B**) Polarization of outer cells results in inactivation of Hippo signalling. Yap can translocate to the nucleus subsequently binding to Tead4 and drive expression of TE specific factors Cdx2 and Gata3. Conversely in unpolarized inner cells, Hippo signalling is activated, leading to phosphorylation and cytoplasmic retention of Yap, thereby preventing co-activation of Tead4.

Specification of the PrE and Epi

The second cell fate decision occurs in the ICM, resulting in specification of the PrE and Epi lineages (Figure 1.5). The PrE becomes morphologically apparent by E4.5 as a layer of epithelial cells on the surface of the ICM, adjacent to the blastocyst cavity. This observation lead to early suggestions that ICM cells adjacent to the cavity differentiated towards PrE, in a positional manner similar to the induction of TE (Rossant, 1975). However, it has since been demonstrated that the ICM contains a heterogeneous population of PrE and Epi precursors which subsequently sorts into two defined populations (Chazaud *et al.*, 2006; Plusa *et al.*, 2008).

Epi cells are marked by the pluripotency-associated factors Nanog, Sox2 and Oct4 whilst PrE cells are marked by Gata6. Nanog and Sox2 are required for maintenance of the Epi (Mitsui *et al.*, 2003; Avilion *et al.*, 2003). Initially all cells of the ICM, up until the 32-cell stage, coexpress Gata6 and Nanog (Chazaud *et al.*, 2006; Plusa *et al.*, 2008). Following the 32-cell stage, cells of the ICM begin to upregulate lineage specific transcription factors, in a mutually exclusive manner, such that cells express either Nanog or Gata6 (Chazaud *et al.*, 2006; Plusa *et al.*, 2008). Fgf signalling has been implicated in the formation of this salt and pepper expression pattern such that, Fgf4 becomes down regulated in some ICM cells, whereas its receptor Fgfr2, is upregulated (Guo *et al.*, 2010). Activation of Fgf signalling in these cells results in the upregulation of Gata6 and the repression of Nanog, biasing cells towards PrE (Frankenberg *et al.*, 2011).

After the 64 cell-stage, the heterogeneous population of PrE and Epi precursors sort into two distinct populations, with the PrE forming an epithelial layer on the surface of the ICM, adjacent to the blastocyst cavity. Live imaging of embryos which express a fluorescent reporter for the PrE marker Pdgfrα revealed that PrE cells reach the cavity by active migration (Plusa *et al.*, 2008). However, cells adjacent to the cavity that were negative for Pdgfrα expression were occasionally seen to upregulate Pdgfrα and subsequently contribute to the PrE, whereas cells that express PrE markers, but do not reach the cavity were observed to undergo apoptosis (Plusa *et al.*, 2008). This suggests that, whilst initial specification of PrE precursors may be independent of positional cues, the eventual sorting and formation of the PrE is position dependent.

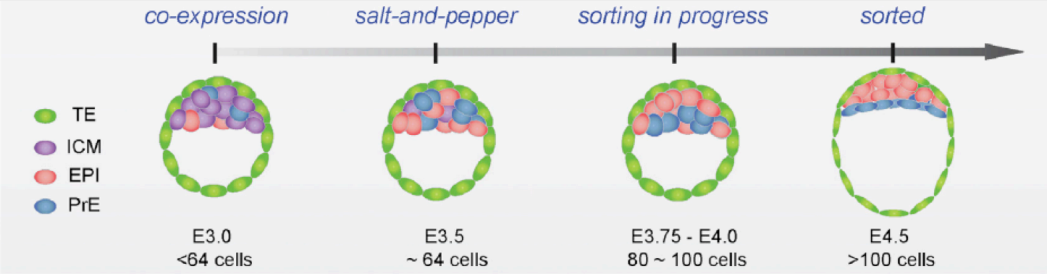

Figure 1.5. Specification of the PrE and Epi lineages. Schematic of the expression of Gata6 (blue) and Nanog (Red) during the specification of the PrE and Epi lineages. E = embryonic day. (Figure from Xenopoulos *et al.*, 2015).

Whether the Hippo signalling pathway is important in the specification and sorting of PrE and Epi has yet to be elucidated. Depletion of Lats by siRNA treatment of embryos has been shown to result in failure of PrE formation (Lorthongpanich *et al.*, 2013). Similarly deletion of the upstream Hippo pathway member Nf2 in embryos resulted in loss of PrE (Cockburn *et al.*, 2013). The exact mechanisms underlying the loss of PrE in these embryos remains unknown.

1.3 Mouse embryonic stem cells

Mouse embryonic stem cells (mESCs) are karyoptypically normal cell lines derived from the ICM of the mouse embryo during pre-implantation development (Evans & Kaufman, 1981; Martin, 1981). Embryonic stem cells are considered pluripotent, in that they retain the capability to differentiate into all lineages of the developing mouse embryo (Beddington & Robertson, 1989; Morgani *et al.*, 2013). mESCs can be cultured *in vitro*, in medium containing leukaemia inhibitory factor (LIF), and foetal calf serum (Smith *et al.*, 1988; Williams *et al.*, 1988). In these culture conditions cells exhibit heterogeneous expression of markers of pluripotency such as Nanog and markers of PrE such as Gata6 or Hex (Chambers *et al.*, 2007; Niakan *et al.*, 2010; Morgani *et al.*, 2013; Canham *et al.*, 2010). LIF binds to a heterodimeric receptor, composed of the LIF receptor (LIFR) and glycoprotein 130 (gp130), resulting in activation of Janus associated tyrosine kinases (JAK) that phosphorylates signal transducer and activator of transcription 3 (STAT3). Subsequent dimerization of STAT3 and translocation to the nucleus allows expression of target genes (reviewed in Hirai, Karian & Kikyo, 2011). Although LIF

activates multiple signalling pathways, including mitogen activated protein kinase (MAPK) and Src family kinase (SFK) pathways, activation of STAT3 is sufficient for mESC self renewal in culture (Burdon *et al.*, 1999; Anneren, 2004; Niwa *et al.*, 1998; Matsuda *et al.*, 1999).

LIF has been shown to activate the SFK Yes, resulting in a subsequent tyrosine phosphorylation of Yap in mESCs (Tamm, Bower & Anneren, 2011). This leads to Tead2 dependent transcription of the Oct4 promoter (Tamm, Bower & Anneren, 2011). Ectopic expression of a constitutively active form of Yap was found to induce expression of Oct4 and promote self-renewal in the absence of LIF (Lian *et al.*, 2010). These findings are in contrast to the studies in pre-implantation mouse embryos, where Yap was restricted to the cytoplasm in cells of the pluripotent ICM (Nishioka *et al.*, 2009).

1.4 Conclusions and experimental aims

Yap is known to be one of the nuclear executors of the Hippo pathway. Regulation of Yap by the Hippo pathway is an important feature in cell fate specification in the mouse embryo. However, in mESCs Yap appears to be involved in self-renewal. Mouse embryonic stem cells provide an attractive model for the study of the function of Yap during self-renewal and differentiation. The aims of this work were therefore to address the role of Yap in these contexts. With the studies in the presented in the following chapters, I intended to:

- Describe the subcellular distribution of Yap in the differentiation of mESCs
- Establish whether Yap is involved in differentiation towards primitive endoderm cell fate *in vitro*
- Establish whether Yap is involved in differentiation towards primitive endoderm cell fate *in vivo*
- Establish whether Yap is absolutely required for self renewal of mESCs

Chapter 2: Materials and Methods

2.1 Cell culture reagents

Media and Supplements

Knockout Serum Replacement + LIF (KOSR+LIF):

Knockout Dulbecco's Modified Eagles Medium (Gibco, 10829-018)

Knockout Serum Replacement 15% (Gibco 10828-028)

Non-essential amino acids, 0.1mM (SIGMA; M7145)

GlutaMAX, 2mM (Gibco, 35050-038)

Sodium Pyruvate, 1mM (Gibco, 11360-039)

2-mercaptoethanol, 0.1mM (Invitrogen, 21985-023)

LIF, 100U/ml (Department of Biochemistry, University of Cambridge)

Serum + LIF (SL):

Glasgow Minimum Essential Medium (Gibco, 11580576)

Foetal Bovine Serum, 10% (Labtech, batch number: 50115)

Non Essential Amino Acids, 0.1mM (SIGMA; M7145)

GlutaMAX, 2mM (Gibco, 35050-038)

Sodium Pyruvate, 1mM (Gibco, 11360-039)

2-mercaptoethanol, 0.1mM (Invitrogen, 21985-023)

LIF, 100U/ml (Department of Biochemistry, University of Cambridge)

Cytokines, Growth Factors and Inhibitors

PD0325901 (PD03) (R&D 4192)

Dobutamine (SIGMA)

Verteporfin (SIGMA)

Other Tissue Culture Reagents

Phosphate Buffered Saline (PBS) (SIGMA D8537)

Gelatin: 0.1% in PBS (SIGMA G1890)

Trypsin: 0.05% Trypsin-EDTA (Thermo 25300-054)

Doxycycline hydrochloride (SIGMA D-9891)

Neomycin (Geneticin G418) (Gibco 11811-023)

Puromycin (SIGMA)

4OHT (tamoxifen) (SIGMA)

Cell Lines

E14Tg2a: mESC line derived from 129/Ola mice (A generous gift from Prof. A. Martinez-Arias, University of Cambridge) (Hooper *et al.*, 1987).

IOUD2: mESC line containing LacZ reporter directly after the Oct4 promoter (Mountford *et al.*, 1994)

Gata6-mCherry: Generous gift from Christian Schröter, mESC line with Gata6-mCherry inducible transgene, based on KH2 mESC line (Schröter *et al.*, 2015)

YapE08: Acquired from Knockout Mouse Project (KOMP) JM8 mESC clone derived from C57BL/6N mice. Contains Yap targeted Knockout-First mutation

2.2 Cell Culture

Routine cell culture:

Mouse embryonic stem cells were cultured in media containing LIF (either KOSR+LIF or SL, (see Media and Supplements) on gelatin-coated tissue culture plastic at a cell density of $2.4x10^4$cells/cm^2, at 37°C, 5% CO_2. The media was changed every day, and cells were passaged every 2-3 days. To passage, cells were washed twice with room temperature PBS, incubated with 0.05% trypsin for 5 minutes at 37°C, and re-suspended in media to neutralise the trypsin. For KOSR culture, any excess trypsin was removed before incubation at 37°C due to the lack of serum in the KOSR

media. Cells were centrifuged at 1000rpm for 3 minutes, re-suspended in fresh media and re-plated at the desired cell density.

Freezing Cells:

To freeze mESCs, cells were washed twice with PBS, incubated with 0.05% trypsin for 5 minutes at 37°C, re-suspended in media to neutralise trypsin, centrifuged at 1000rpm for 3 minutes, re-suspended in media containing 10% dimethyl-sulfoxide (DMSO), aliquoted into cryovials (Nunc 368-632) and immediately transferred to -80°C. The following day, the cryovials were transferred to liquid nitrogen for long-term storage. To thaw frozen cells, cryovials were removed from liquid nitrogen and warmed in a water bath at 37°C. Cells were re-suspended in 10ml of media and centrifuged at 1000rpm, before resuspension and plating on gelatin-coated tissue culture plastic.

2.3 Cell culture assays

LIF Removal:

mESCs were cultured in KOSR+LIF for at least two passages prior to experiments. Cells were trypsinised and re-plated onto gelatin-coated 25mm tissue culture plastic round coverslips (Nunc, 174-985) in 6-well tissue culture plates (GreinerBioOne, 657160) at a density of $2.4x10^4$cells/cm^2, in media with or without LIF. Media was changed daily, and replaced with media with or without LIF. Following 48 hours cells were washed twice with BBS-$CaCl_2$ (see Reagents for immunostaining) before fixation with 4% PFA for subsequent immunostaining.

Spontaneous Differentiation towards PrE:

mESCs were cultured in KOSR+LIF for at least two passages prior to experiments. Cells were trypsinised and re-plated onto gelatin coated 25mm tissue culture plastic round coverslips in 6-well tissue culture plates at a density of $2.4x10^4$cells/cm^2 in KOSR+LIF. Media was changed daily. Following 48 hours, cells were washed twice with BBS-$CaCl_2$ (see Reagents for immunostaining) before fixation with 4% PFA for subsequent immunostaining.

Embryoid Bodies: Hanging Drop method

mESCs were trypsinised and re-suspended in KOSR+LIF at a density of $1x10^5$ cells/ml. 10µl drops of media, containing approximately 1000 cells were placed onto the underside of a sterile petri dish lid, before being inverted and cultured at 37°C, 5% CO_2. The petri dish contained PBS to prevent the drops from drying out. After 48 hours embryoid bodies, were collected by washing with PBS and either fixed in 4% PFA or transferred into petri dishes containing KOSR+LIF for continued suspension culture.

Embryoid Bodies: Cell aggregate method

The method of generating embryoid bodies by cell aggregation was adapted from (Li & Yurchenco, 2006). mESCs were cultured on mouse embryonic fibroblasts in KOSR +LIF. When confluent, cells were washed twice with PBS and then trypsinised. Crucially, trypsinisation was monitored under a microscope and neutralised by addition of media only when the mESC colonies lifted up off the fibroblasts. The mESC colonies were collected into a 15ml tube and allowed to pellet by gravity. The supernatant was then aspirated and the pellet re-suspended using a glass Pasteur pipette. The mESC aggregates were then allowed to pellet by gravity a second time before re-suspending in 2ml of KOSR+LIF media (see Media and Supplements) and trituration with a Pasteur pipette in order to create clusters of cells containing 3-7 cells each. The mESC clusters were then transferred to a sterile petri dish at a density of approximately 10^3 cell clusters per dish and incubated at 37°C, 5% CO_2. The media was changed after 3 days of culture and then every day up to a maximum of 7 days. Embryoid bodies that displayed endodermal differentiation (assessed by the presence of an outer later of flattened cells visible under phase-contrast microscopy) and cavitation were selected and fixed in 4% PFA for subsequent immunofluorescence analysis.

Inducible Gata6-inducible model of differentiation:

Gata6-inducible mESCs were cultured in S+L for at least two passages prior to experiments. Cells were trypsinised and re-plated onto gelatin

coated 25mm tissue culture plastic round coverslips in 6-well tissue culture plates at a density of $5x10^4$ cells per well, in S+L containing 1μM PD03. Thereafter the media was changed daily. After 3 days, PD03 was excluded from the media and Gata6 was induced by addition of 500ng/ml doxycycline. After 6 hours of induction, cells were either washed twice in BBS-$CaCl_2$ and fixed in 4% PFA or placed in S+L for a further 24 hours before washing and fixation in 4% PFA. No-doxycycline treated control cells were fixed alongside the 6h doxycycline-treated cells. The Hippo signalling inhibitors were added to the media with doxycycline following 3 days of PD03 treatment, and either removed after 6 hours, or kept in the media for the following 24 hours.

Cell culture on hydrogels of varying compliance

Hydrogels were prepared as described in (Cretu, Castagnino & Assoian, 2010):

Table 2.1. Reagents for preparation of polyacrylamide hydrogels

Name	Source
Glutaraldehyde 70%	SIGMA G7776
3-Aminopropyltrimethosilane (3-APTMS)	SIGMA 281778
SurfaSil Siliconizing Fluid	Thermo 42800
NHS (N-Hydroxysuccinimide Ester)	SIGMA A-8060

Coverslip preparation:

Glass coverslips were sterilized by autoclave, and covered in 1M NaOH for 3 minutes. NaOH was aspirated and coverslips were covered in 3-APTMS and incubated for 3 minutes. 3-APTMS (Table 2.1) was aspirated and coverslips washed 3x10 minutes in deionized water. Excess water was aspirated and coverslips were coated in 0.5% glutaraldehyde in sterile deionized water and incubated for 30 minutes. Glutaraldehyde was

aspirated and coverslips washed 3x10 minutes in deionized water, before being dried completely in air.

Hydrogel preparation:

Acrylamide (AC), bis-acrylamide (Bis-AC), water, APS, TEMED and NHS (Table 2.1) were added to a micro-centrifuge tube in varying ratios depending on the desired compliance, as in Table 2.2.

Table 2.2. Volumes of reagents for acrylamide hydrogels

	0.7kPA	4kPA	40kPA
Water	618	522	402
AC	150	150	150
Bis-AC	24	120	240
APS	8	8	8
TEMED	1	1	1
NHS	228	228	228

The contents of the micro-centrifuge tube were vortexed and immediately poured onto pre-treated coverslips. A siliconized coverslip was used to 'sandwich' the acrylamide solution onto the coverslip, allowing the solution to solidify. Once the hydrogel had solidified, the siliconized coverslip was removed and discarded, and the now hydrogel coated coverslip was placed into a 6 well tissue culture dish and washed 3x5 minutes in PBS. Hydrogels were coated with a 0.2mg/ml solution of Type 1 collagen in PBS overnight at 4°C. The collagen solution was then aspirated, and hydrogels washed twice with PBS. mESCs could then be plated onto the hydrogels, as in routine cell culture.

2.4 Electroporation, Selection and picking of colonies

Transient expression of pCAGGS-FLP-PURO

One day prior to electroporation 40µg pCAGGS-Flp-Puro plasmid was precipitated with ethanol, washed twice with 70% ethanol and re-suspended in 0.1ml PBS in a micro-centrifuge tube. The media was

changed on cells 3-4 hours prior to electroporation. Cells were trypsinised as routine and re-suspended in PBS. Cells were centrifuged at 1000rpm for 3 minutes, re-suspended in 0.7ml room temperature PBS and added to the micro-centrifuge tube containing the pCAGGS-Flp-Puro plasmid. Cell and plasmid suspension was transferred to an electroporation cuvette (0.4cm gap; BioRad) and electroporated using a BioRad Gene Pulser II with high capacitance extender unit, set to 250V / 500μF giving approximately 6-7ms time constant. Cells were allowed to recover for 20 minutes before being plated in KOSR+LIF onto gelatin-coated 10cm tissue culture dishes (Nunc) at $5x10^6$, $2x10^6$ or $1x10^6$ cells per dish. The medium was changed daily. 36 hours post electroporation; the media was replaced with medium containing 1μg/ml puromycin, and selection was maintained for 48 hours. Following removal of the selection antibiotic, surviving colonies were cultured until they reached approximately 1mm in diameter.

Targeting the Yap locus using KOMP knockout first targeting vector

Cells were electroporated as described in Transient expression of pCAGGS-FLP-PURO with the following modifications:

- 15μg of Yap targeting Vector plasmid was linearised by restriction digest with AsiSI
- $2\text{-}3x10^7$ cells were electroporated
- BioRad Gene Pulser II with high capacitance extender unit, set to 800V / 3μF giving approximately 0.04ms time constant
- Cells plated at $5x10^6$, $2x10^6$ and $1x10^7$ cells per dish.
- 24 hours after electroporation, drug selection began with the addition of 150μg/ml G418 to the culture medium. Selection was maintained until colonies grew to approximately 1mm in diameter.

Targeting $CreER^{T2}$ to the ROSA26 locus

Cells were electroporated as described in Transient expression of pCAGGS-FLP-PURO with the following modifications:

- 5µg of pMB80 plasmid was linearised by restriction digest with AscI,
- One confluent 25cm^2 tissue culture flask was electroporated
- BioRad Gene Pulser II with high capacitance extender unit, set to 230V / 500µF giving approximately 6-7.5ms time constant
- Cells were re-suspended in 3ml of media. 1 and 2ml of cell suspension were made up to 10ml in S+L and plated onto two gelatin coated 10cm tissue culture dishes
- 24 hours after electroporation, drug selection began with the addition of 1µg/ml puromycin to the culture medium. Selection was maintained until colonies grew to approximately 1mm in diameter.

Picking clonal colonies

Media in the 10cm dish was replaced with PBS and colonies were picked in a volume of 15µl using a 20µl Pipetteman under a dissecting microscope. Each colony was dispensed into a well of a 96-well round bottom plate containing 15µl of trypsin and incubated for 15 minutes at 37°C. 170µl of media+LIF was then added to the wells, and the cell suspensions transferred to a gelatinized 96-well tissue culture plate. Media was changed every day until most of the clones became confluent.

2.5 Mouse Husbandry

All mouse work was approved by the University of Bath Animal Welfare and Ethical Review Body (AWERB) and undertaken under UK Home Office license PPL 30/3219 in accordance with the Animals (Scientific Procedures) Act incorporating EU Directive 2010/63/EU. CD1 Mice were maintained by in-house breeding on a lighting regime of 14 hours light and 10 hours darkness with food and water supplied *ad libitum*. Embryos were generated by natural mating. Detection of a copulation plug confirmed successful mating. The resulting embryos were then considered to be embryonic day 0.5 (E0.5). Blastocysts were collected at E3.5 and E4.5.

2.6 Blastocyst collection

Pregnant female mice were sacrificed by cervical dislocation. The abdominal cavity was cut open using fine scissors and fat and digestive organs were moved to the side to facilitate visualisation of the uterus. The uterus was held with fine forceps, cut across the cervix and lifted in order to remove mesometrium membrane before removal by cutting of the utero-tubal junction as shown in Figure 2.1. The uterine horns were placed in a 35mm petri dish containing PBS. Using a Leica MZ12 stereomicroscope, the remaining fat and mesometrium were carefully removed from the uterine horns. Using fine scissors, the end side of each uterine horn was cut, and embryos were flushed from the uterus by injection of M2 medium (Millipore; MR-015-D) into the cervix. Embryos were collected from the medium by mouth pipette and placed into a fresh drop of M2 media, before subsequent processing.

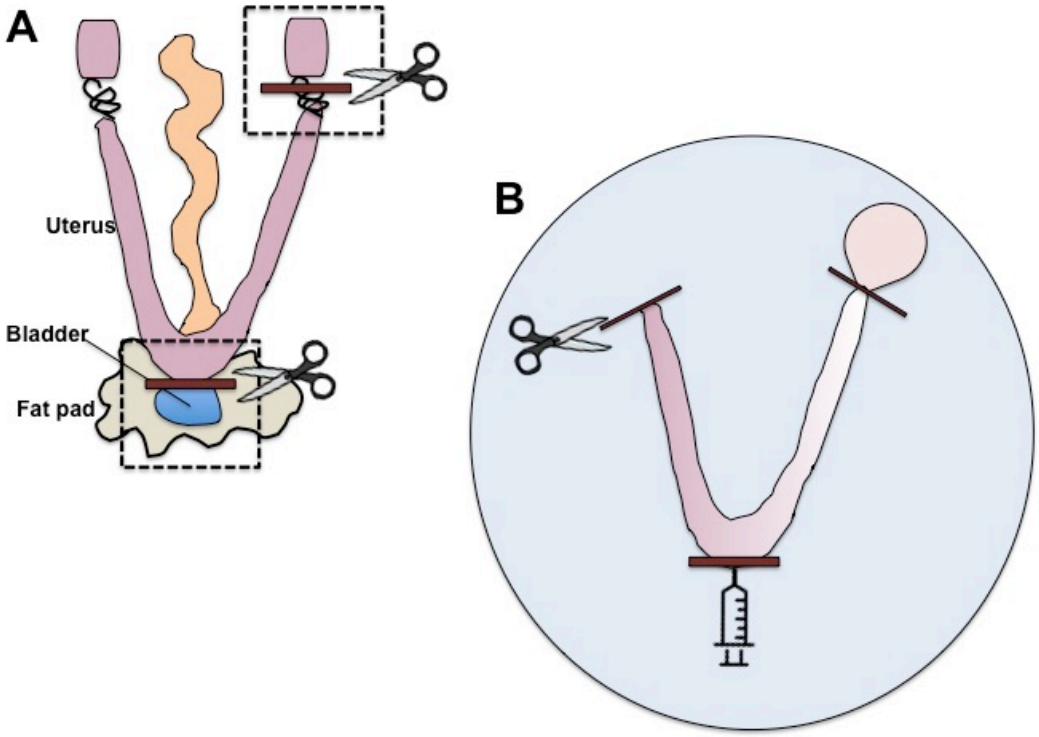

Figure 2.1. Dissection of the mouse uterus. (**A**) Illustration of mouse uterus, indicating where cuts were made across the cervix and utero-tubal junction. (**B**) Illustration of the mouse uterus being flushed by injection of M2 media into the cervix. Adapted from Manipulation of the mouse Embryo, Third Edition.

2.7 Staining techniques

Reagents for immunostaining

BBS: 25mM BES Salt (SIGMA B2891)
140mM NaCL
0.75mM Na_2HPO_4

BBT-BSA: BBS
1mM $CaCl_2$
0.1% Triton-X100
0.5% Bovine Serum Albumin (Roche)

BBS-$CaCl_2$: BBS
1mM $CaCl_2$

Paraformaldehyde (PFA): 4% PFA diluted in BBS + 1mM $CaCl_2$

Immunostaining of mESCs

Following fixation in 4% PFA in BBS+$CaCl_2$, samples were permeabilised by rinsing 3 times before 3 washes of 15 minutes in BBT-BSA (see Reagents for immunostaining). Samples were then incubated with primary antibody (Table 2.3) diluted in BBT-BSA and incubated in a humid chamber at 4°C overnight. The following day, primary antibody was removed by rinsing 3 times before 3 washes of 15 minutes in BBT-BSA. Samples were then incubated with the appropriate secondary antibody (Table 2.4) diluted in BBT-BSA for 2 hours at room temperature, away from light. Secondary antibody incubations were performed sequentially if any were raised in the same species as the primary antibodies. A nuclear stain (Table 2.5) was included in the secondary antibody incubation. Secondary antibody was removed by rinsing 3 times before 3 washes of 10 minutes in BBS+CaCl2. Samples on coverslips were placed cell side up on a glass slide, before mounting a glass coverslip on top with HMM (4% N-propyl-galate, 80% glycerol).

Immunostaining of mouse pre-implantation embryos

The zona pellucida of E3.5 embryos was removed using Tyrode's acidic solution (SIGMA T1788). Embryos were transferred to a siliconised glass dish and fixed in 4% PFA in BBS+$CaCl_2$ for 15 minutes at room temperature. Following a rinse in PBS/PVP (PBS containing polyvinylpyrrolidone-40 (SIGMA)), embryos were permeabilised in a solution containing 0.25% Triton-X100 in PBS/PVP for 30 minutes at room temperature. Embryos were subsequently blocked for 15 minutes in a blocking buffer containing 0.1% BSA, 0.01% Tween20 and 2% donkey serum (SIGMA D9663) in PBS. Embryos were then incubated with primary antibody (Table 2.3) diluted in blocking buffer at 4°C overnight in a humid chamber. The following day, primary antibody was removed by washing the embryos 3 times for 15 minutes in blocking buffer. Embryos were subsequently incubated with secondary antibody (Table 2.4) diluted in blocking buffer for 1-3 hours at room temperature away from light. Secondary antibody incubations were performed sequentially if any were raised in the same species as the primary antibodies. Either Hoechst or Topro3 (Table 2.5) was included as a nuclear stain, in the secondary antibody incubation. Secondary antibody was removed by washing the embryos 3 times for 15 minutes in blocking buffer. To mount, embryos were taken through an increasing concentration series of Vectashield (Vector Laboratories) and mounted in 100% Vectashield on glass slides.

Table 2.3. List of Primary antibodies used for immunofluorescence

Antibody	Host	Manufacturer	Catalogue number	Dilution
Yap	Rabbit	Cell Signalling	4912	1:200
Yap	Rabbit	Santa Cruz	15407	1:200
pYap(S127)	Rabbit	Cell Signalling	4911	1:200
Oct4	Mouse	Santa Cruz	5279	1:200
Nanog	Rat	eBIOSCIENCE	14-5761-80	1:200
Gata4	Rabbit	Santa Cruz	SC9053	1:200
Gata6	Goat	R&D Systems	AF1700	1:200

Table 2.4. List of secondary antibodies used for immunofluorescence

Antibody	Host	Manufacturer
Alexa Fluor 488 – conjugated anti Mouse	Goat	Invitrogen
Alexa Fluor 488 – conjugated anti Rabbit	Goat	Invitrogen
Alexa Fluor 488 – conjugated anti Goat	Donkey	Invitrogen
Alexa Fluor 546 – conjugated anti Rabbit	Goat	Invitrogen
Alexa Fluor 568 – conjugated anti Mouse	Goat	Invitrogen
Alexa Fluor 568 – conjugated anti Goat	Donkey	Invitrogen
Alexa Fluor 633 – conjugated anti Mouse	Goat	Invitrogen
Alexa Fluor 633 – conjugated anti Rabbit	Goat	Invitrogen
Alexa Fluor 633 – conjugated anti Rat	Goat	Invitrogen
Alexa Fluor 568 – conjugated anti Rat	Goat	Invitrogen

Table 2.5. List of nuclear stains used for immunofluorescence

Nuclear stain	Manufacturer	Dilution
Hoechst 3342	Invitrogen	1: 1000
Topro3	Invitrogen	1: 1000

Histochemical staining of mESCs with X-gal

To stain for β-galactosidase, 0.1M-phosphate buffer was prepared by dissolving 3.74g/L monobasic sodium phosphate and 10.35g/L dibasic sodium phosphate in distilled water, and adjusting the pH to 7.3 using a p.H. meter. Media was aspirated and cells were fixed in fix solution (5nM EGTA, 2mM $MgCl_2$ and 0.2% glutaraldehyde in phosphate buffer) for 5 minutes. The fixed solution was aspirated and cells washed twice for 5 minutes in wash solution (2mM $MgCl_2$ in phosphate buffer). Cells were then incubated in staining solution (2mM $MgCl_2$, 5mM potassium ferrocyanide, 5mM potassium ferricyanide, 1mg/ml X-Gal in phosphate buffer and filtered before use) overnight at 37°C. Presence of β-galactosidase was indicated by a blue colour.

2.8 Molecular Biology

Genomic DNA isolation from mESCs

Cells were lysed in lysis buffer (20mM Trizma-HCl pH8, 50mM EDTA, 50mM KCl, 100mM NaCl, 0.5% (wt/vol) SDS, 0.1% (vol/vol) Igepal, 0.1% (vol/vol) Tween-20, 400µg/ml RNAseA, Proteinase K 1mg/ml) at 60°C overnight. DNA was precipitated using 100% isopropanol, washed twice in 70% ethanol and re-suspended in TE containing 20µg/ml RNAseA.

Genomic PCR

PCR Master mix:	2X PCR ReddyMix (Thermo)	10µl
(per reaction)	Forward Primer 10µM	1µl
	Reverse Primer 10µM	1µl
	H_20	6 µl
	DNA template	1µl

PCR Cycle: Step 1: 94°C

Step 2: 94°C

Step 3: 58°C

Step 4: 72°C

Step 5: Repeat steps 2-4 for 30 cycles

Step 6: 72°C

Step 7: hold at 4°C

PCR was amplified using an MJ research PTC200 thermocycler. Resulting PCR products were run on a 1% agarose gel. Primers used in PCR analysis are listed in Table 2.6.

Long-Range PCR

PCR MasterMix: 2 µL 5X LongAmp *Taq* Reaction Buffer

0.16 µL DMSO
0.3 µL 10 mM dNTPs
0.4 µL 10 µM Forward Primer
0.4 µL 10 µM Reverse Primer
10-50 ng Template DNA
0.4 µL LongAmp *Taq* DNA Polymerase
Nuclease-free water to 10 µL

PCR Cycle: Step 1: 93°C 3 mins
Step 2: 93°C 15 secs
Step 3: 65°C 30 secs decreasing 1°C/cycle
Step 4: 65°C 9 mins
Step 5: Repeat steps 2-4 for 8 cycles
Step 6: 92°C 15 secs
Step 7: 55°C 30 secs
Step 8: 65°C 8 mins increasing 20 sec/cycle
Step 9: 65°C 9 mins
Step 10: hold at 4°C

LongAmp Taq PCR Kit (New England Biolabs) was used for long range PCR amplification. PCR was amplified using an MJ research PTC200

thermocycler. Resulting PCR products were run on a 1% agarose gel. Primers used in PCR analysis are listed in Table 2.6.

Analysis of mRNA expression (RT-PCR)

Cells cultured in 6 well plates were washed twice with PBS. RNA was extracted using Tri reagent (SIGMA). Chloroform was used to separate the RNA, which was then precipitated using isopropanol. Following centrifugation, the resulting pellet was washed with 75% ethanol, dried, and suspended in RNAse-free water. RNA was quantified using a nanophotometer (Implen, Munich, Germany). Contaminating DNA was removed via treatment with DNase (Ambion). cDNA was generated with the SuperScript II Reverse transcriptase kit (Invitrogen). cDNA was amplified by PCR using intron spanning primers, and compared to β-actin as a control.

Table 2.6. List of primers used in PCR analysis

Primer Name	Sequence 5'-3'
F Yap Exon3	ATCAGACAACAACATGGCAGGAC
F5' Yap Crit	GTCTTTGTTAGGGCTCTTTGG
R3' Yap Crit	CGTGATGGTAGGAGAACAGAC
YAP rt F	ACCCTCGTTTTGCCATGAAC
YAP rt R	TGTGCTGGGATTGATATTCCGTA
En2R: 5'	TGTTAGTCCCAACCCCTTCCTCC
NF: 5'	GGTACCGCGTCGAGAAGTTCCTATT
LR: 5'	TGAACTGATGGCGAGCTCAGACCAT
5' YAP (GF4)	CAGACTTCACTCTTGCCAAGCTTGGTGC
5' YAP (GF3)	CTCTCACTCCAGACTTCACTCTTGCCAAGC
3' YAP (GR4)	CAAGGTTCTATAAGTACAATAAGTCCAATC
3' YAP (GR3)	CAACTCAATACAACTACTCTGGTATGTAC
β-actin F	AAGAGCTATGAGCTGCCTGA
β-actin R	TACGGATGTCAACGTCACAC

2.9 Image acquisition and analysis

Imaging mouse embryonic stem cells

To allow for quantitative comparison between cells under different conditions in an experiment, all cells were stained at the same time with the same staining conditions and imaged in one session. An average of 5-10 mESC colonies from each condition were imaged. 512x512 pixels (201.64μm x 201.64μm) fluorescent images of mESCs were acquired using a Zeiss LSM 510 Meta confocal laser-scanning microscope, and a Plan-Apochromat 63x/1.4 Oil Ph3 objective with 0.7x zoom and 246.03μm x 246.03μm images acquired using a Leica SP5-II confocal laser scanning microscope Zeiss LSM 510 Meta confocal laser-scanning microscope and a HCX PL APO CS 63.0x1.40 OIL UV objective. A representative section of each colony was analysed using MINS.

Imaging pre-implantation mouse embryos

To allow for quantitative comparison between embryos in an experiment, all embryos were immunostained together at the same time with the same staining conditions. 512x512 pixels (201.64μmx201.64μm) with optical section thickness of 1μm fluorescent images of mouse embryos were acquired using a Zeiss LSM 510 Meta confocal laser-scanning microscope, using a Plan-Apochromat 63x/1.4 Oil Ph3 with 0.7x zoom.

Segmentation using MINS

Fluorescent images of mESCs and embryos were segmented and quantified using modular interactive nuclear segmentation (MINS), a MATLAB based segmentation tool designed for counting cells and measuring fluorescent intensity of 2D and 3D image data (Lou *et al.*, 2014). MINS detects nuclei from the nuclear label e.g. Hoechst, segments individual nuclei and applies an overlay mask which allows measurements of fluorescent intensity values from all channels (Figure 2.2).

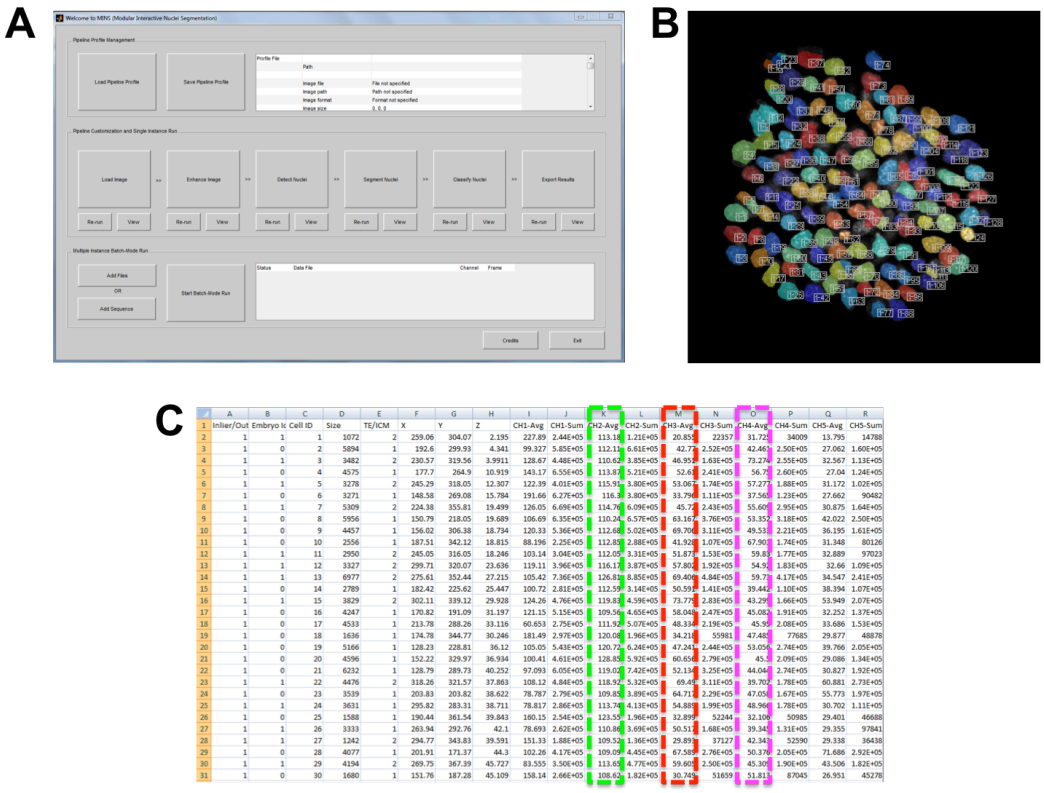

Figure 2.2. Modular Interactive Nuclear Segmentation (MINS), (**A**) The main graphical user interface (GUI) of MINS (**B**), the result of segmentation of mESCs showing overlay of individual cells of a colony (**C**) and array of data produced with average fluorescent intensity values of cells for each channel highlighted.

Classification of cell lineage in pre-implantation mouse embryos

In the analysis of embryos, MINS will also automatically assign a cell identity of either trophectoderm or inner cell mass based on the distance from the centre of the embryo (Figure 2.3). These classifications were checked manually by comparing Z-stack images embryos to the assigned overlay identities. Cells of the PrE in E4.5 embryos were classified manually by their location and expression of Gata6. Trophectoderm and inner cell mass cells were analysed independently.

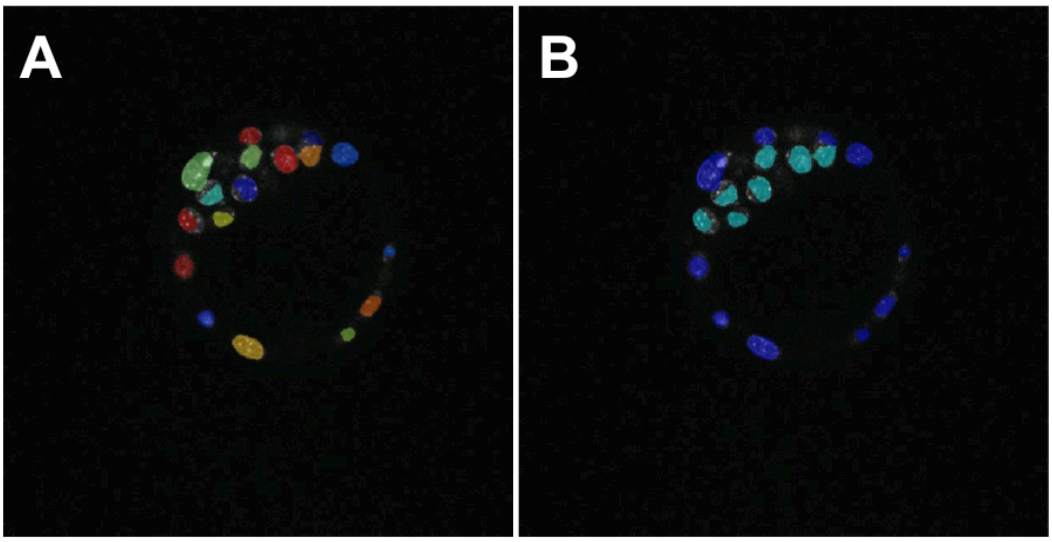

Figure 2.3. MINS Segmentation of embryo nuclei and assignment of lineage. (**A**) MINS segmentation of nuclei in one Z-section of an embryo, (**B**) MINS allocation of lineage, cells of the ICM and TE are assigned.

Adjusting for image intensity loss along the Z-axis

Image acquisition using confocal imaging leads to fluorescent intensity loss with depth due to absorption or scattering of excitation and fluorescence. In order to correct for this, embryos were mildly compressed upon mounting to reduce the thickness of the sample. Furthermore, the fluorescence intensity of each channel in each cell was plotted against the Z-axis, such that the drop in intensity could be visualised (Figure 2.4). Cells above the Z-location in which fluorescence intensity starts to drop were discarded from any analysis.

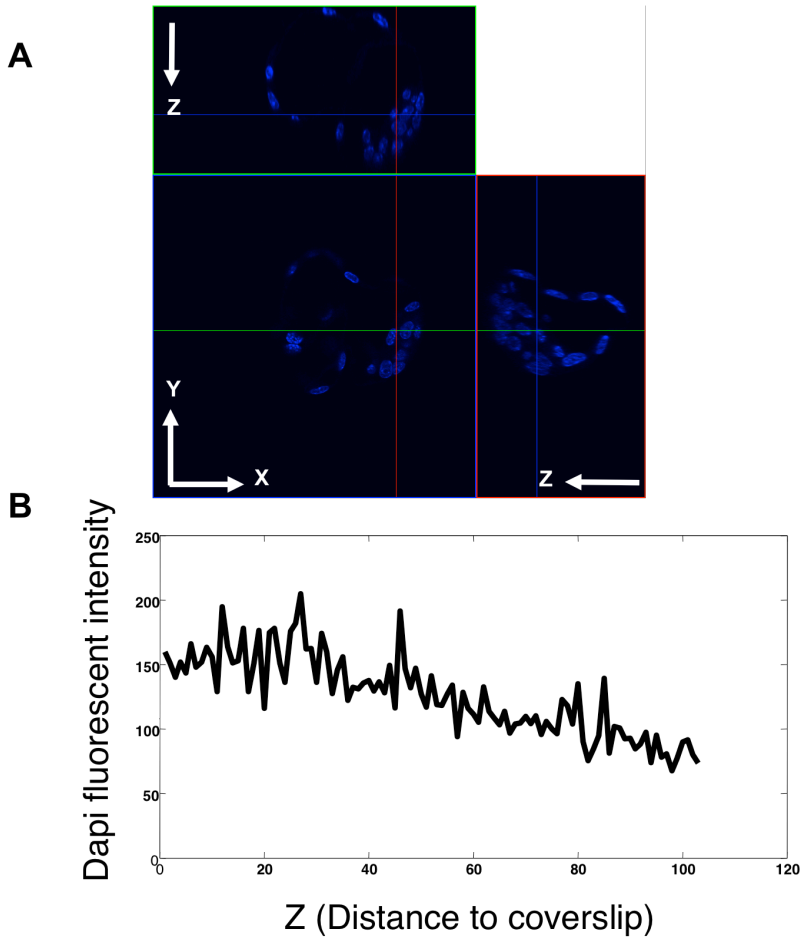

Figure 2.4. Fluorescence intensity loss along the Z-axis in mouse embryos. (**A**) Representative confocal section with orthographic projections of the Z-axis. (**B**) Graph representing fluorescent intensity (arbitrary units) decay as Z (μM) increases.

Staging of mouse embryos

In order to study molecular mechanisms of mouse pre-implantation development, correct staging of embryos is important. Developmental staging of embryos is based on time since fertilization and morphological features therefore developmental stages can encompass a range of molecular events. Factors such as genetic background of mice can affect developmental timing (Molls, Zamboglou & Streffer, 1983), Embryos were therefore staged according to their total cell number and expression pattern of Gata6 and Nanog (Table 2.7).

Table 2.7. Staging of mouse pre-implantation embryos

	Gata6/Nanog Expression pattern	Total cell number
E3.5	Co-expression	32-60
E4.0	'Salt and Pepper'	60-120
E4.5	Sorted	>120

Defining thresholds using mixture analysis

In order to determine whether cells were positive for expression of markers over background levels, threshold limits were defined using mixture analysis. Mixture analysis is a method for estimating the parameters of two or more univariate normal distributions based on pooled data. Fluorescent intensity values of Gata6 or Nanog were determined from MINS analysis and mixture analysis was performed using Paleontological Statistics (PAST) data analysis software. Thresholds were determined as where the two estimated distributions met (Figure 2.5), with mixture analysis automatically allocating each data point into one of the two groups. Mixture analysis was performed using data from E4.5 embryos, and end stage of PrE differentiation in mESCs, as at these points it was considered that Gata6 and Nanog levels in cells exist in bimodal states i.e. protein is either expressed or not at these time points. These thresholds were then applied to earlier stages in order to generate population data based on Gata6 and Nanog expression.

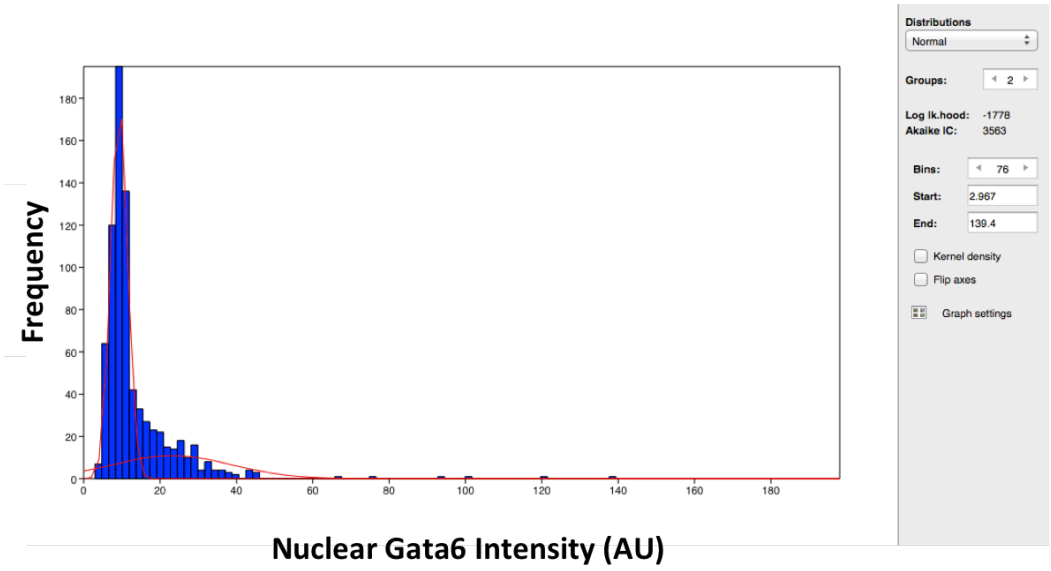

Figure 2.5. Mixture analysis using PAST. An example of mixture analysis, Gata6 intensity values are plotted as a histogram, with the predicted normal distributions displayed in red. The likelihood that the data can be represented as the specified number of groups (in this case 2) is displayed as the likelihood value, with lower negative log values indicating increased likelihood. Threshold value is determined as where the two populations meet.

Fluorescent intensity profiling

For quantifying cytoplasmic Immunofluorescence intensity, linear profiles were generated using ImageJ. Grayscale values for each linear profile were plotted as a histogram and averaged to obtain the mean intensity value. At least 3 intensity profiles were analysed per experimental group.

2.10 Statistical Analysis

Statistical analysis was performed using GraphPad Prism 6 software. Significant difference between experimental groups was determined by one-way ANOVA followed by Tukey's *post hoc* test for experiments with three or more groups and Student's T-test for experiments with two groups.

A statistically significant difference was accepted if $P<0.05$. Significance is indicated on graphical representations of the data by the marks: *P<0.05, **P<0.01, ***P<0.001.

Chapter 3: The role of Yap in differentiation of mouse embryonic stem cells

3.1 Background

While the role of Yap as an oncogene and as an effector of the Hippo pathway is well established (Overholtzer *et al.*, 2006; Zender *et al.*, 2006; Steinhardt *et al.*, 2008), its role in cellular differentiation is less well known. Yap is involved in cellular differentiation in several contexts. In the developing airways of the mouse embryonic lung, ablation of Yap results in the loss of epithelial differentiation (Mahoney *et al.*, 2014). Yap is also required for optic vesicle progenitors to adopt a retinal pigment epithelia cell fate in zebrafish (Miesfeld *et al.*, 2015), and in mouse pre-implantation development, nuclear Yap increases expression of Cdx2, which leads to differentiation towards the trophectoderm (TE) fate (Nishioka *et al.*, 2009). It may therefore be possible that nuclear Yap is a general feature for differentiation in any cellular context.

Mouse embryonic stem cells (mESCs) are pluripotent cells derived from the pre-implantation mouse blastocyst, which retain the potential to differentiate into cells of all lineages (Evans & Kaufman, 1981; Beddington & Robertson, 1989). mESCs are therefore an excellent model system in which to study the expression of Yap during differentiation. As Yap mRNA is enriched in mESCs compared to differentiated cells (Ramalho-Santos *et al.*, 2002), this indicates that this model is valid for the study of Yap during differentiation.

3.2 Expression of Yap during differentiation of mESCs

In order to investigate the role of Yap in the differentiation of mESCs, one approach is to remove the signal maintaining the pluripotent state and determine the expression of Yap. LIF is an essential cytokine for the maintenance of pluripotency and in its absence mESCs spontaneously differentiate (Smith *et al.*, 1988; Williams *et al.*, 1988). If levels of Yap change following LIF withdrawal, this would suggest that regulation of Yap changes upon differentiation.

mESCs were induced to differentiate by LIF withdrawal, and nuclear Yap levels were measured. As Yap acts as a transcriptional co-activator, nuclear localization is required for activation of target gene expression

(Zhao *et al.*, 2007). Yap activity can be regulated via phosphorylation by the Hippo signalling pathway leading to cytoplasmic retention and thus prevention of transcriptional co-activation. Therefore the amount of Yap in the nucleus provides an indication of Yap activity. Nuclear Yap intensity was measured by quantitative immunofluorescence following segmentation of cell nuclei with MINS (Modular Interactive Nuclear Segmentation) (Lou *et al.*, 2014). This method allows measurement of fluorescent intensity of immunostaining in the nucleus at the single cell level, which infers the levels of proteins (Muñoz Descalzo *et al.*, 2012). E14Tg2a mESCs were cultured for either 24 or 48 hours with or without LIF, fixed and then immunostained for Yap and the markers of pluripotency Nanog and Oct4 (Figure 3.1A) and analyzed by quantitative immunofluorescence analysis (Figure 3.1B,C). The results of this analysis for each protein are shown using distribution plots (Figure 3.1B) and box and whisker plots (Figure 3.1C). As expected the nuclear intensity of Nanog and Oct4 decreased following 48-hours of LIF withdrawal compared to cells grown in the presence of LIF indicating that the mESCs were indeed differentiating (Figure 3.1B,C). Following 24-hours of LIF withdrawal, nuclear Yap intensity was increased compared to control. However after 48-hours of LIF withdrawal, nuclear Yap intensity was found to be lower than control (Figure 3.1B,C). This transient increase in nuclear Yap upon LIF withdrawal suggests that Yap could be involved in the early phase of mESC differentiation. Interestingly, following 24-hours of LIF withdrawal, nuclear Oct4 intensity was also increased (Figure 3.1B,C). Elevated levels of Oct4 have previously been shown to be associated with differentiation of mESCs (Niwa, Miyazaki & Smith, 2000) and Oct4 is required for specification of the Primitive Endoderm (PrE) in pre-implantation mouse embryos (Le Bin *et al.*, 2014).

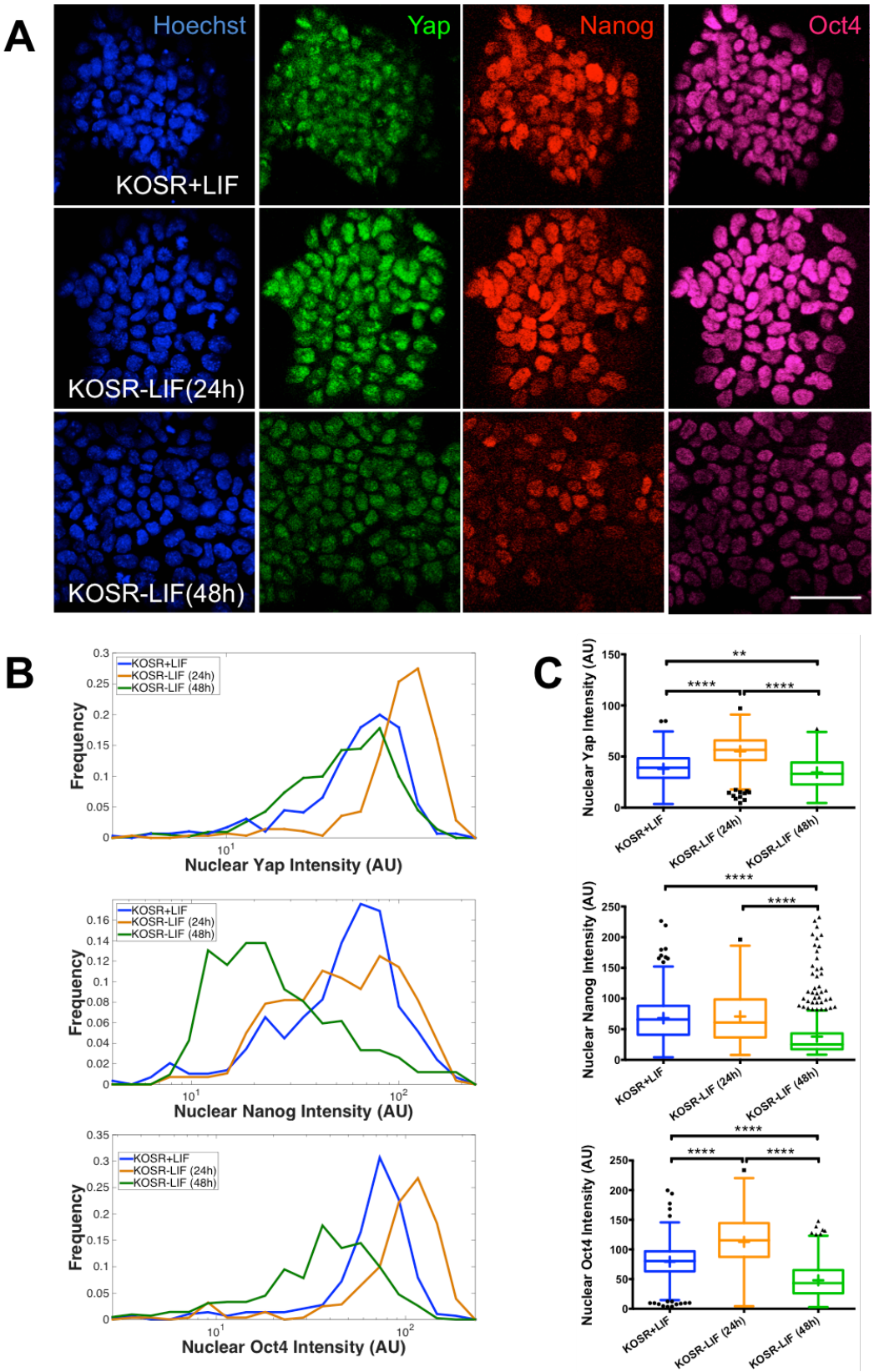
A
Hoechst
Yap
Nanog
Oct4
KOSR+LIF
KOSR-LIF(24h)
KOSR-LIF(48h)
B
KOSR+LIF
KOSR-LIF (24h)
KOSR-LIF (48h)
Frequency
Nuclear Yap Intensity (AU)
Nuclear Nanog Intensity (AU)
Nuclear Oct4 Intensity (AU)
C
Nuclear Yap Intensity (AU)
Nuclear Nanog Intensity (AU)
Nuclear Oct4 Intensity (AU)
**
****

Figure 3.1. Nuclear Yap intensity increases following withdrawal of LIF. (**A**) Representative confocal images of E14Tg2A cells stained for Hoechst (blue), Yap (green), Nanog (red) and Oct4 (Magenta) grown in KOSR for 48 hours with LIF as indicated. Scale bar: 50 μm. (**B**) Distributions of Yap, Nanog and Oct4 in E14Tg2A cells cultured in KOSR+LIF (blue line), KOSR-LIF(24h) (orange line) and KOSR-LIF(48h) (green line). Fluorescence levels (grayscale) were quantified for each individual cell, binned in 20 logarithmically spaced classes (x axis); the frequency of each bin is shown on the y-axis here and in similar graphs. (**C**) Box and whisker plots displaying intensity levels of Yap, Nanog and Oct4 in indicated culture conditions. Solid line indicates median values, while cross indicates mean value here and in similar graphs. **=P<0.001, ****=P<0.0001 by one-way ANOVA with Tukey's post-hoc test. n=at least 280 cells per culture condition. Data shown is representative of two independent experiments.

A previous study has shown that mESCs can spontaneously differentiate into PrE-like cells in standard mESC culture conditions i.e. serum + LIF (Niakan *et al.*, 2010). To examine if expression of Yap in this spontaneous differentiation towards PrE-like cells, E14Tg2a mESCs were cultured in standard mESC culture conditions and then immunostained for Yap, Nanog and Gata6 (Figure 3.2A). Gata6 is an early marker of PrE (Cai *et al.*, 2008). Immunostaining revealed spontaneously differentiating cells that express Gata6, with low expression levels of Nanog (Figure 3.2B). The cells expressing Gata6 appeared to have increased nuclear Yap when compared to the surrounding cells (Figure 3.2B). In this experiment 3.2% of cells spontaneously expressed Gata6. Immunostaining was then analyzed using quantitative immunofluorescence analysis. Nuclear Gata6 intensity of each cell was plotted against nuclear Nanog intensity to give a graphical representation of the population of cells (Figure 3.2C). Nuclear Yap intensity of each cell was then plotted as a heat-map, revealing that cells with higher nuclear Gata6 (bottom right of the graph) intensity also have higher nuclear Yap intensity compared to cells not expressing Gata6 (Figure 3.2B). This is further evidence that upon differentiation of mESCs, nuclear Yap expression increases.

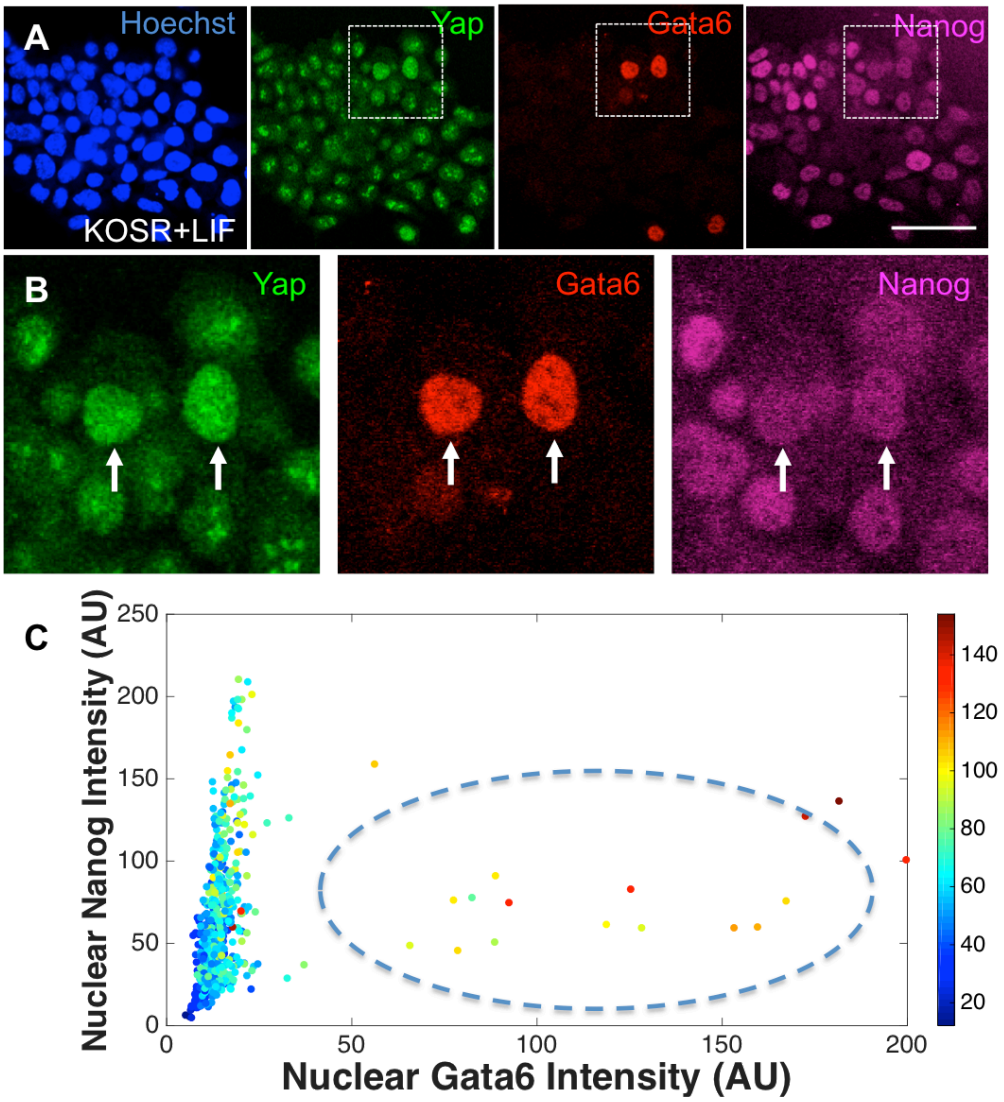

Figure 3.2. Nuclear Yap intensity is increased in cells spontaneously differentiating towards PrE fate (**A**) Representative confocal images of E14Tg2A cells stained for Hoechst (blue), Yap (green), Gata6 (red) and Nanog (Magenta) grown in KOSR for 48 hours with LIF, Scale bar: 50 μm (**B**) Magnified sections of dashed areas in A. Arrows indicate cells expressing Gata6. (**C**) Scatter plot showing Gata6 (x-axis), Nanog (y-axis) and Yap (heat map, side bar) nuclear intensity in fluorescence arbitrary units (AU). Each dot represents the levels in a single cell. 564 cells were analysed. Dashed oval indicates cells expressing Gata6. Images shown are representative of two independent experiments.

Later markers of PrE such as Gata4 have also been shown to be expressed in standard culture of mESCs (Niakan *et al.*, 2010). Expression of Gata4 was examined in mESCs cultured in standard culture conditions. IOUD2 cells were cultured for 72 hours, fixed and expression of Gata4 or Yap was examined by immunostaining. Expression of Gata4 was most often observed in cells located at the

periphery of colonies (Figure 3.3B). This is analogous to expression of Gata4 in the PrE of the pre-implantation mouse embryo, which is located at the edge of the inner cell mass adjacent to the blastocoel (Plusa *et al.*, 2008).

Yap was also expressed in the nuclei of cells located at the periphery of colonies (Figure 3.3A). Cells towards the centre of colonies exhibited a more diffuse Yap expression. This was not due to antibody penetration as co-staining using a pan-cadherin antibody displayed staining throughout the colony (Figure 3.3A). Expression of nuclear Yap in cells at the periphery of mESC colonies correlates with the expression of later marker of PrE, Gata4. This, together with increased expression of nuclear Yap in Gata6 positive cells raised the possibility that nuclear Yap may be associated with PrE cell fate.

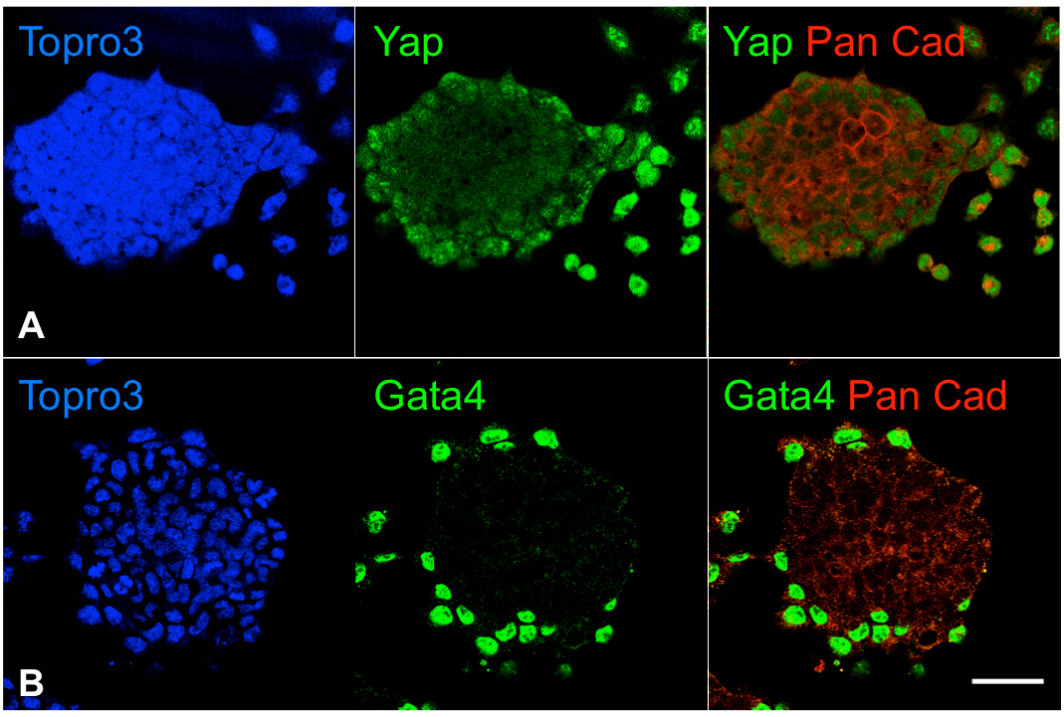

Figure 3.3. Nuclear Yap and Gata4 are expressed in cells located at the periphery of mESC colonies. (A) Representative confocal image of a colony IOUD2 cells stained for Topro3 (blue), Yap (green), and Pan-Cadherin (red) grown in KOSR with LIF (**B)** Representative confocal image of a colony of IOUD2 cells stained for Topro3 (blue), Gata4 (green), and Pan-Cadherin (red) grown in KOSR with LIF. Scale bar 50μm. Images shown are representative of five colonies from two independent experiments.

3.3 Embryoid Bodies as a model of PrE differentiation

The previous results suggest that Yap might be involved in PrE differentiation. Spontaneous differentiation towards PrE is a relatively rare event in mESCs. However aggregation of mESCs into embryoid bodies facilitates PrE differentiation (Hamazaki *et al.*, 2004; Li & Yurchenco, 2006). Embryoid bodies can recapitulate early steps of pre-implantation development, including differentiation of endoderm on the surface of the inner cell mass, differentiation of a columnar epithelium and subsequent formation of a central cavity (Coucouvanis & Martin, 1995).

In order to study Yap in differentiation towards primitive endoderm, mESCs were cultured as embryoid bodies using two methods. In the first method, IOUD2 mESCs were cultured as aggregates in hanging drop suspension culture for 2 days and subsequently transferred into suspension culture for extended culture (Figure 3.4A). Presence of an endodermal outer layer was examined using phase contrast microscopy (Figure 3.4B). Even after 9 days in suspension culture, embryoid bodies formed using the hanging drop method did not appear to form an endodermal layer of cells on the surface of the embryoid bodies (Figure 3.4B).

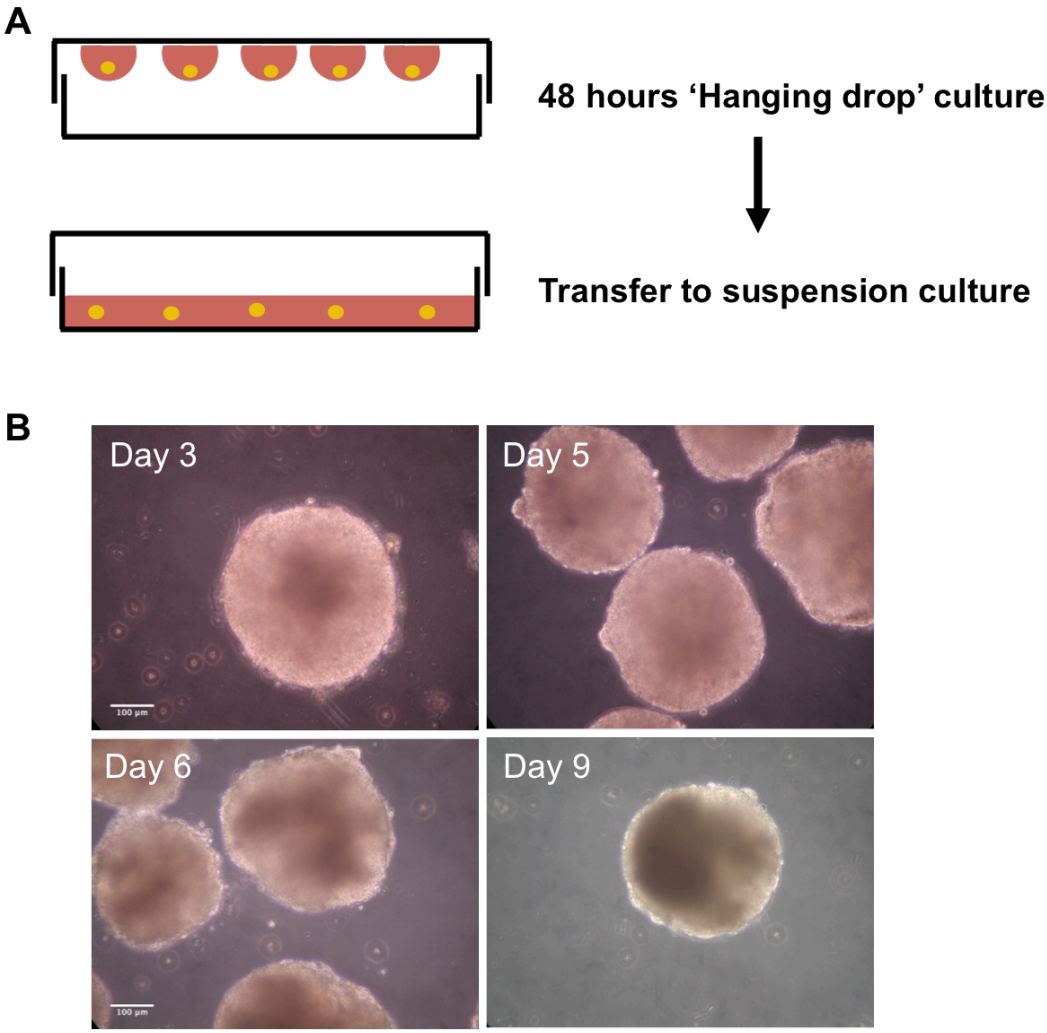

Figure 3.4. Culture of embryoid bodies in 'hanging drop' suspension culture. (**A**) Schematic illustrating culture of mESCs in hanging drop culture on lid of cell culture dish, prior to transfer to suspension culture. (**B**) Phase contrast images of Embryoid bodies at indicated time points. Scale bars 100µm.

As no clear endoderm layer was formed using the 'hanging drop' method, a second method of forming embryoid bodies was used. IOUD2 mESCs were cultured as small cell clusters in suspension culture (Figure 3.5). After 3 days in culture, some embryoid bodies with a clear endodermal layer were visible (Figure 3.5B). After 4 days in culture these embryoid bodies would start to form a central cavity (Figure 3.5C) and could be could be maintained in culture for up to 7 days (Figure 3.5D-F). However efficiency of endodermal differentiation was low and many of the embryoid bodies did not form an endodermal layer, (as visible in Figure 3.5C).

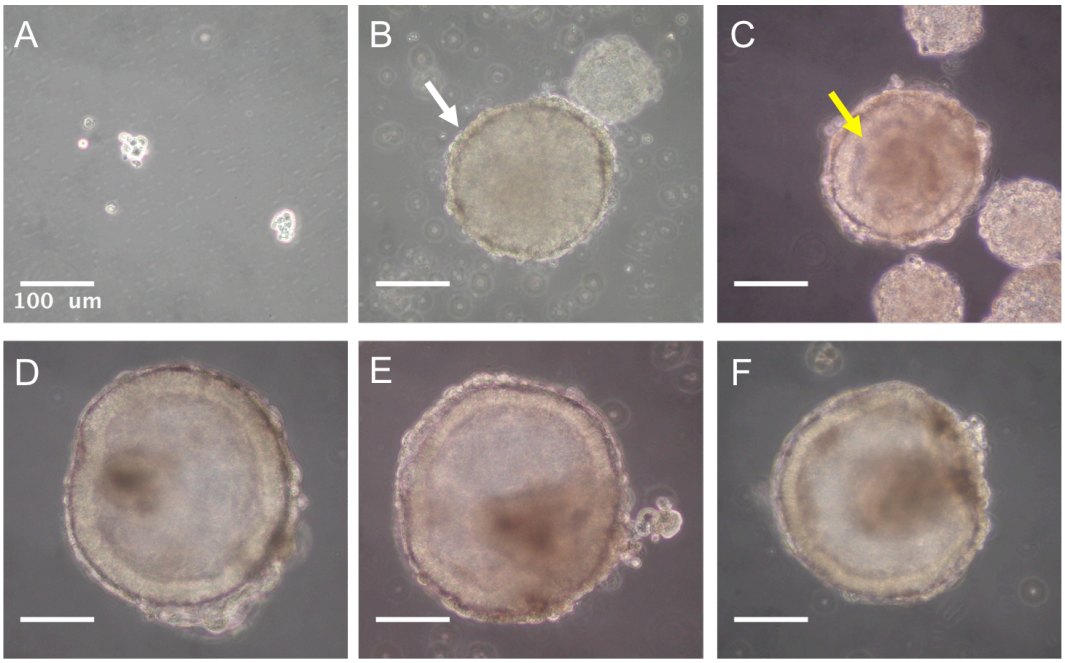

Figure 3.5. Culture of embryoid bodies in cell aggregate suspension culture. Phase contrast images of (**A**) initial cell clusters, Embryoid bodies after, (**B**) 3 days (white arrow indicates endodermal cells), (**C**) 4 days (Yellow arrow indicates formation of cavity), (**D**) 5 days, (**E**) 6 days and (**F**) 7 days in culture. Scale bars 100µm.

Embryoid bodies that had formed a visible outer layer of endodermal cells were selected and expression of Yap was examined by immunostaining (Figure 3.6). The embryoid bodies were quite delicate and during the process of staining, cells on the surface would easily detach. However, strong nuclear staining could be seen in some cells on the outer surface (Figure 3.6A,B). Due to the low frequency of embryoid bodies forming an endodermal layer and the challenges in immunostaining it was not possible to examine whether the outer cells were expressing markers of primitive endoderm such as Gata4 and Gata6. Furthermore, as the frequency of embryoid bodies that formed a visible endoderm was low, the analysis of the expression of Yap in early events in differentiation could sadly not be monitored.

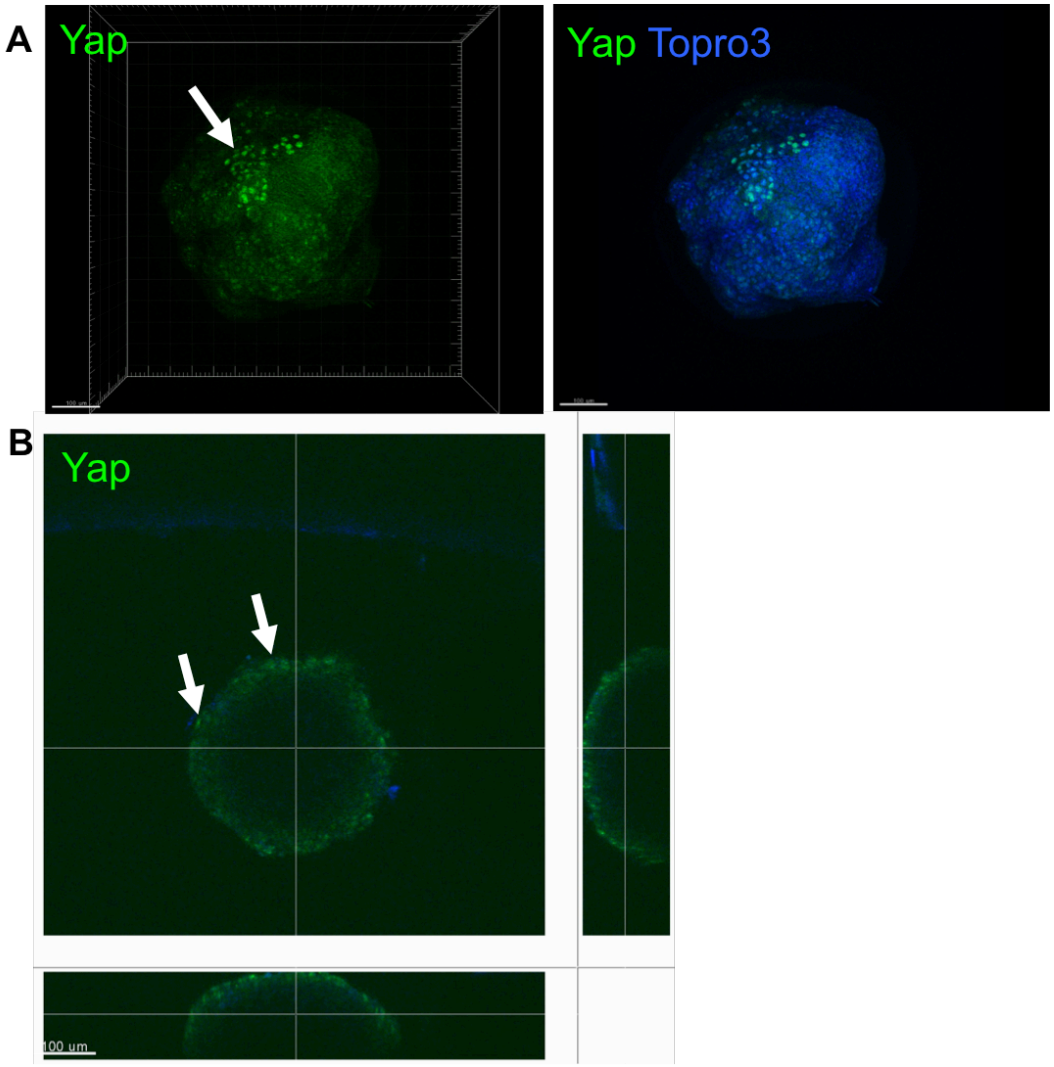

Figure 3.6. Yap is expressed in cells on the surface of embryoid bodies. (**A**) Confocal image of an embryoid body following 3 days in suspension culture stained for Topro3 (blue) and Yap (green). (**B**) Single confocal section of an embryoid body following 3 days in suspension culture stained for Yap (green). Optical orthogonal sections following the white lines in the main image are shown. White arrows indicate nuclear Yap expression. Scale bars: 100μm.

3.4 Gata6-inducible model of PrE differentiation

Differentiation of mESCs towards PrE-like cells can also be achieved through over-expression of Gata6 (Wamaitha *et al.*, 2015). mESCs which express Gata6 under the control of a doxycycline-inducible promoter can be used to model the cell fate decision between PrE and Epiblast (Schröter *et al.*, 2015). A short 6-hour pulse of doxycycline results in co-expression of Gata6 and Nanog. Subsequent removal of doxycycline, followed by a chase period of 24 hours results in a resolution of cell fate decision with cells expressing either Gata6 or Nanog, which resemble

PrE or Epiblast cell fates respectively (Figure 3.7A,B). Pretreatment of these cells with the MEK inhibitor PD0325901 (hereafter referred to as PD) for 3 days enhances extra-embryonic differentiation potential (Schröter *et al.*, 2015). This experimental model allows the analysis of mESCs before, during and after differentiation towards PrE like cells.

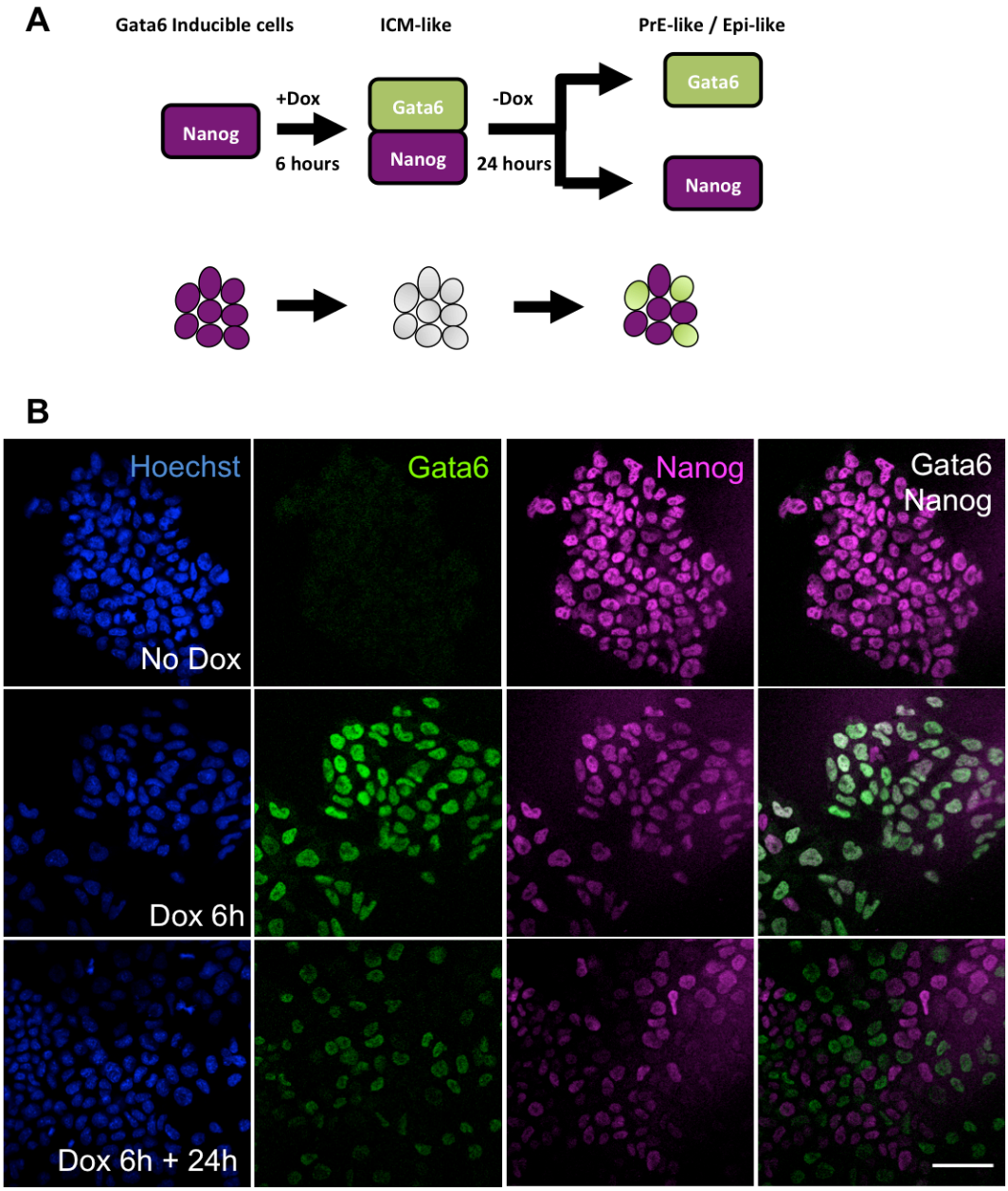

Figure 3.7. Gata6-inducible model of PrE differentiation. (**A**) Schematic indicating Gata6-inducible differentiation protocol. Cells initially express Nanog and following addition of doxycycline (Dox) for 6 hours cells co-express both Nanog and Gata6. Removal of doxycycline and culture for 24 hours in S+L media results in differentiation towards PrE-like cells expressing Gata6 or Epi like cells expressing Nanog. (**B**) Representative confocal images of Gata6-inducible cells stained for Hoechst (blue), Gata6 (green) and Nanog (Magenta) grown in indicated conditions, Scale bar: 50μm. Images shown are representative of six independent experiments.

To validate the experimental model, Gata6-inducible mESCs were treated with a 6-hour pulse of doxycycline and were then either fixed immediately or after a 24-hour chase in standard mESC culture media. These cells were then immunostained for Gata6 and Nanog and analyzed using

quantitative immunofluorescence. The nuclear Gata6 intensity of individual cells was plotted against its nuclear Nanog intensity so as to provide a graphical representation of the population of cells under each experimental condition (Figure 3.8). In order to define cells as positive or negative for Gata6 or Nanog, threshold intensities were created. Threshold intensity values were defined using mixture analysis (see Materials and Methods). Briefly, mixture analysis estimates the parameters of two or more distributions from pooled data; i.e. in this case the two distributions being Positive or Negative for Gata6 or Nanog. Mixture analysis was applied to the 24-hour chase, at which point cells express Gata6 and Nanog in a mutually exclusive manner. Intensities of Gata6 or Nanog above the threshold value were considered positive, and levels below threshold considered negative, therefore allowing four populations of cells in each experimental condition, *Gata6-Nanog-*, *Gata6+Nanog+, Gata6+Nanog- and Gata6-Nanog+*.

As expected, in the untreated control almost all of the cells are negative for expression of Gata6, and positive for expression of Nanog i.e. *Gata6-Nanog+* (Figure 3.8). Following a 6-hour pulse of doxycycline the majority of cells (78.76%) are co-expressing Gata6 and Nanog, i.e. *Gata6+Nanog+*. After a 24-hour chase a large proportion of cells are expressing either Gata6 or Nanog in a mutually exclusive manner, i.e. *Gata6+Nanog-* or *Gata6-Nanog+*, which represent cell fates of PrE or Epi respectively. The proportion of cells that express Gata6 following the 24-hour chase resembles the proportion of cells that differentiate towards PrE in the ICM of the mouse embryo (Kang *et al.*, 2012).

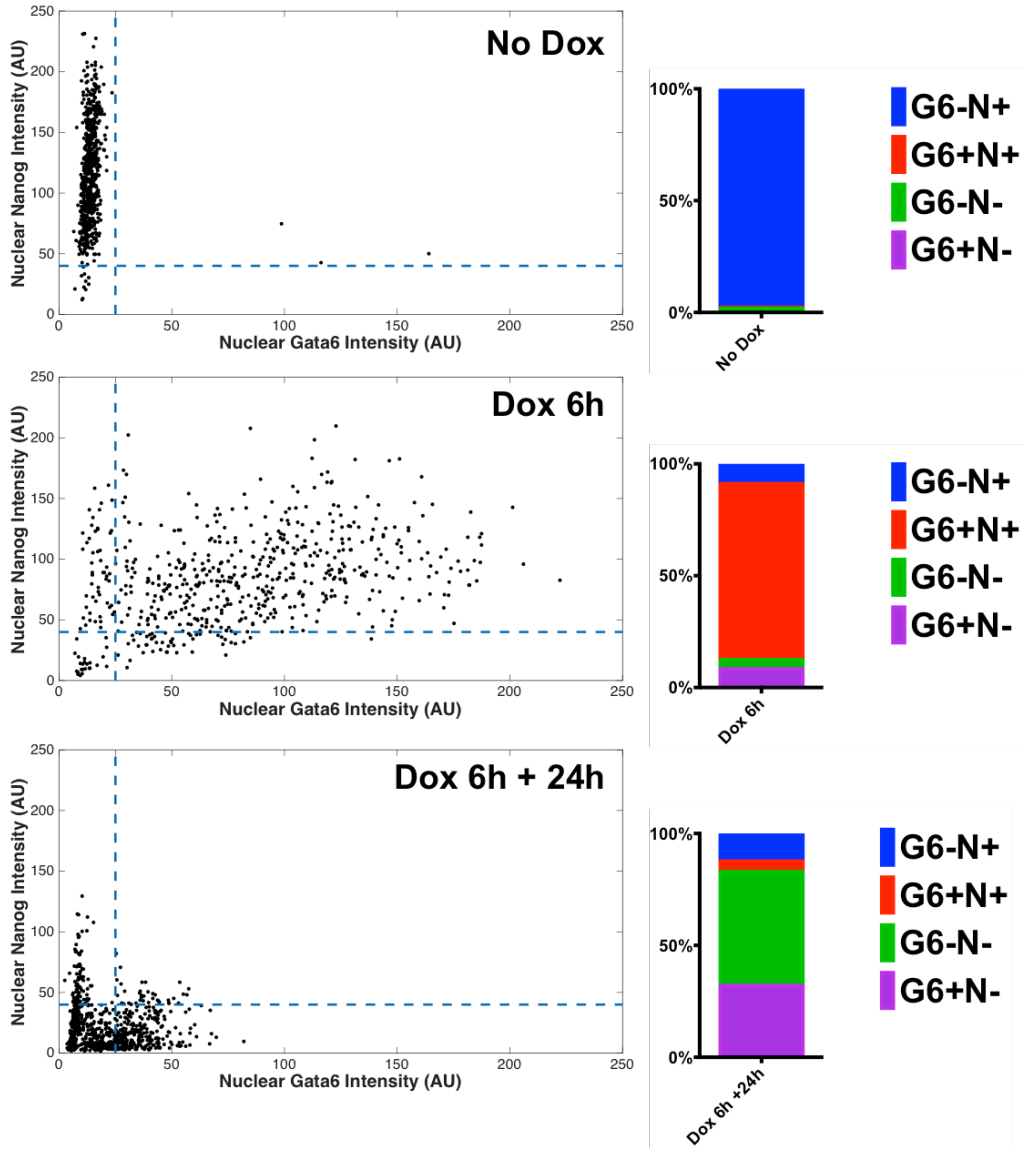

Figure 3.8. Quantitative analysis of Gata6 and Nanog expression in Gata6-inducible model of PrE differentiation. Scatter plots showing Gata6 (x-axis) and Nanog (y-axis) nuclear intensity in fluorescence arbitrary units (AU) from immunostaining of Gata6-inducible cells in the indicated conditions. Each dot represents the levels in a single cell. Dashed lines represent threshold limits for Gata6 and Nanog. Bar charts indicate proportion of cells in each population. >597 cells were analysed in each culture condition. Data shown is representative of six independent experiments.

3.5 Expression of Yap in Gata6-inducible model of PrE differentiation

To investigate Yap regulation during differentiation towards PrE, nuclear Yap intensity was measured in the Gata6 inducible mESC model of PrE differentiation. Cells were treated with a 6-hour pulse of doxycycline and fixed either immediately or after a 24-hour chase in standard mESC culture media. These cells were then immunostained for Yap and

analyzed with quantitative immunofluorescence analysis (Figure 3.9). Immediately after a 6-hour pulse of doxycycline, nuclear Yap intensity was increased compared to an untreated control. Following a 24-hour chase, nuclear Yap Intensity decreased to levels below that of the untreated control (Figure 3.9). This shows that upon induction of Gata6, Yap is more abundant in the nucleus, and that upon differentiation, levels of Yap in the nucleus decrease.

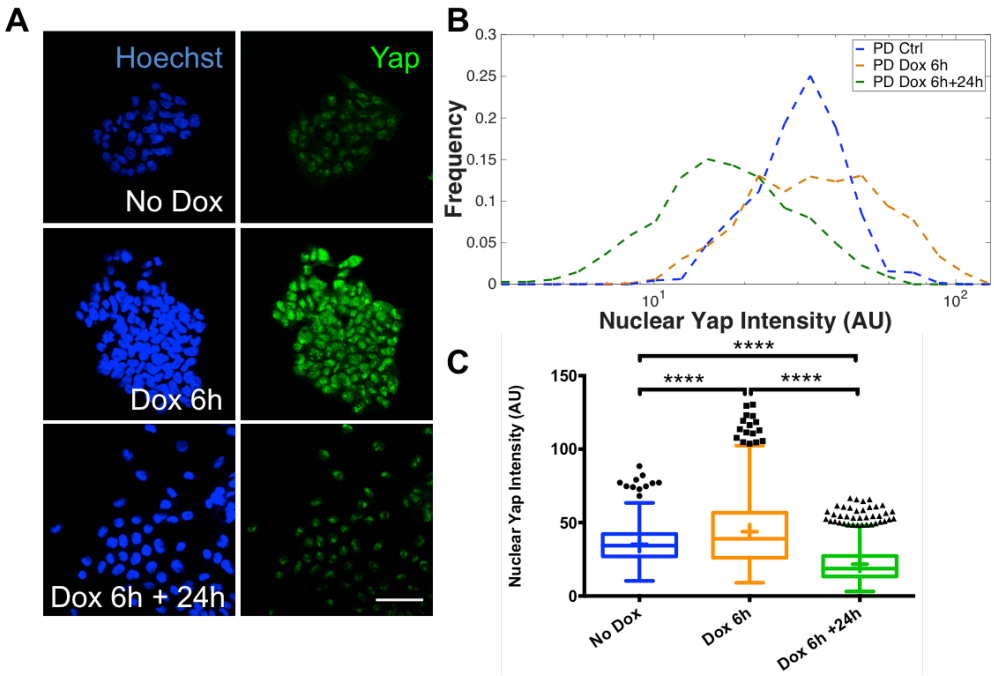

Figure 3.9. Nuclear Yap intensity increases following induction of Gata6. (**A**) Representative confocal images of Gata6-inducible cells stained for Hoechst (blue) and Yap (green) grown in indicated conditions, Scale bar: 50μm. (**B**) Distributions of Yap in Gata6-inducible cells cultured in S+L (blue line), Dox 6h (orange line) and Dox6h+24h (green line). (**C**) Box and whisker plot displaying intensity levels of Yap in indicated culture conditions. ****=P<0.0001 by one-way ANOVA and Tukey's post-hoc test. n=at least 638 cells for each culture condition. Data shown is representative of two independent experiments.

The specificity of the antibody (Cell Signalling 4912) used in these experiments has recently been called into question (Hirate *et al.*, 2012; Saha, Home & Paul, 2012). In order to confirm the transient rise in Yap upon differentiation by induction of Gata6, the experiment was repeated with a separate Yap antibody from another supplier (Santa Cruz 15407). Using this second antibody, similar results were obtained whereby nuclear Yap intensity increased following induction of Gata6 expression, and decreased after the subsequent 24-hour chase (Figure 3.10). As

similar results were obtained with two separate antibodies, this suggests that Yap expression is indeed increased transiently upon induction of Gata6. The Yap antibody from Santa Cruz was used in preference in subsequent experiments.

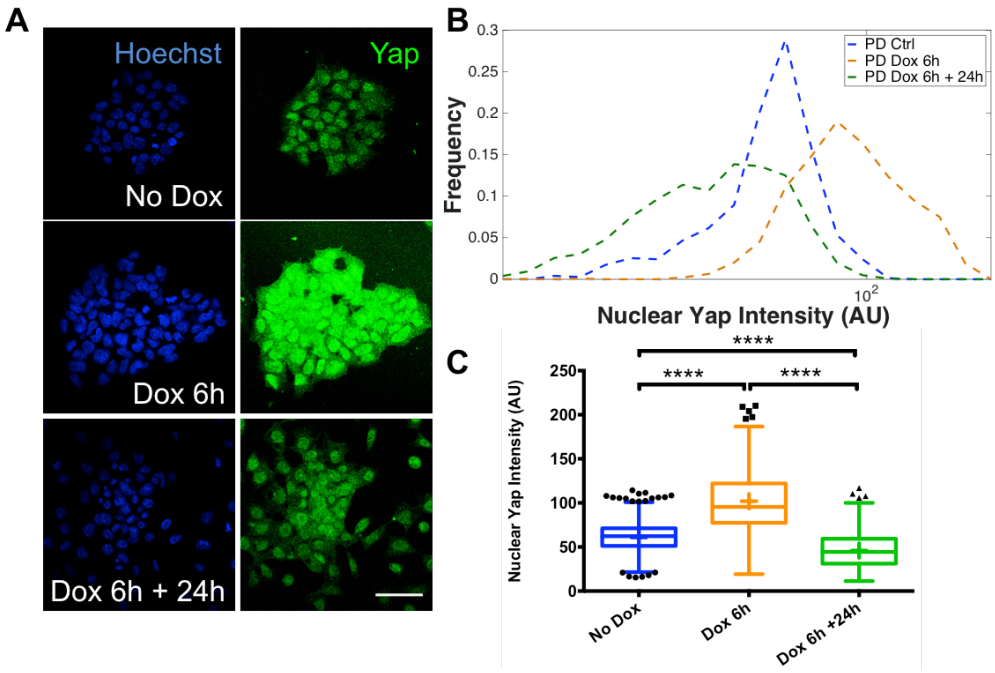

Figure 3.10. Increase in nuclear Yap is reproduced using the Santa Cruz Yap antibody (**A**) Representative confocal images of Gata6-inducible cells stained for Hoechst (blue) and Yap (green) grown in indicated conditions, Scale bar: 50μm. (**B**) Distributions of Yap in Gata6-inducible cells cultured in S+L (blue line), Dox 6h (orange line) and Dox6h+24h (green line). (**C**) Box and whisker plot displaying intensity levels of Yap in indicated culture conditions. ****=P<0.0001 by one-way ANOVA with Tukey's post-hoc test. n=at least 748 cells for each culture condition. Data shown is representative of five independent experiments.

3.6 Expression of nuclear Yap is associated with PrE cell fate

As nuclear Yap intensity was increased in cells spontaneously differentiating towards PrE and also upon induction of Gata6, increased nuclear Yap may therefore be specifically associated with the PrE cell fate in mESCs. The Gata6 inducible cells provide an experimental model of cell fate choice between *Gata6+Nanog-* PrE and *Gata6-Nanog+* Epi. To determine whether the increased nuclear Yap is associated with *Gata6+Nanog-* PrE like cell fate, Gata6 inducible cells were treated with a 6-hour pulse of Doxycycline and fixed either immediately or after a 24-hour chase period in standard mESC culture media. Nanog and Gata6

expression was determined using immunostaining along with Yap (Figure 3.11) and analyzed by quantitative immunofluorescence (Figure 3.12). As previously shown in Figure 3.10, nuclear Yap intensity increased following a 6-hour pulse of doxycycline, and decreased following the 24-hour chase period.

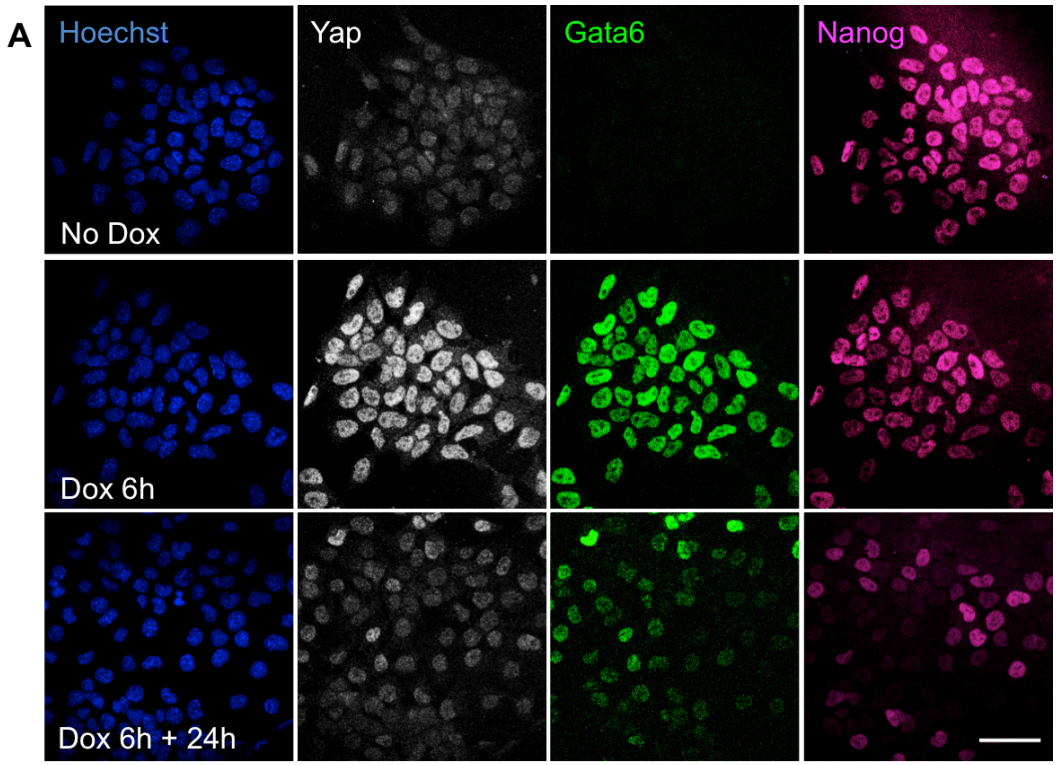

Figure 3.11. Examining Yap expression in relation to cell fate. (**A**) Representative confocal images of Gata6-inducible cells stained for Hoechst (blue), Yap (white), Gata6 (green) and Nanog (magenta) grown in indicated conditions, Scale bar: 50μm. Images shown are representative of three independent experiments.

The Gata6 nuclear intensity of individual cells was plotted against the Nanog nuclear intensity and the threshold intensities for Gata6 and Nanog were defined using mixture analysis. The nuclear intensity of Yap from individual cells was then plotted as a heat-map to give a graphical representation of Gata6, Nanog and Yap in individual cells (Figure 3.12A). As in Figure 3.7, after a 6-hour pulse of doxycycline, Gata6 and Nanog showed co-expression (Figure 3.12A). In mESCs cultured under these conditions, nuclear Yap intensity appears to be highest, and specifically in cells co-expressing Gata6 and Nanog (Figure 3.12B). Following the 24-hour chase; Gata6 and Nanog were expressed in a mutually exclusive

manner representing PrE and Epi cell fates respectively. Nuclear Yap intensity is significantly higher in *Gata6+Nanog-* cells compared to *Gata6-Nanog+* cells (Figure 3.12C). This therefore suggests that PrE (and not Epi) cell fate is associated with increased nuclear Yap.

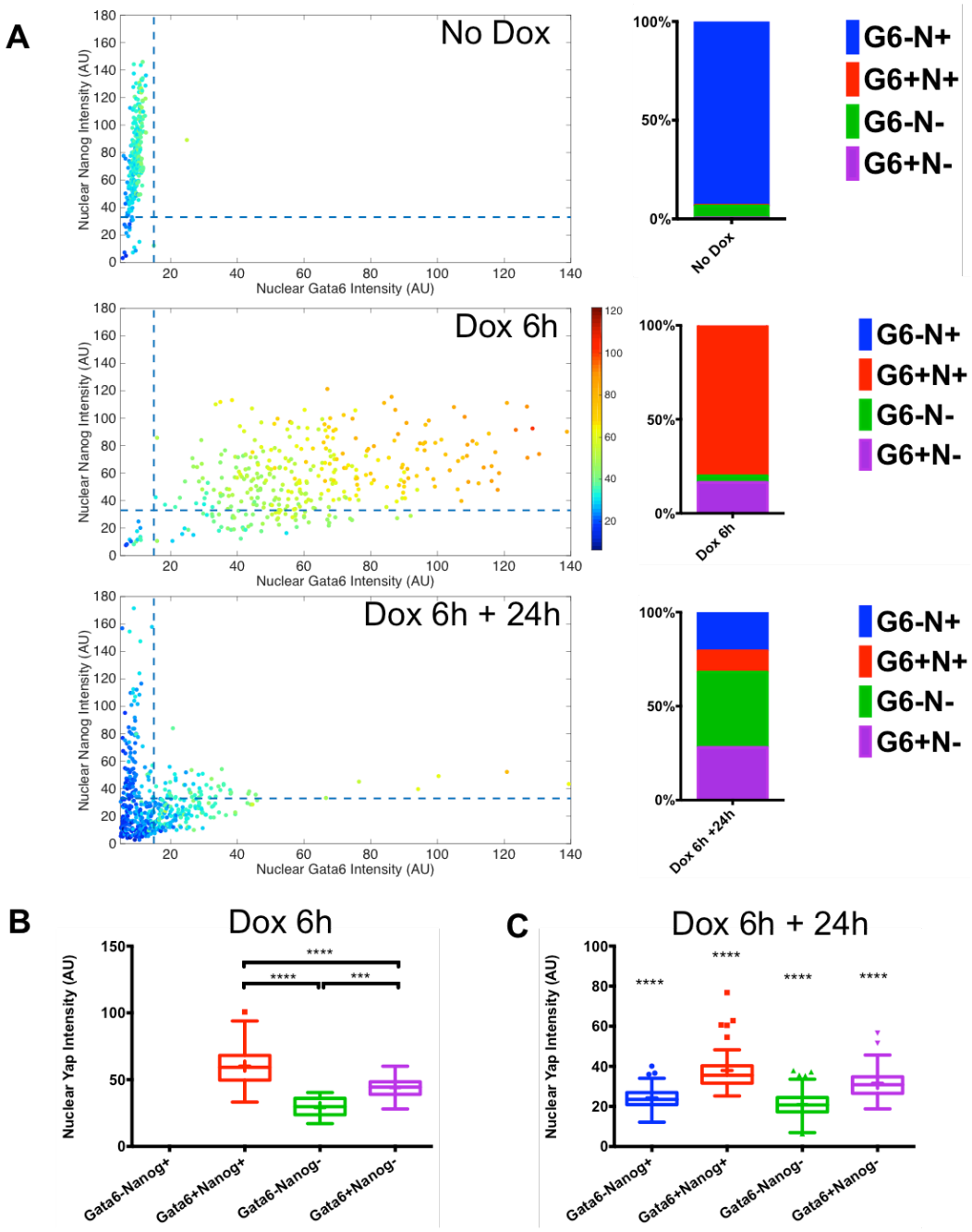

Figure 3.12: Quantitative analysis of nuclear Yap intensity in cell populations differentiating towards Epi or PrE cell fate (A) Scatter plots showing Gata6 (x-axis) Nanog (y-axis) and Yap (heat-map, side) nuclear intensity in fluorescence arbitrary units (AU) from immunostaining of Gata6-inducible cells in the indicated conditions. Each dot represents the levels in a single cell. Dashed lines represent threshold limits for Gata6 and Nanog. Bar charts indicate proportion of cells in each population. (**B,C**) Box and whisker plots displaying intensity levels of Yap in indicated cell populations following (**B**) 6 hours of doxycycline treatment and (**C**) 24 hours chase following 6 hours of doxycycline treatment. All populations in C are significantly different from each other. ***=P<0.001, ****=P<0.0001 by one-way ANOVA with Tukey's post-hoc test. n=at least 294 cells for each culture condition. Data shown is representative of three independent experiments.

3.7 Hippo regulation of Yap during PrE differentiation

Yap can be regulated by the Hippo signalling pathway through phosphorylation by Lats at S112 leading to interaction with 14-3-3 proteins and cytoplasmic retention, thus rendering Yap unable to act as a transcriptional co-activator (Zhao *et al.*, 2007). The previously observed increase in nuclear Yap upon differentiation towards PrE may therefore be a result of a decrease in phosphorylation at S112 by Lats allowing Yap to translocate to the nucleus. Phosphorylation of Yap during differentiation towards PrE was measured using an antibody directed against pYap-S127 (Human Yap S127 is analogous to mouse Yap S112, hereafter referred to as pYap) (Figure 3.13A). Expression of pYap was quantified by fluorescence intensity profiles (Figure 3.13B). Expression of pYap did not appear to change following a 6-hour pulse of doxycycline (Figure 3.13A,B). This suggests that the increase in nuclear Yap expression upon differentiation may not be due to decreased phosphorylation and cytoplasmic retention. 24-hours after the pulse of doxycyxline, expression of pYap appeared reduced (Figure 3.13A,B). This is in accordance with the total expression level of Yap being decreased following differentiation. This experiment suggests that the observed increase in nuclear Yap expression upon differentiation towards PrE may not be due to decreased phosphorylation at YapS112.

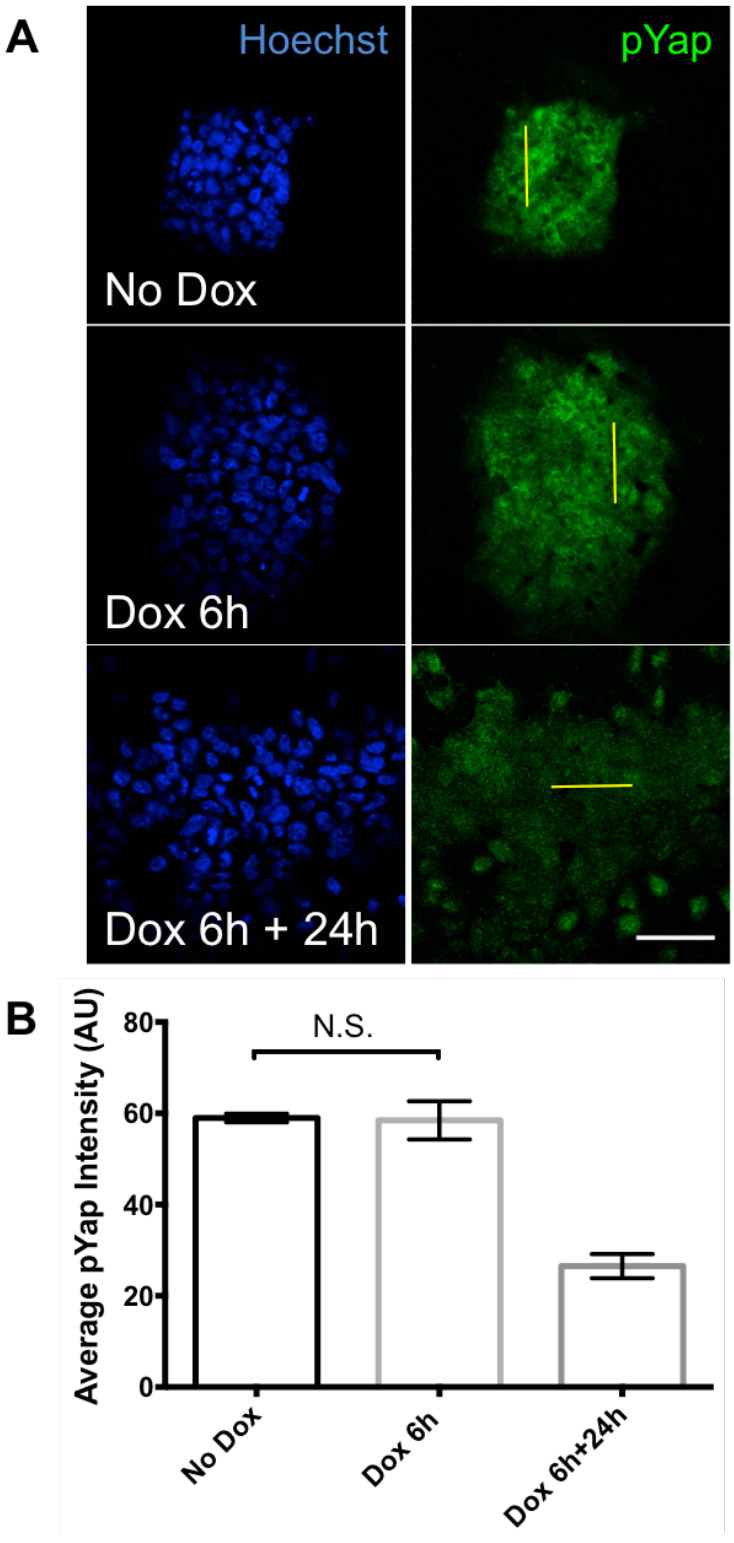

Figure 3.13. Expression of pYap in Gata6 inducible model of PrE differentiation: (**A**) Representative confocal images of Gata6-inducible cells stained for Hoechst (blue) and pYap (green), grown in indicated conditions, Yellow lines indicate example intensity profiles. Scale bar: 50μm. (**B**) Bar chart displaying average fluorescence intensity, derived from intensity profiles. N.S.= no significant difference by one-way ANOVA with Tukey's post-hoc test. n=3 measurements per condition

3.8 Modulating subcellular localization of Yap through varying compliance of cell culture surface

The subcellular localization of Yap has been shown to be regulated by stiffness of the extra-cellular matrix (Dupont *et al.*, 2011). Culture of cells on stiff culture substrates (≥40kPa) results in expression of nuclear Yap, whereas culture of cells on soft substrates (0.7kPa) results in cytoplasmic retention of Yap (Dupont *et al.*, 2011). This therefore presents the possibility of using soft culture substrates as a means to induce cytoplasmic retention of Yap and subsequently examine if differentiation of mESCs towards PrE is affected, due to the lack of Yap transcriptional activity. If nuclear Yap is required for differentiation towards PrE, preventing Yap translocating to the nucleus would inhibit differentiation towards PrE.

To examine if compliance of the culture surface affects subcellular localization of Yap in mESCs, IOUD2 cells were cultured on polyacrylamide hydrogels of varying compliance (Figure 3.14). mESCs cultured on softer (0.7kPa) hydrogels appeared to form round colonies, whereas mESCs on hydrogels of increasing stiffness (4kPa, 40kPa) formed more irregular shaped colonies and showed more indication of cell spreading Figure 3.14.

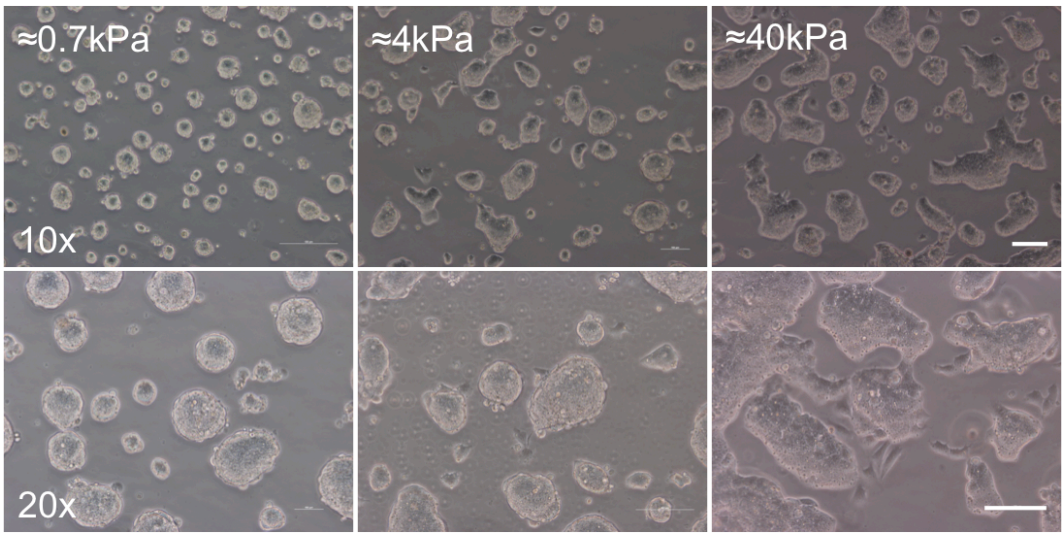

Figure 3.14. culture of mESCs on hydrogels of varying compliance. Representative phase contrast images of IOUD2 cells grown on polyacrylamide hydrogels. Approximate compliance is given in kPa. Scale bars 100μm

The subcellular localization of Yap in cells cultured on soft hydrogels was determined by immunostaining (Figure 3.15). Unfortunately, immunostaining of cells grown on hydrogels resulted in large amounts of non-specific staining (Figure 3.15), thus preventing analysis of the subcellular localization of Yap.

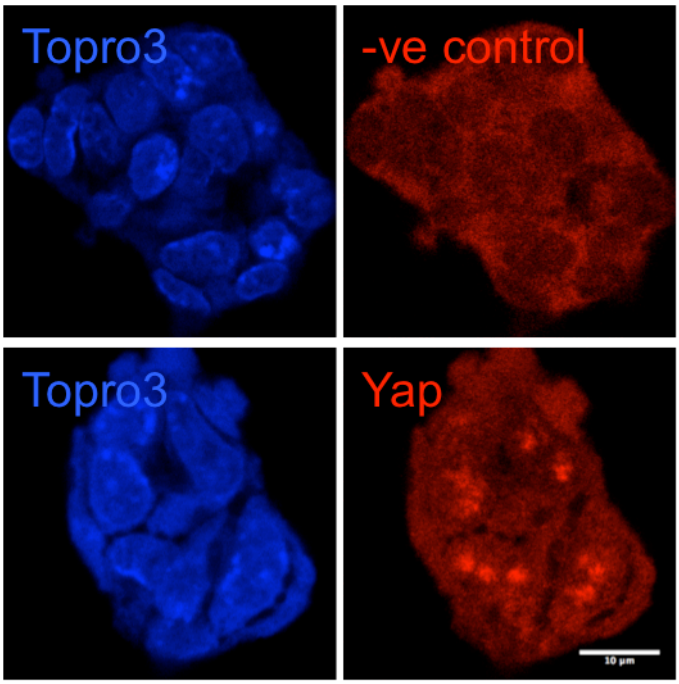

Figure 3.15. Immunostaining of mESCs cultured on soft (0.7kPa) hydrogel. Representative confocal images of IOUD2 cells stained for Topro3 (blue) and Yap (Red). –ve control indicates no primary antibody. Scale bar: 10µm

3.9 Small molecule Inhibition of Yap in Gata6 inducible model of PrE differentiation

To examine if nuclear Yap is required for differentiation towards PrE, small molecules, dobutamine and verteporfin, were used to inhibit nuclear Yap. Dobutamine is a β-adrenergic receptor agonist which has been shown to induce phosphorylation and cytoplasmic retention of Yap (Bao *et al.*, 2011). Verteporfin is a small molecule inhibitor, which binds to Yap, subsequently preventing its association with Tead transcription factors (Liu-Chittenden *et al.*, 2012). If nuclear Yap is required for mESC differentiation towards PrE, inhibition of nuclear Yap through cytoplasmic retention, or inability to bind transcriptional co-activator Tead should prevent differentiation towards PrE.

The effect of these inhibitors on nuclear Yap was examined in the Gata6-inducible model of PrE differentiation. Gata6-inducible mESCs were treated with a 6-hour pulse of doxycycline together with either 10μM dobutamine or 2.5μM verteporfin (Figure 3.16), as nuclear Yap expression was previously found to be highest following this time point. Addition of verteporfin resulted in widespread cell death, preventing further analysis (Figure 3.16).

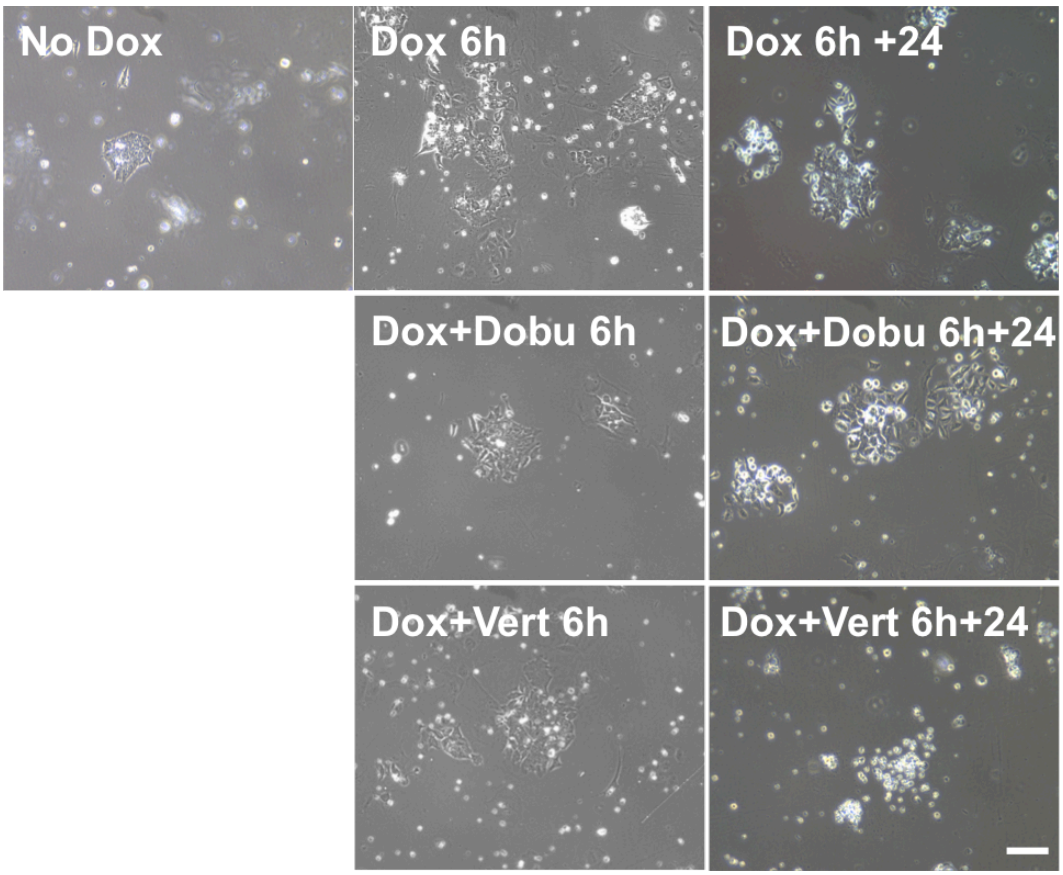

Figure 3.16. Inhibition of nuclear Yap with dobutamine and verteporfin: Representative phase contrast images of Gata6 inducible cells cultured under the indicated conditions. Scale bar: 50μm**.** Images shown are representative of two independent experiments.

To investigate the effects of addition of dobutamine on cell fate choice, Gata6-inducible mESCs were treated with a 6-hour pulse of doxycycline together with dobutamine and fixed either immediately or following a 24-hour chase in standard mESC culture media. Yap, Nanog and Gata6 expression was determined using immunostaining (Figure 3.17A) and analysed by quantitative immunofluorescence. Addition of dobutamine during the 6-hour pulse of doxycycline significantly reduced nuclear Yap

expression compared to addition of doxycycline alone (Figure 3.17). Unexpectedly, addition of dobutamine resulted in expression of Nanog in both the nuclei and cytoplasm of cells.

As increased nuclear Yap expression was previously found to be associated with PrE cell fate, Gata6 expression was examined 24-hours following the doxycycline pulse together with dobutamine. At this time point cells are either positive for Gata6 or Nanog. A threshold limit for Gata6 expression was defined by mixture analysis. Addition of dobutamine resulted in a decreased proportion of cells positive for Gata6 expression compared to doxycycline alone (Figure 3.17C). This suggests that reduction of nuclear Yap expression results in fewer cells differentiating towards a PrE-like cell fate.

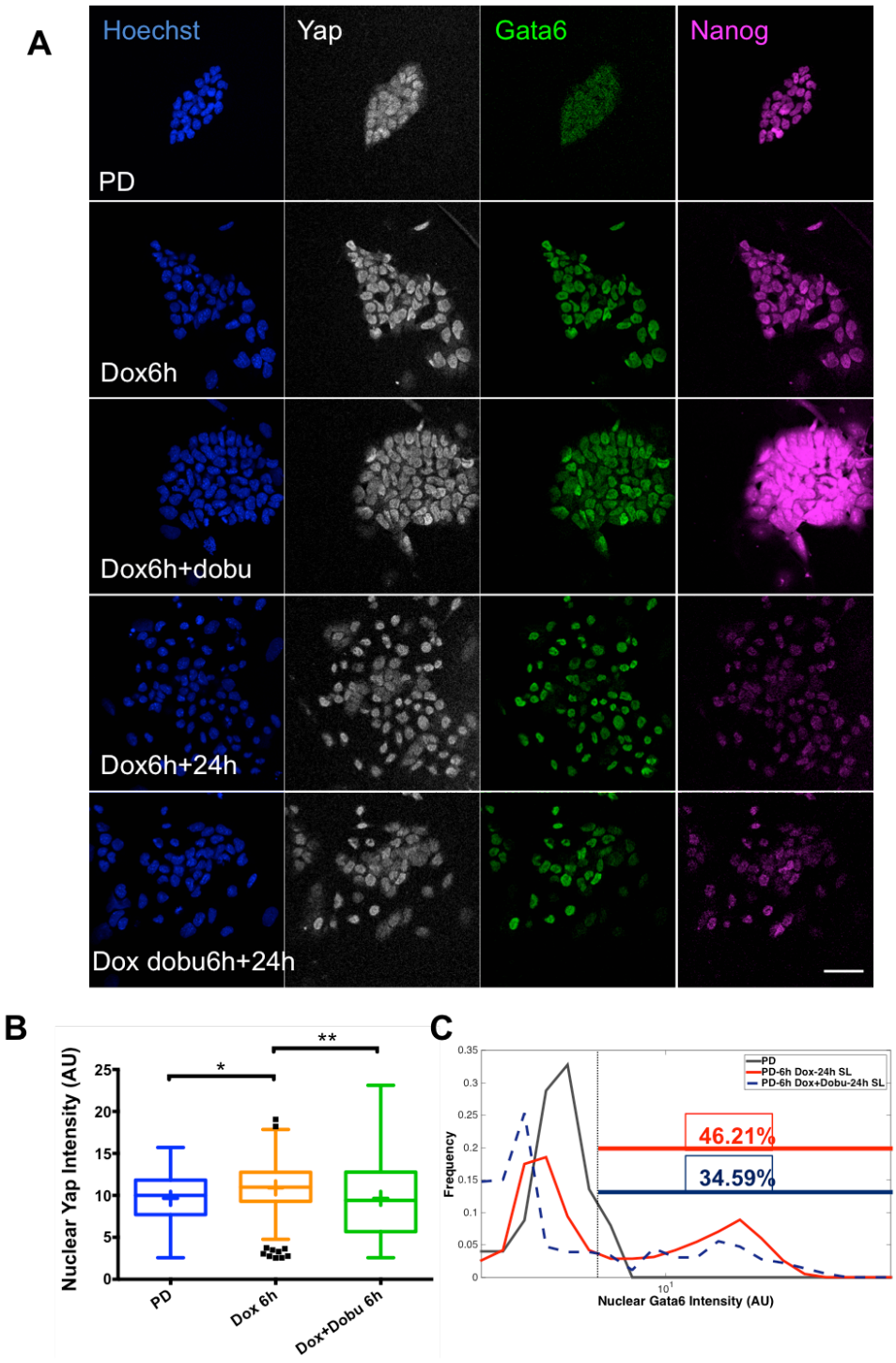

Figure 3.17. Dobutamine reduces nuclear Yap expression, which results in reduced Gata6 expression. (**A**) Representative confocal images of Gata6-inducible cells stained for Hoechst (blue), Yap (white), Gata6 (green) and Nanog (magenta) grown in the indicated conditions, Scale bar: 50μm. (**B**) Box and whisker plot displaying intensity levels of Yap in indicated culture conditions. *=P<0.05, **=P<0.01 by one-way ANOVA with Tukey's post-hoc test. n=at least 294 cells per culture condition (**C**) Distributions of Yap in Gata6-inducible cells cultured in S+L (grey line), Dox 6h+24h (red line) and Dox+Dobu6h+24h (dashed blue line). Percentages of cells above Gata6 threshold limit are indicated. Data shown is representative of two independent experiments.

3.10 Summary

- In mESCs, Nuclear Yap expression initially increases before decreasing upon differentiation induced by withdrawal of LIF
- Nuclear Yap expression is increased in mESCs spontaneously differentiating towards PrE
- Yap expression is high in endoderm-like cells on the surface of embryoid bodies
- Gata6-inducible mESCs can model PrE cell fate choice
- Nuclear Yap increases upon induction of Gata6 and is higher in cells that have differentiated towards PrE-like cell fate
- Nuclear Yap increases upon induction of Gata6 is not associated with decreased pYap expression
- Attenuation of Nuclear Yap with dobutamine resulted in a reduced proportion of cells differentiating towards PrE-like cell fate

3.11 Discussion

Nuclear Yap in the differentiation of mESCs

In this Chapter it is shown that there is a decrease in total Yap expression upon differentiation of mESCs Figure 3.1. This is in agreement with previous studies (Tamm, Bower & Anneren, 2011; Lian *et al.*, 2010). Here, in this Chapter, a more detailed analysis on Yap during differentiation is performed, showing an initial increase in nuclear Yap expression prior to differentiation, indicating dynamic regulation of Hippo signalling during this process (Figure 3.1). This initial increase in nuclear Yap expression may have been missed in the studies by Tamm *et al.* and Lian *et al.,* due to the fact that only self-renewing conditions and end-points of differentiation were assayed.

The same previous studies also highlight a potential role for Yap in the maintenance of mESC self-renewal, with Yap regulating the expression of Oct4 (Tamm, Bower & Anneren, 2011; Lian *et al.*, 2010). A correlation in the behaviour of Oct4 and Yap can be seen in Figure 3.1, whereby upon induction of differentiation via the removal of LIF, an increase in both

Oct4 and Yap nuclear expression is observed. Despite its role in maintenance of pluripotency, Oct4 has also been shown to be required for differentiation in a number of contexts (Radzisheuskaya *et al.*, 2013; Niwa, Miyazaki & Smith, 2000; Le Bin *et al.*, 2014). ESCs and induced pluripotent stem cells (iPSCs) with lowered Oct4 levels maintain self renewal and fail to differentiate upon induction of differentiation cues (Radzisheuskaya *et al.*, 2013), whilst over expression of Oct4 in ESCs leads to differentiation towards PrE (Niwa, Miyazaki & Smith, 2000). Deletion of Oct4 in the pre-implantation mouse embryo, induced during the transition from morula to blastocyst, results in cells of the inner cell mass failing to commit to either Epi or PrE lineages (Le Bin *et al.*, 2014). It is thus apparent that Oct4 is required for exit from the pluripotent state, and the regulation of Oct4 by Yap could be involved in this context.

Yap in differentiation towards PrE

The results in this chapter show that differentiation towards PrE-like cell fate is accompanied by increased nuclear Yap expression (Figure 3.12). Nuclear Yap is increased in spontaneously differentiating mESCs that express Gata6, which is one of the earliest markers of PrE (Plusa *et al.*, 2008). This could suggest that Yap may be involved in early phases of PrE differentiation. Increased nuclear Yap expression was also observed in Gata6 expressing cells that had down regulated Nanog in the gata6-inducible model of PrE differentiation (Figure 3.12) as well as in endodermal cells in embryoid bodies (Figure 3.6). This could suggest that increased nuclear Yap expression is also associated with maintenance of PrE cell fate. This could be confirmed by looking for expression of later markers of PrE such as Gata4 (Plusa *et al.*, 2008), and seeing if nuclear Yap expression remains high in cells that express Gata4. Furthermore, the role of Yap in PrE differentiation can be assessed *in vivo*, by examination of Yap expression in the mouse pre-implantation embryo.

Increase in nuclear Yap expression following induction of Gata6

As induction of Gata6 resulted in increased expression of nuclear Yap (Figure 3.9 and Figure 3.10), it is possible that Gata6 is directly regulating

the expression of Yap. In a recent study by Wamaitha *et al.* Chromatin immunoprecipitation (ChIP) followed by high throughput sequencing (ChIP-seq) analysis of Gata6 binding targets, in a Gata6-inducible mESC line, did not identify *Yap* as a Gata6 bound region (Wamaitha *et al.*, 2015). Furthermore, in the same study, RNA sequencing in a Gata6-inducible human embryonic stem cell line did not lead to an increase in expression of Yap RNA (Wamaitha *et al.*, 2015). Taken together, these results from the study by Wamaitha *et al.* imply that upon induction of Gata6, Gata6 is not directly regulating expression of Yap.

Regulation of Yap by Hippo during differentiation towards PrE

If the increase of nuclear Yap expression is not due to an increase in expression of Yap, another possibility is that induction of Gata6 leads to decreased Hippo signalling, which results in decreased phosphorylation of Yap by Lats at YapS112. Phosphorylation of YapS112 results in cytoplasmic retention of Yap (Zhao *et al.*, 2007), Thus, decreased Hippo signalling could result in increased nuclear Yap localization.

Interestingly, immunostaining of pYap-S112 did not show decreased levels following 6-hours of doxycycline induced Gata6 expression (Figure 3.13A,B). This suggests that increased nuclear levels of Yap at this time point is not due to decreased Yap S112 phosphorylation by Lats i.e. less cytoplasmic retention of Yap. This could therefore suggest that there may be more Yap protein in total due to either increased transcription of Yap, or increased stability of Yap. An increase in total Yap could potentially overcome Lats mediated phosphorylation and subsequent cytoplasmic retention. To test for an increase in expression of Yap, reverse transcriptase PCR could be used to detect an increase in Yap mRNA following induced expression of Gata6. If there is no increase in Yap mRNA then it is possible that the increased levels of nuclear Yap are due to increased Yap stability. This experiment was attempted, but due to the relatively low number of cells in the Gata6-inducible model of PrE differentiation assay, insufficient RNA was extracted for RT-PCR analysis.

It would be interesting to repeat this experiment, scaling up the amount of cells in the assay, such that sufficient RNA for analysis could be extracted.

A recent study introduced a *YapS112A* knock-in mutation into the endogenous *Yap* locus, such that YapS112 cannot be phosphorylated by Lats and therefore evades cytoplasmic retention (Chen *et al.*, 2015). The *YapS112A* mice appear phenotypically normal, which is surprising considering that they show nuclear localization of YapS112A, overexpression of which has previously been shown to induce aberrant tissue expansion (Camargo *et al.*, 2007). The *YapS112A* mutant mice were found to be able to regulate the expression of Yap protein levels through increased phosphorylation by Lats of another serine residue YapS381 (Chen *et al.*, 2015). Phosphorylation of YapS381 by Lats primes Yap for subsequent phosphorylation by Casein Kinase 1 (CK1), resulting in the generation of a 'phosphodegron', a motif that is recognised by β-transducin repeat-containing protein (β-TRCP) (Zhao *et al.*, 2010). β-TRCP is an adaptor for SCF E3 ubiquitin ligases, which subsequently poly-ubiquitinates Yap, leading to its destruction by the proteasome (Zhao *et al.*, 2010). Therefore in these mice, Yap transcriptional activity was regulated primarily through stability of the protein as opposed to its subcellular localisation. It is therefore possible that the transient increase in nuclear Yap upon induction of Gata6 is due to increased stability of Yap. To test this hypothesis, the half-life of Yap could be measured following induction of Gata6 by treatment with the inhibitor of protein synthesis, cycloheximide. Measuring the total amount of Yap following cycloheximide treatment could indicate if induction of Gata6 increases the stability of Yap.

The half-life of Yap has been reported to be less than 3 hours in conditions that promote active Hippo signalling, such as high cell density (Levy *et al.*, 2008; Zhao *et al.*, 2010). The C-terminus of Yap contains a tyrosine residue, which upon phosphorylation by c-ABL, increases the stability of Yap (Levy *et al.*, 2008). The same tyrosine residue has been reported to be phosphorylated by YES, downstream of LIF in mESCs, resulting in increased Yap dependent transcriptional activity (Tamm,

Bower & Anneren, 2011). It is therefore possible that Yap is stabilized downstream of LIF, allowing Yap to overcome Hippo mediated cytoplasmic retention. Interestingly, recent studies indicate a role for LIF in the expansion of PrE primed mESCs in cell culture, and the expansion of PrE cells *in vivo* (Morgani *et al.*, 2013; Morgani & Brickman, 2015). Therefore it is possible to speculate that this LIF induced expansion of PrE is associated with increased nuclear Yap. Indeed, increased nuclear Yap is observed in mESCs spontaneously differentiating towards PrE in the presence of LIF (Figure 3.2). This is further evidence that increased nuclear Yap expression is associated with differentiation towards PrE, however the question remains; what is the function of nuclear Yap in relation to differentiation towards PrE?

Nuclear targets of Yap

Increased nuclear Yap is associated with PrE differentiation in spontaneous differentiation (Figure 3.2), embryoid bodies (Figure 3.6) and in a Gata6 inducible model of differentiation (Figure 3.10). Furthermore inhibition of nuclear Yap resulted in a decreased proportion of cells differentiating towards PrE Figure 3.17, suggesting a requirement for nuclear Yap. In specification of the TE in the mouse pre-implantation embryo, nuclear Yap co-activates expression of TE specific transcription factors Cdx2 and Gata3 (Nishioka *et al.*, 2009; Ralston *et al.*, 2010). Interestingly, a recent study has shown that in embryonic pancreatic progenitor cells, Yap, Tead and Gata6 bind to enhancers of genes associated with pancreatic development, notably Hhex and Fgfr2 (Cebola *et al.*, 2015). Hhex and Fgfr2 are associated with PrE development (Thomas, Brown & Beddington, 1998; Arman *et al.*, 1998), which suggests the possibility that during differentiation, Yap acts with Gata6 to enhance transcription of endodermal associated targets. It would be interesting to examine transcriptional targets of Yap in mESCs differentiating towards PrE by methods such as ChIP-seq analysis.

Inhibition of Yap during PrE differentiation using small molecules

In this Chapter, the small molecules dobutamine and verteporfin were used in order to inhibit nuclear Yap (Figure 3.16 &Figure 3.17). Unfortunately, due to time limitations, only one concentration of each was used in these experiments. In the case of verteporfin, a concentration of 2.5μM resulted in cell death (Figure 3.16). The concentration of 2.5μM was chosen as this was shown to be the minimum concentration still able to provide >50% inhibition of Yap Tead interaction as measured by a Gal4-Tead reporter assay in HEK293 cells (Liu-Chittenden *et al.*, 2012). The resulting cell death in mESCs could suggest a role for Yap and Tead in cell survival, however it could also be a result of concentration dependent non-specific activity of verteporfin. Examining the effects of lower concentrations of verteporfin in mESCs would provide insight into this matter.

The other small molecule used to inhibit nuclear Yap was the β-adrenergic receptor agonist dobutamine Figure 3.17. Treatment with dobutamine reduced the increase in nuclear Yap expression upon induction of Gata6 (Figure 3.17B), which resulted in a decreased proportion of cells differentiating towards PrE (Figure 3.17C). This is in accordance with Yap being required for differentiation towards PrE. Interestingly, treatment with dobutamine for 6 hours resulted in an increase in Nanog expression, in both the nucleus and cytoplasm. It is a possibility that due to reduced nuclear Yap, Gata6 repression of Nanog is impaired, resulting in excess Nanog protein in the cell. However there is also the possibility that this observed affect on Nanog is due to unknown downstream mechanisms of the β-adrenergic receptor. Indeed, the exact mechanisms resulting in the increased phosphorylation of Yap downstream of dobutamine activation of the β-adrenergic receptor is unknown.

To examine if Yap is absolutely required for PrE differentiation, the effect of a knockout of Yap in the Gata6 inducible cells could be examined. If Yap is required for PrE differentiation, knockout of Yap would prevent PrE

differentiation upon induction of Gata6. Furthermore, this would rule out the possibility of off target effects as seen with the use of small molecules. Conversely, it would be interesting to see if increasing nuclear Yap results in increased efficiency of differentiation towards PrE.

Chapter 4: The role of Yap in mouse pre-implantation development

4.1 Background

During mouse pre-implantation development, two key cell fate decisions occur. The first takes place after compaction, around embryonic day 3 (E3.0) of development, where the trophectoderm (TE) and the inner cell mass (ICM) are specified. The TE is an extra-embryonic lineage, which will form the foetal portion of the placenta (reviewed in Schrode *et al.*, 2013). The Hippo signalling pathway has been shown to be important in specification of the TE (Nishioka *et al.*, 2008; 2009). Cells from the ICM exhibit increased Hippo signalling, leading to increased phosphorylation and subsequent cytoplasmic retention of Yap (Nishioka *et al.*, 2009). In contrast, the polarized outer cells exhibit decreased Hippo signalling, which results in increased nuclear Yap expression, leading to increased Tead4-dependent transcription of Cdx2, a TE specific transcription factor (Nishioka *et al.*, 2009).

The second cell fate choice occurs around E3.5, when cells of the ICM separate into two populations, primitive endoderm (PrE) and epiblast (Epi). The PrE will contribute to extra-embryonic membranes such as the parietal and visceral endoderm of the yolk sac and the Epi will give rise to the embryo proper (reviewed in Schrode *et al.*, 2013). Initially, all cells of the ICM co-express the transcriptional regulators Gata6 and Nanog, which are markers of PrE and Epi respectively. Around E4.0, as the embryo develops, expression of Gata6 and Nanog becomes mutually exclusive, forming a “salt and pepper” expression pattern. These cells then undergo sorting, where the Gata6-expressing PrE precursors migrate towards the surface of the ICM, in contact with the blastocoel of the blastocyst, where they will form the PrE. PrE precursor cells that do not reach the blastocoel will undergo apoptosis or downregulate PrE gene expression and contribute to the epiblast(Plusa *et al.*, 2008; Saiz *et al.*, 2013; Chazaud *et al.*, 2006). Positional cues are therefore important for the proper formation of the PrE. As positional cues direct Hippo signalling in the differentiation of the TE (Nishioka *et al.*, 2009), it is possible that Hippo signalling also has a role in the formation of the PrE. However, this possibility has currently not been explored.

4.2 Yap is expressed in the nuclei of primitive endoderm cells

To investigate the role of Yap in the differentiation of PrE and Epi, localization of Yap was examined by immunostaining embryos from E3.0 to E4.5 with a polyclonal Yap antibody (Santa Cruz 15407) (Figure 4.1 & Figure 4.2). Yap was found to be expressed in the nuclei of outer cells of morulae and in the TE of early blastocysts, as previously described (Figure 4.1)(Nishioka *et al.*, 2009). However, Yap was also clearly detected in the nuclei of inner cells in these embryos, albeit at a lower level. Recently Home *et al.* reported that Yap was consistently nuclear in both inner and outer cells, using an antibody from Cell Signalling (Home *et al.*, 2012). However, the signal observed using the Cell Signalling antibody was shown to be present in $Yap^{-/-}$ embryos, suggesting that it is a non-specific artefact of the antibody (Hirate *et al.*, 2012). In order to confirm that Yap expression was higher in the outer cells compared to inner cells, E3.0 and E3.5 embryos were analysed using a software tool called Modular Interactive Nuclear Segmentation (MINS). Using MINS, inner and outer cells were classified automatically based on distance from the centre of the embryo. These classifications were confirmed manually and mean nuclear Yap intensity was determined (Figure 4.1A). Mean nuclear Yap intensity was found to be significantly higher in outer cells compared to inner cells (Figure 4.1B). This confirms that the antibody used for experiments in this chapter (Santa Cruz 15407) yields similar results as those described by Nishioka *et al*.

In mid to late blastocysts, Yap was expressed in nuclei of TE cells and diffusely throughout cells of the ICM (Figure 4.2). In E4.5 embryos, when the Gata6-positive cells have segregated and formed the PrE, Yap was highly expressed in the nuclei of cells forming the PrE, with low expression in cells of the Epi (Figure 4.2, bottom row). In summary, this data shows that Yap is expressed in the nuclei of cells that form the TE and in cells of the PrE following segregation. These observations are in agreement with a previous study of Yap in mouse pre-implantation embryos (Frankenberg *et al.*, 2013). Altogether this suggests that Yap may be involved in the lineage commitment of PrE

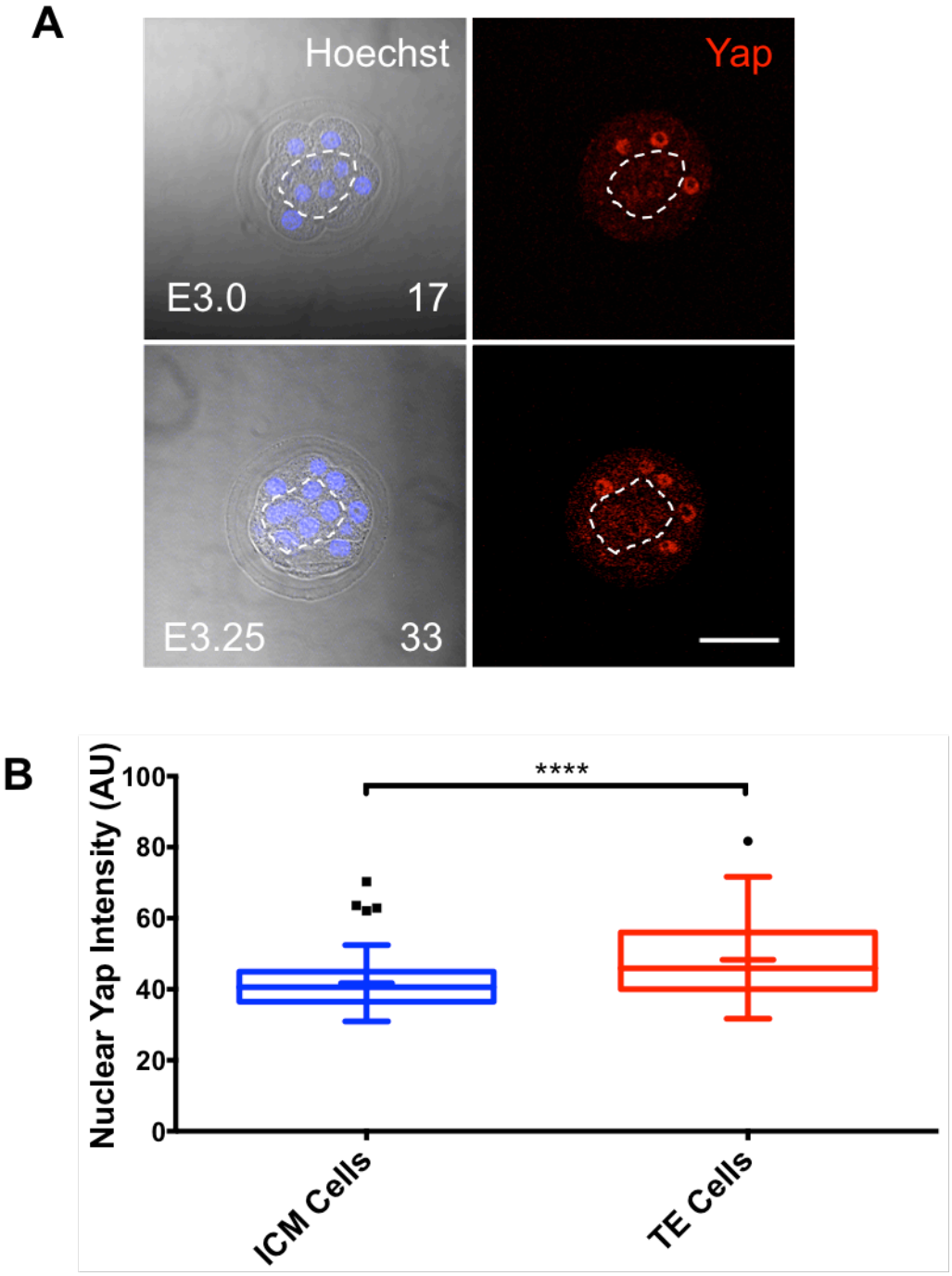

Figure 4.1. Nuclear Yap is more highly expressed in outer cells compared to inner cells, (**A**) Representative confocal section of mouse pre-implantation embryos at E3.0 and E3.25 immunostained for Yap (red). Total cell number is displayed for each embryo shown. Dashed white lines indicate inner cells. Scale bar: 50μm. (**B**) Box and whiskers plot displaying nuclear Yap intensity, Solid line indicates median values, while cross indicates mean value. ****=P<0.0001 by Students unpaired t-test. n= 394 cells from 9 embryos.

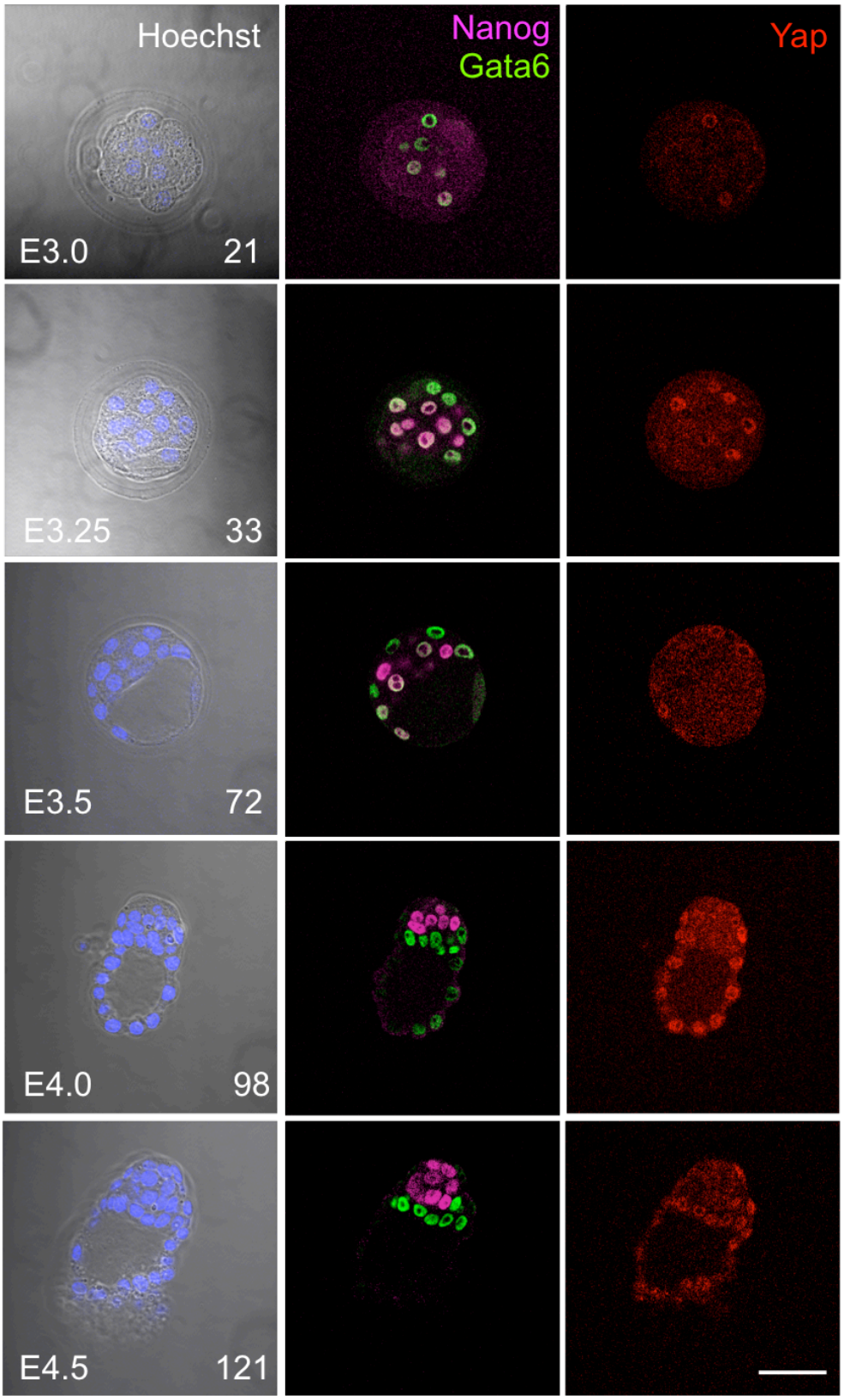

Figure 4.2. Yap is expressed in the nuclei of PrE cells at E4.5, Representative confocal sections of mouse embryos at successive stages of pre-implantation development, immunostained for Nanog (magenta), Gata6 (green) and Yap (red). Embryonic Day (E) with total cell number for each embryo is shown. Scale bar: 50μm.

4.3 Nuclear Yap expression in PrE Precursors

The expression of Yap in the nuclei of PrE cells of E4.5 embryos may indicate a potential role for Yap in PrE specification. To determine if Yap is involved in specification of PrE, cells of the ICM of E3.5-E4.5 embryos were examined in more detail, using quantitative image analysis. Mouse embryos were collected at E3.5 and E4.5 and immunostained for Yap, Gata6 and Nanog. The total cell number and the expression of Gata6 and Nanog were used to classify embryos into the developmental time points E3.5 (32-60 cells), E4.0 (60-120 cells) and E4.5 (>120 cells) (Figure 4.3).

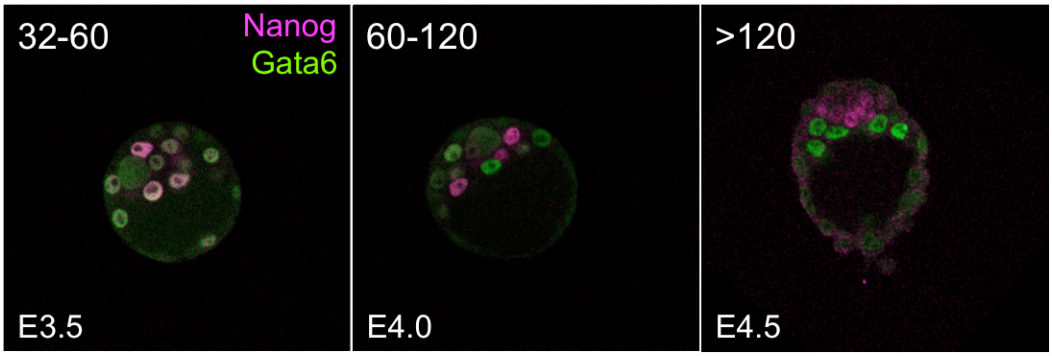

Figure 4.3. Classification of embryos into developmental time points based on total cell number, Representative confocal sections of mouse pre-implantation embryos at E3.5, E4.0, E4.5 immunostained for Gata6 (green) and Nanog (magenta). The images illustrate the initial co-expression (left panel), then salt and pepper pattern (middle panel) and eventual sorting of Gata6 and Nanog expression into separate populations (right panel). These developmental time points were classified by total cell number by the ranges indicated in the main text.

Fluorescence intensities were measured by quantitative immunofluorescence following segmentation of cell nuclei with MINS. In order to classify cells as positive or negative for Gata6 or Nanog, threshold intensities were defined. Threshold intensity values were defined using mixture analysis applied to intensity values from E4.5 embryos, as at this stage cells are in clear populations expressing either Gata6 or Nanog (see Materials and Methods). Intensities of Gata6 or Nanog above the threshold value were considered positive, and levels below threshold considered negative, therefore four populations of cells at each embryonic stage could be defined: *Gata6-Nanog-*, *Gata6+Nanog+, Gata6+Nanog- and Gata6-Nanog+*. The nuclear Gata6

intensity of individual cells of the ICM was then plotted against its nuclear Nanog intensity so as to provide a graphical representation of the population of cells at each embryonic stage (Figure 4.4, Figure 4.5 and Figure 4.6).

In E3.5 embryos Gata6 and Nanog are co-expressed (Figure 4.4A,B). Although Yap was occasionally expressed in the nuclei of cells in the ICM, no significant difference in mean nuclear Yap intensity was found between populations (Figure 4.4A,C). In E4.0 embryos, Gata6 and Nanog are expressed in a “salt and pepper” manner in the ICM (Figure 4.5A,B). Mean nuclear Yap intensity was found to be higher in *Gata6+Nanog+* cells compared to *Gata6-Nanog+* cells (Figure 4.5C). In E4.5 embryos, Gata6 and Nanog are expressed in the PrE and Epi respectively. Yap was expressed in the nuclei of cells that formed the PrE (Figure 4.6A,B) and mean nuclear Yap was significantly increased in *Gata6+Nanog-* cells of the PrE as compared to *Gata6-Nanog+* cells of the Epi (Figure 4.6C).

In summary, quantitative analysis of nuclear Yap intensity across the developmental time points examined appears to show that when cells begin to specify fate *i.e.* when cells begin to express either Gata6 or Nanog, nuclear Yap intensity is higher in cells expressing Gata6. This suggests that Yap may be involved in initial specification of PrE precursors as well as lineage commitment.

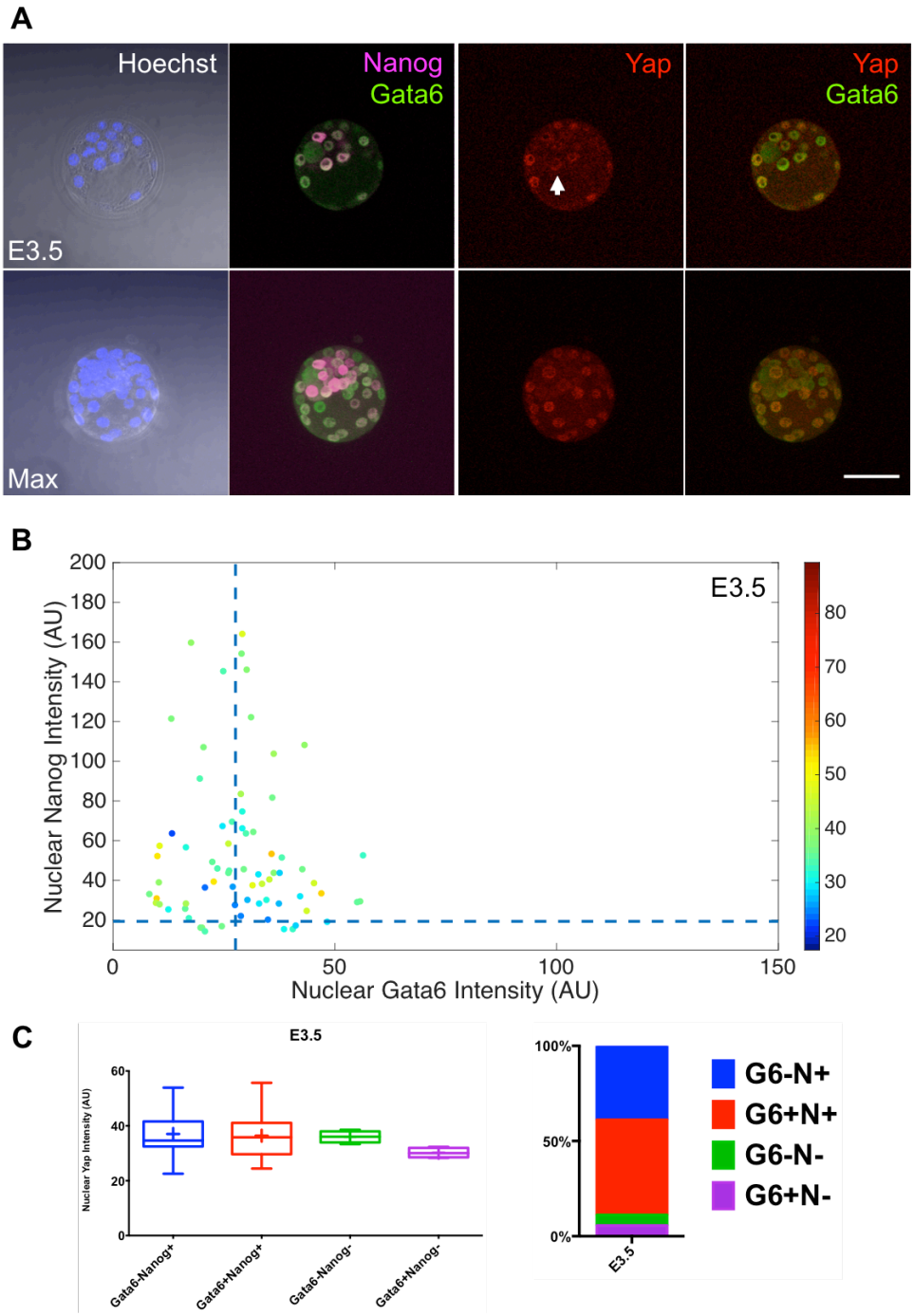

Figure 4.4. Quantification of Yap expression in E3.5 embryos, (**A**) Representative confocal section (upper row) and maximum projection (lower row) of mouse pre-implantation embryos at E3.5 immunostained for Nanog (magenta), Gata6 (green) and Yap (red). Arrow indicated ICM cell expressing nuclear Yap. Scale bar: 50µm. (**B**) Scatter plots showing Gata6 (x-axis), Nanog (y-axis) and Yap (heat map, side bar) nuclear intensity in fluorescence arbitrary units (AU). Each dot represents the levels in a single cell. Dashed lines represent threshold limits for Gata6 and Nanog (**C**) Box and whisker plots displaying intensity levels of Yap in defined populations. Solid line indicates median values, while cross indicates mean value. Bar chart to the right indicates proportion of cells in each population. 72 cells were analysed from 4 embryos.

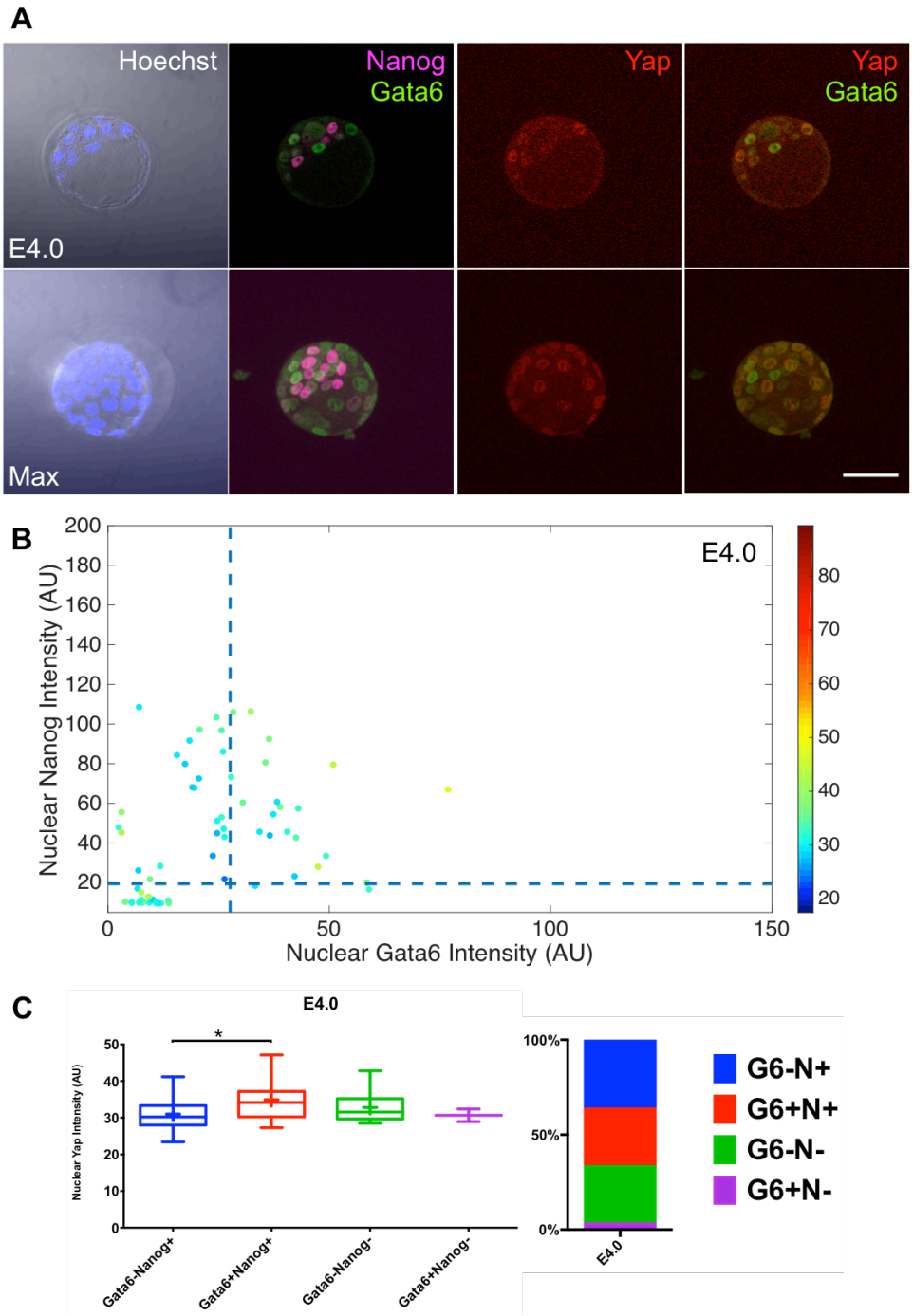

Figure 4.5. Quantification of Yap expression in E4.0 embryos, (**A**) Representative confocal section (upper row) and maximum projection (lower row) of mouse pre-implantation embryos at E4.0 immunostained for Nanog (magenta), Gata6 (green) and Yap (red). Scale bar: 50μm. (**B**) Scatter plots showing Gata6 (x-axis), Nanog (y-axis) and Yap (heat map, side bar) nuclear intensity in fluorescence arbitrary units (AU). Each dot represents the levels in a single cell. Dashed lines represent threshold limits for Gata6 and Nanog (**C**) Box and whisker plots displaying intensity levels of Yap in defined populations. Solid line indicates median values, while cross indicates mean value. Bar chart to the right indicates proportion of cells in each population. *=P<0.05 by one-way ANOVA with Tukey's post-hoc test. n=66 cells from 3 embryos.

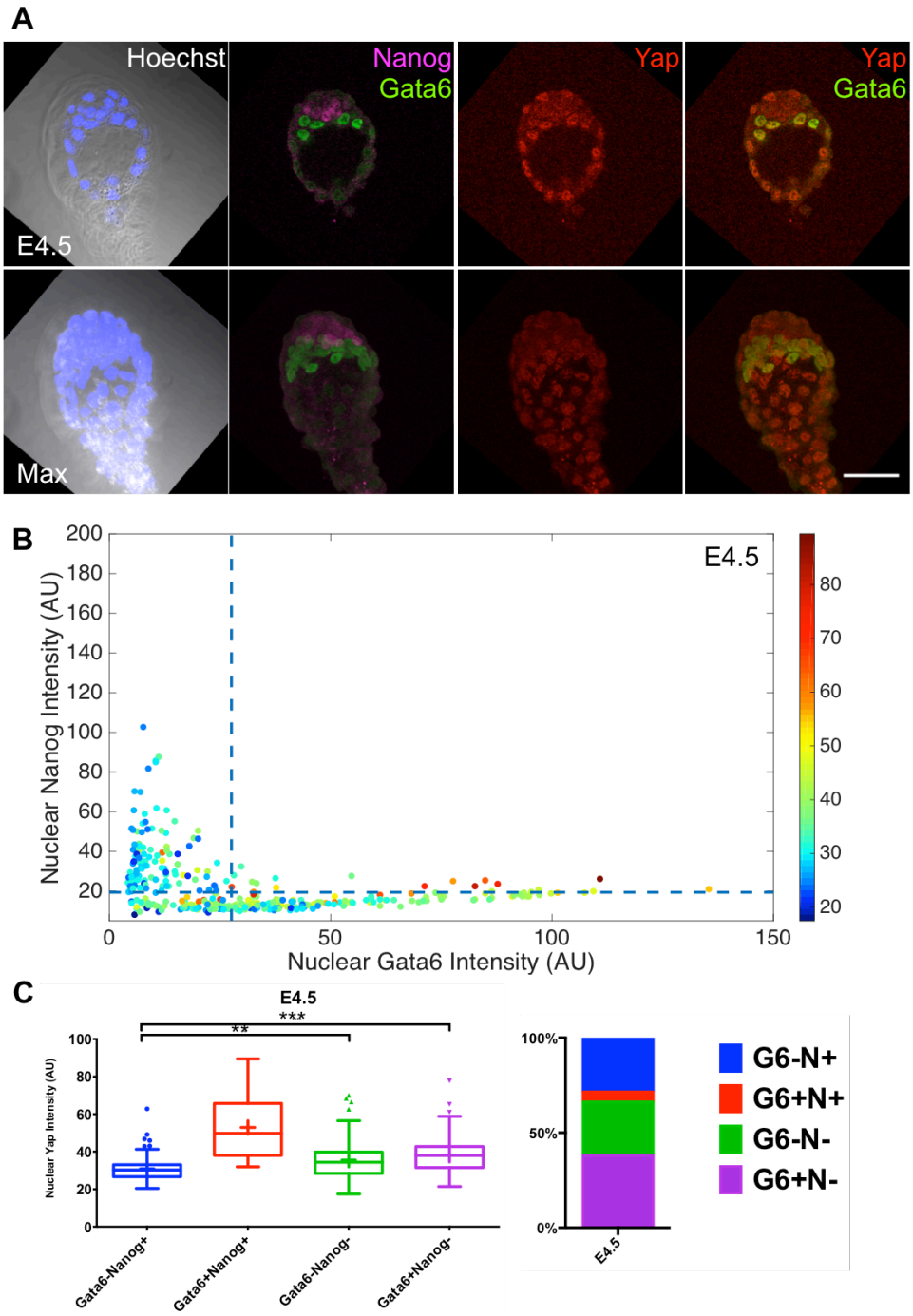

Figure 4.6. Quantification of Yap expression in E4.5 embryos, (**A**) Representative confocal section (upper row) and maximum projection (lower row) of mouse pre-implantation embryos at E4.5 immunostained for Nanog (magenta), Gata6 (green) and Yap (red). Scale bar: 50μm. (**B**) Scatter plots showing Gata6 (x-axis), Nanog (y-axis) and Yap (heat map, side bar) nuclear intensity in fluorescence arbitrary units (AU). Each dot represents the levels in a single cell. Dashed lines represent threshold limits for Gata6 and Nanog (**C**) Box and whisker plots displaying intensity levels of Yap in defined populations. Solid line indicates median values, while cross indicates mean value. Bar chart to the right indicates proportion of cells in each population. **=P<0.001, ***=P<0.0001 by one-way ANOVA with Tukey's post-hoc test. n=340 cells from 6 embryos.

4.4 pYap expression does not decrease in PrE

Yap can be regulated by the Hippo signalling pathway through phosphorylation at S112. Phosphorylation of Yap at S112 leads to the creation of a 14-3-3 binding site allowing Yap to bind to 14-3-3 proteins (Basu *et al.*, 2003). 14-3-3 proteins retain Yap in the cytoplasm thus rendering Yap unable to act as a transcriptional co-activator (Zhao *et al.*, 2007). In order to examine if increased nuclear Yap in cells expressing higher levels of Gata6 is due to decreased Hippo signalling activity resulting in rescued cytoplasmic retention of Yap, E3.5 and E4.5 embryos were immunostained with an antibody directed against pYap-S127 (Figure 4.7A) (Human Yap S127 is analogous to mouse Yap S112, hereafter referred to as pYap). Visually in E3.5 embryos, pYap expression was higher in the cytoplasm of cells of the ICM compared to outer cells that form the TE. In E4.5 embryos, pYap expression was also higher in the cytoplasm of cells of the ICM compared to cells of the TE. There was no visible decrease in cytoplasmic pYap expression in Gata6-expressing cells that form the PrE in E4.5 embryos. To quantify the immunostaining, fluorescence intensity profiles were created using Gata6 as a marker of PrE (Figure 4.7B). Intensity profiles revealed that expression of pYap is not significantly different between cells of the PrE and the Epi (Figure 4.7C). This suggests that the increase of nuclear Yap observed in cells expressing higher levels of Gata6 is not due to decreased cytoplasmic retention of Yap. pYap staining was visible in nuclei of cells expressing Gata6. However, this could potentially be the result of antibody cross reactivity, as pYap is generally expected to be excluded from the nucleus, and Nishioka *et al.* did not observe nuclear staining of pYap in E3.0 mouse embryos (Nishioka *et al.*, 2009).

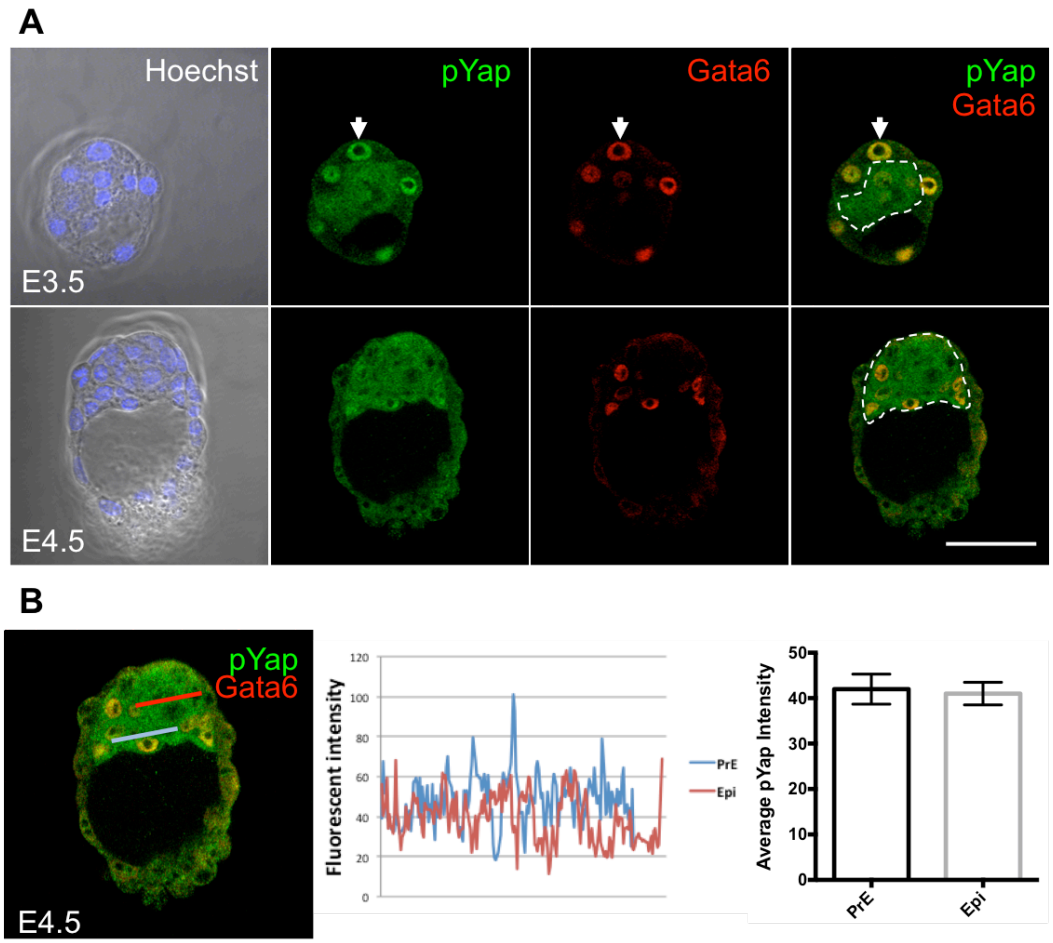

Figure 4.7. Expression of pYAP in E3.5 and E4.5d embryos. (**A**) Representative confocal sections of mouse pre-implantaion embryos at E3.5 and E4.5 immunostained for pYap (green) and Gata6 (red). Dashed white lines indicate inner cell mass. Arrows indicate example of nuclear pYap. Scale bar: 50μm. (**B**) Quantification of cytoplasmic pYap in E4.5. Fluorescence intensity profiles along the lines drawn either through PrE or Epi. (**C**) Bar chart comparing average intensity from n=3 measurements from one embryo. Bar chart displays mean ± standard error of the mean.

4.5 Culture of mouse pre-implantation embryos with inhibitors of Yap leads to a decrease in Gata6 expression

To test if Yap is important in the specification of PrE, embryos were cultured with inhibitors of Yap during the time period in which this process occurs. E3.5 embryos can be cultured *in vitro*, during which time patterning of the embryo will still occur (Dietrich & Hiiragi, 2007). In order to inhibit Yap, dobutamine, a β-adrenergic agonist that has been shown to induce phosphorylation and cytoplasmic retention of Yap (Bao *et al.*, 2011), and verteporfin, a small molecule that inhibits Tead-Yap binding (Liu-Chittenden *et al.*, 2012) were used. Dobutamine was used at a

concentration of 10μM as this was found to reduce nuclear Yap expression in mESCs in the previous Chapter. Verteporfin was used at 2.5μM as this concentration has been reported to reduce expression of Cdx2 in early mouse embryos (Rayon *et al.*, 2014). E3.5 embryos were cultured in the absence or presence of dobutamine or verteporfin for 24 hours (Figure 4.8). Control embryos cultured in KSOM for 24 hours had expanded and formed blastocoels. In comparison, embryos cultured with dobutamine had not expanded as much as the control embryos. Culturing embryos with verteporfin lead to widespread cell death, precluding further analysis.

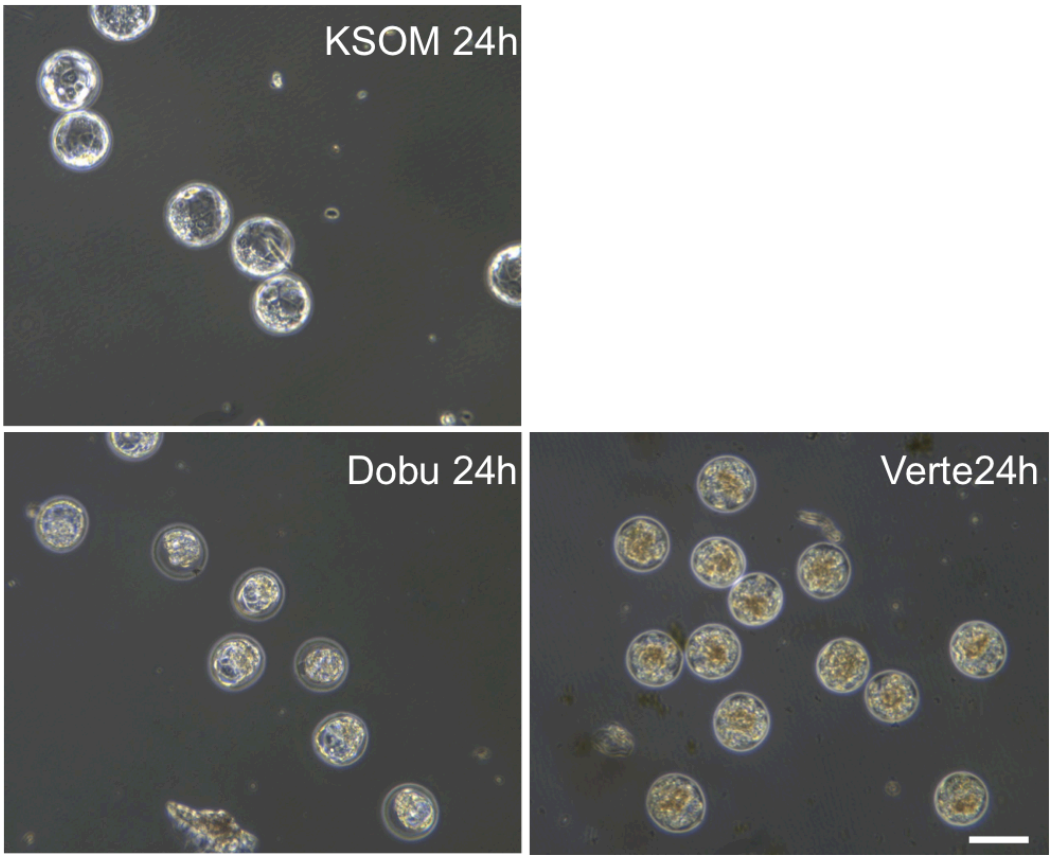

Figure 4.8. Culture of E3.5 embryos with inhibitors of Yap, Bright field images of E3.5 embryos following 24h culture in KSOM, Dobutamine 10μM (Dobu) or Verteporfin 2.5 μM (Verte). Scale bar: 100μm.

To examine the effect of dobutamine on specification of PrE and Epi lineages, the proportion of ICM cells expressing Gata6 or Nanog was determined. Control and dobutamine treated embryos were fixed and immunostained for Yap, Gata6 and Nanog (Figure 4.9A). Embryos were analysed using MINS in order to determine expression levels in individual

cells. Dobutamine treatment of embryos appeared to reduce nuclear Yap intensity with fewer cells displaying high Yap levels (Figure 4.9A,B,C) Although this difference was not statistically significant, it suggests that Dobutamine treatment results in cytoplasmic retention of Yap (Figure 4.9C). The nuclear Gata6 intensity of individual cells of the ICM was plotted against its nuclear Nanog intensity so as to provide a graphical representation of the population of cells (Figure 4.9B). To classify cells as positive or negative for Gata6 or Nanog, threshold intensities were defined, using mixture analysis on intensity values from control embryos. Treatment with dobutamine appeared to reduce the proportion of cells that are positive for expression of both Gata6 and Nanog (Figure 4.9B). Indeed the mean nuclear intensity of Gata6 and Nanog for cells in the ICM was found to be significantly lower in dobutamine treated embryos, compared to control embryos (Figure 4.9D and E respectively).

To assess if treatment of embryos with dobutamine was affecting growth and survival of cells, the number of cells in the blastocyst compartments was determined. No significant difference was found between the number of cells comprising the ICM in control and dobutamine-treated embryos. This result suggests that treatment with dobutamine does not affect growth of the ICM. However, a significant decrease was observed in the number of TE cells in dobutamine-treated embryos compared to control embryos. This suggests that dobutamine may inhibit growth of the TE.

In summary, these results suggest that treatment of embryos with dobutamine results in decreased expression of both Gata6 and Nanog in the cells of the ICM. Growth of the ICM is not affected by dobutamine treatment. However a reduction in TE cell number is observed. The effects of dobutamine treatment may be due to a reduction in nuclear Yap expression.

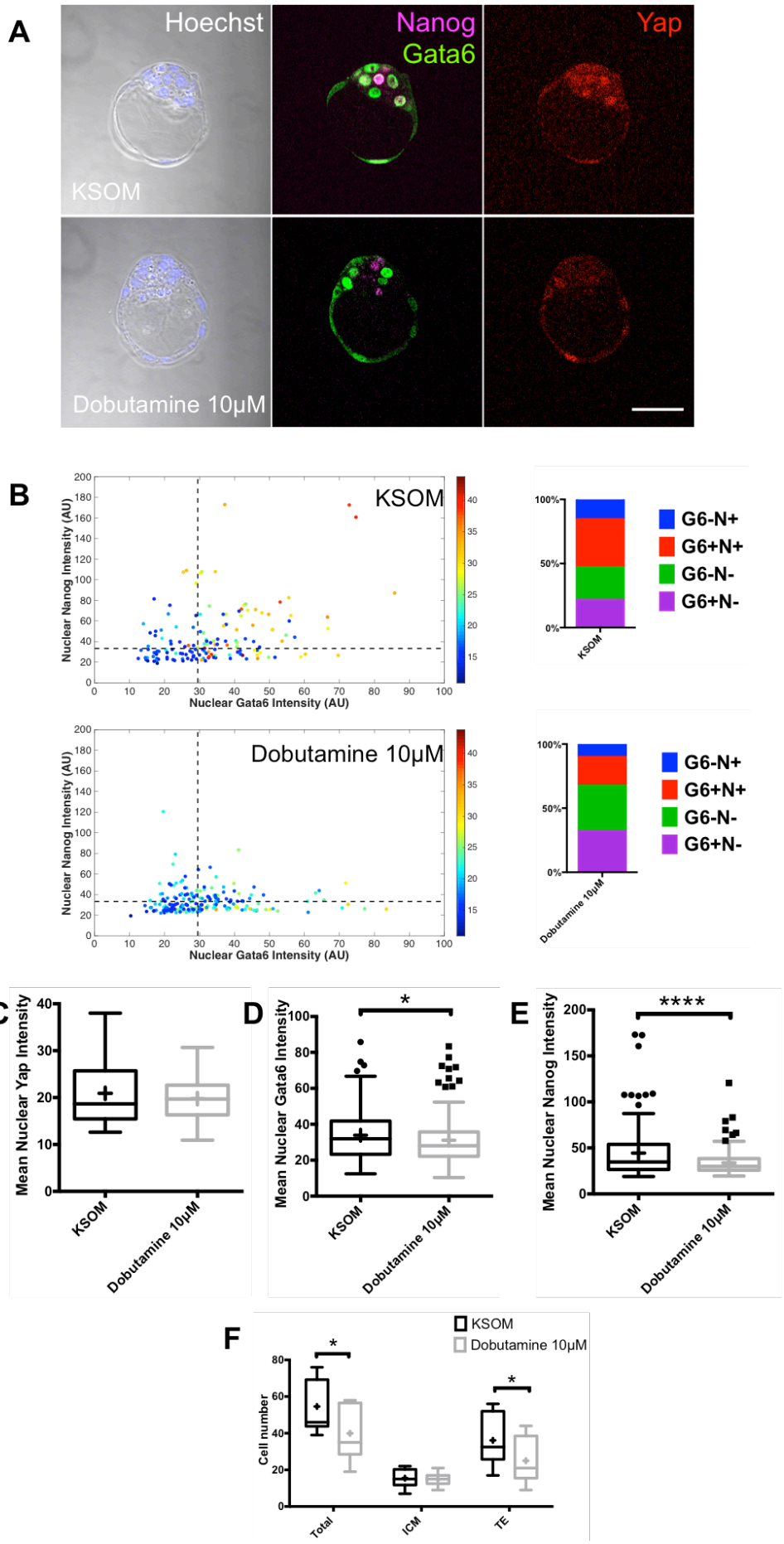
A
Hoechst
Nanog
Gata6
Yap
KSOM
Dobutamine 10μM
B
KSOM
Dobutamine 10μM
Nuclear Nanog Intensity (AU)
Nuclear Gata6 Intensity (AU)
G6-N+
G6+N+
G6-N-
G6+N-
C
Mean Nuclear Yap Intensity
D
Mean Nuclear Gata6 Intensity
E
Mean Nuclear Nanog Intensity
F
Cell number
Total
ICM
TE

Figure 4.9: Dobutamine treatment of E3.5 embryos leads to decreased expression of Gata6 and Nanog and a reduction in TE cell number, (**A**) Representative confocal sections of embryos cultured for 24 hours in either KSOM or KSOM+Dobutamine 10μM, Scale bar: 50μm (**B**) Scatter plots showing Gata6 (x-axis), Nanog (y-axis) and Yap (heat map, side bar) nuclear intensity in fluorescence arbitrary units (AU) in KSOM (upper graph) or dobutamine treated embryos (lower graph). Each dot represents the levels in a single cell. Dashed lines represent threshold limits for Gata6 and Nanog with bar charts indicating proportion of cells in each population. (**C,D,E**) Box and whisker plots displaying intensity levels of Yap(**C**), Gata6(**D**) and Nanog(**E**) in KSOM and Dobutamine treated embryos respectively. Solid line indicates median values, while cross indicates mean value. *=P<0.05, ****=P<0.0001 by Students unpaired t-test. n=155 cells from 10 KSOM treated embryos and 194 cells from 10 Dobutamine treated embryos. (**F**) Box and whisker plot displaying cell counts of ICM and TE lineages upon treatment with dobutamine. *=P<0.05, Students unpaired t-test. 10 embryos were analysed per culture condition.

4.6 Summary

In this Chapter, mouse pre-implantation embryos from E3.5 to E4.5 were immunostained in order to examine expression of Yap in the cell fate decision between PrE and Epi. Nuclear Yap intensity was found to be higher in *Gata6+Nanog-* cells of the PrE compared to *Gata6-Nanog+* cells of the Epi. Although nuclear Yap intensity was increased, this did not appear to be due to decreased Hippo-dependent phosphorylation of YapS127. Treatment of embryos with dobutamine resulted in decreased expression of Gata6 and Nanog, and a reduction in TE cell number.

4.7 Discussion

Yap in specification of PrE

During amniotic development, formation of the primitive endoderm is an important event in order to generate extra-embryonic tissues (as reviewed in Schrode *et al.*, 2013). Separation of pluripotent epiblast cells and PrE precursors occurs through active cell sorting, with PrE precursors moving towards the blastocoel. Cells that remain misplaced undergo selective apoptosis, which suggests the possibility of a mechanism in which cells can sense their position in order to ensure the correct placement of PrE and Epi cells.

The results in this Chapter show that Yap is expressed in nuclei of cells of the PrE at E4.5 (Figure 4.2). This observation may suggest that, following

sorting of cells, polarization of PrE cells located adjacent to the blastocoel leads to inhibition of Hippo signalling, thus allowing un-phosphorylated Yap to translocate to the nucleus. Indeed it has been shown that at E4.5, atypical protein kinase C (aPKC), a protein involved in apicobasal polarity, is polarised apically on the surface of PrE cells (Saiz *et al.*, 2013). aPKC has been shown to inhibit Hippo signalling in TE specification, allowing Yap to translocate to the nucleus in outer, polarised cells of the embryo (Hirate *et al.*, 2013). Therefore nuclear localization of Yap in the PrE of E4.5 embryos may be downstream of polarization. Disruption of this polarization using inhibitors of aPKC results in apoptosis of PrE cells, despite the correct localization, suggesting that cells are unable to perceive positional information (Saiz *et al.*, 2013). It is tempting to speculate that Yap is therefore involved in the protection of correctly positioned PrE cells from apoptosis, such that misplaced cells expressing PrE markers do not polarize and subsequently do not inactivate Hippo signalling.

Although Yap was found predominantly nuclear in the PrE at E4.5, nuclear Yap was also seen in cells of the ICM at earlier stages, with higher nuclear Yap in cells expressing higher levels of Gata6 (Figure 4.5). This could indicate that Yap also has a function in the initial specification of PrE cells. Following co-expression in the ICM of E3.5 embryos, cells down-regulate expression of either Gata6 or Nanog leading to a “salt and pepper’ expression pattern of lineage markers (Chazaud *et al.*, 2006; Plusa *et al.*, 2008). FGF signalling has been shown to be instrumental in this specification through up-regulation of Gata6 and down-regulation of Nanog (Chazaud *et al.*, 2006; Kang *et al.*, 2012; Yamanaka, Lanner & Rossant, 2010; Nichols *et al.*, 2009; Bessonnard *et al.*, 2014). Ras, a small GTPase downstream of FGF receptor, has been shown to promote Yap stability through down-regulation of the ubiquitin ligase complex substrate recognition factors SOCS5/6 (Hong *et al.*, 2014). This raises the possibility that, in cells of the ICM, FGF signalling enhances the stability of Yap, thus leading to increased levels of Yap in the cell. Increased levels of Yap could subsequently overcome Hippo-dependent

phosphorylation and cytoplasmic retention, therefore entering the nucleus and exerting a transcriptional effect.

siRNA knockdown of TEAD4 in cells of the ICM has been shown to lead to a bias towards Epi cell fate choice (Mihajlović, Thamodaran & Bruce, 2015). This is in accordance with the findings described here, in that increased nuclear Yap is associated with PrE, thus loss of the transcription factor with which Yap binds prevents PrE specification. Tead4 has been shown, via CHIP-Seq, to bind to the proximal promoter regions of *Fgfr2*, *Dab2* and *Lrp2* in trophoblast stem cells (Home *et al.*, 2012). In accordance with this result, clonal knockdown of TEAD4 in cells of the ICM was shown to result in reduced expression of Fgfr2 (Mihajlović, Thamodaran & Bruce, 2015). Yap may therefore have a role in reinforcing PrE cell fate specification in a positive feedback mechanism, in which activation of Fgfr2 results in increased stability of Yap, which in turn leads to increased expression of Fgfr2.

Derivatives of the PrE will form the yolk sac of the embryo, and are also important for induction of signals in the adjacent embryonic tissue, particularly in the establishment of the anterior-posterior axis (Thomas & Beddington, 1996; Varlet, Collignon & Robertson, 1997). Interestingly, mice carrying a targeted disruption of the Yap gene undergo developmental arrest at E8.5, revealing defects in yolk sac vasculogenesis, and a shortened body axis. These observations can be explained by an earlier requirement for Yap during formation of the PrE, which is supported by the data presented here. It would be interesting to see if specification of the PrE in $Yap^{-/-}$ embryos is disrupted.

Hippo regulation of Yap during specification of PrE

Despite increased nuclear Yap expression in cells of the PrE compared to Epi in E4.5 embryos, no difference was observed in cytoplasmic pYap (Figure 4.7C). Phosphorylation of YapS112 results in binding to 14-3-3 proteins and cytoplasmic retention (Zhao *et al.*, 2007). This may suggest that the increased nuclear Yap is not a result of decreased Hippo dependent cytoplasmic retention. Yap can also be regulated by

phosphorylation at S381, which results in subsequent ubiquitination and degradation of Yap (Zhao *et al.*, 2010). The increased nuclear Yap expression in PrE may therefore be due to increased stability of Yap allowing Yap to overcome Hippo dependent cytoplasmic retention.

Disruption of upstream Hippo signalling components also leads to defects in formation of the PrE. Loss of the Hippo pathway member neurofibromain 2 (Nf2, orthologue of *Drosophila* Merlin), leads to loss of PrE formation (McClatchey *et al.*, 1997). As Hippo pathway members are negative regulators of Yap, this would suggest that increased nuclear Yap is not involved with PrE formation. However, subsequent studies into loss of Hippo pathway members Nf2 or Lats show that cells of the ICM mis-express the TE marker Cdx2 (Hirate *et al.*, 2013; Cockburn *et al.*, 2013; Lorthongpanich *et al.*, 2013). Aberrant expression of Cdx2, along with Gata6 and Nanog in the ICM may result in incompatible developmental programs, or inhibition of the proper specification of PrE and Epi lineages. Consequently, the loss of PrE following ablation of upstream Hippo pathway members may be due to ectopic expression of Cdx2 in the ICM. Therefore it is important to allow correct specification of TE and ICM before studying the effects of loss of Yap or Hippo pathway members on PrE specification.

Inhibition of Yap during specification of PrE

In this chapter, two small molecules, dobutamine and verteporfin, were used in an attempt to inhibit the nuclear effect of Yap during specification of PrE. Treatment with Verteporfin resulted in embryonic cell death, which could suggest an important role for Yap-Tead binding in cell growth and survival during pre-implantation development. However, the observed cell death could also be the result of non-specific effects of verteporfin. Verteporfin has been used previously to inhibit Yap-Tead interactions during specification of TE in mouse embryos, resulting in a reduction of Cdx2 expression (Rayon *et al.*, 2014). The same concentration of verteporfin used by Rayon *et al.* was used in the experiments in this

chapter. It would be interesting to see if lower concentrations of verteporfin were still cytotoxic.

Treatment with dobutamine resulted in a reduction in expression of Gata6 and Nanog in cells of the ICM. Dobutamine is a β-adrenergic receptor agonist, which has been shown to induce phosphorylation and subsequent cytoplasmic retention of Yap, although the exact mechanism of action is unknown (Bao *et al.*, 2011). The results in this chapter may therefore suggest that nuclear Yap expression is required for correct segregation of PrE and Epi lineages. However, this experiment did not determine whether treatment with dobutamine prevents correct cell fate specification, only that expression of Gata6 and Nanog are reduced. In order to examine if dobutamine prevents cell fate specification, later markers of PrE could be used for example Sox7, which is expressed only following sorting of PrE precursor cells (Artus, Piliszek & Hadjantonakis, 2011).

ICM cell number was not affected by dobutamine treatment, however a decrease in TE cell number was observed. As Yap is required for specification of TE and is shown here to be expressed in the nuclei of TE cells throughout pre-implantation development (Figure 4.2), this may suggest that nuclear Yap is required for growth of TE cells.

Although a decrease in nuclear Yap intensity was observed following treatment of embryos with dobutamine for 24 hours, this decrease was not found to be statistically significant. It is possible that the effects of dobutamine were transient, and that fixation after 24 hours had missed the maximum reduction in nuclear Yap. To determine if this is the case, a time course analysis of the effects of dobutamine on Yap would be required.

Chapter 5: Creation of an inducible knockout of Yap in mouse embryonic stem cells

5.1 Background

Yap is believed to have a critical role in the maintenance of self-renewal and pluripotency in mouse embryonic stem cells (mESCs) (Tamm, Bower & Anneren, 2011; Lian *et al.*, 2010). Tamm *et al.* report that Yap increases the activity of Oct4 and Nanog promoters downstream of LIF, whereas Lian *et al.* report that ectopic expression of Yap induces expression of Oct4 and Sox2 (Tamm, Bower & Anneren, 2011; Lian *et al.*, 2010). However, the results obtained in the previous chapters show a requirement for increased nuclear Yap upon differentiation towards primitive endoderm (PrE) implying that the absence of Yap in mouse embryonic stem cells (mESCs) would favour stable pluripotency. Therefore, ablation of Yap in mESCs would provide a model system in which to assess the importance of Yap in maintenance of self-renewal and pluripotency in mESCs.

Ablation of a gene and observing the effects is one of the most direct methods to study the function of a gene. Embryonic stem cells can be genetically modified through homologous recombination (Thomas & Capecchi, 1987). This method involves the introduction of genomic DNA into a cell, whereby it can recombine into its corresponding genomic locus. Addition of a selectable marker, for example resistance to an antibiotic, allows for positive selection of cells in which recombination has occurred. Targeting of the selectable marker into an essential part of the gene of interest leads to creation of a null allele, i.e. an allele that cannot produce a functional protein (Figure 5.1). In order to generate a homozygous mutant, both alleles need to be targeted.

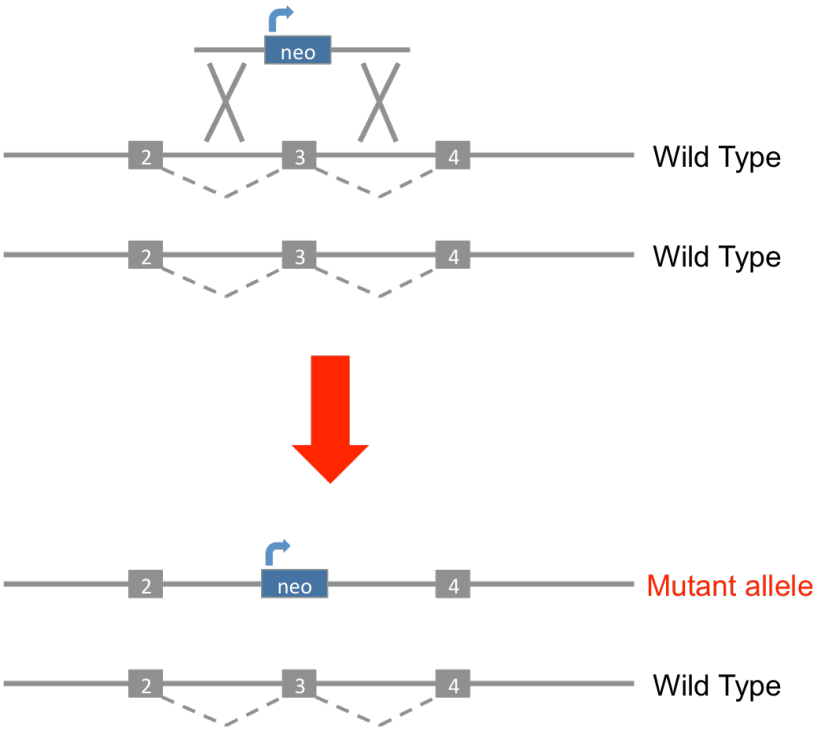

Figure 5.1. Genome editing via homologous recombination. Schematic illustrating homologous recombination. The homology arms on the targeting vector recombine with the endogenous locus resulting in insertion of a neomycin (neo) selectable marker. Dashed lines represent mRNA transcription.

Bi-allelic mutations can be generated in a variety of ways. A common method is to target each allele sequentially, using targeting vectors with different selectable markers, thus allowing selection of cells that carry a mutation in both alleles (Riele *et al.*, 1990). An alternative method relies on loss of heterozygosity, whereby following targeting of one allele, cells spontaneously duplicate the selectable marker, thus losing the remaining wild-type allele (Mortensen *et al.*, 1992). These cells therefore express double the amount of selectable marker and can be selected using increasing concentrations of the appropriate antibiotic (Mortensen *et al.*, 1992; Lefebvre *et al.*, 2001). However, these methods will lead to constitutive mutations, and are therefore incompatible with genes essential for cell growth, viability or pluripotency, as induction of the mutation will lead to death or differentiation of the mESCs. As Yap has been reported to be associated with cell proliferation (Zhao *et al.*, 2007; 2008) and in mESC self renewal (Lian *et al.*, 2010; Tamm, Bower & Anneren, 2011), derivation of targeted mutant Yap cells using these strategies could be ineffective .

To circumvent the problem associated with direct mutation leading to cell death or differentiation, conditional mutagenesis using site-specific recombinases can be used (Gu, Zou & Rajewsky, 1993). The bacteriophage P1 Cre protein can catalyze recombination between loxP sites in mammalian cells (Sauer & Henderson, 1988). LoxP sites can be introduced on either side of an exon, and subsequent expression of Cre will lead to recombination and removal of the exon (Figure 5.2). This allows for derivation of cells that contain the conditional mutation in both alleles, such that only experimental expression of Cre will lead to a knockout.

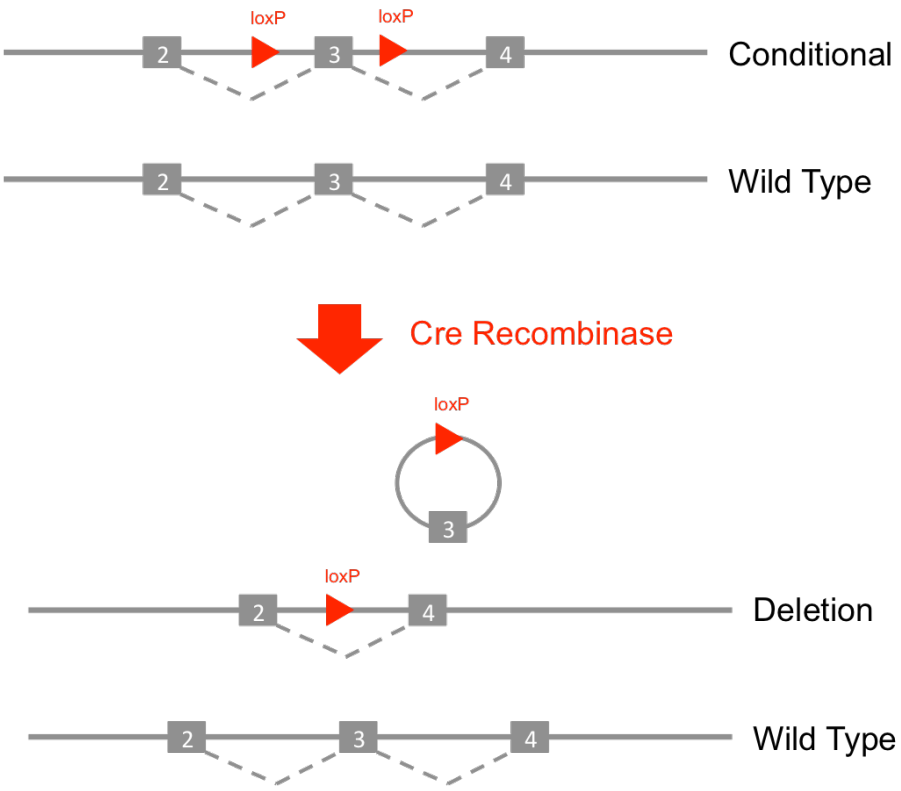

Figure 5.2. Excision of an exon via Cre-mediated recombination. Schematic illustrating Cre mediated recombination. In this example loxP sites (red triangles) flank exon 3. Expression of Cre recombinase results in site-specific recombination between loxP sites, leading to excision of exon3.

Large-scale gene knockout consortia have been established, including the European Conditional Mouse Mutagenesis Program (EUCOMM) and the KnockOut Mouse Project (KOMP), with the aim of generating a comprehensive and public resource of heterozygous reporter tagged mESCs for each gene in the mouse genome (Ringwald *et al.*, 2010). The

majority of these are generated using the "knockout-first" targeting strategy (Testa *et al.*, 2004). In this strategy, a targeting vector introduces loxP sites either side of a critical exon, together with a selection cassette, which contains neomycin resistance and a β-galactosidase reporter gene. FRT sites either side of the selection cassette allow for its removal by expression of the recombinase, Flipase (Flp). Removal of the selection cassette will result in the formation of a conditional allele (Figure 5.3). A splice acceptor in the selection cassette, and a subsequent polyadenylation signal terminates the endogenous mRNA transcript such that the gene is not transcribed downstream of the cassette site, creating a knockout allele (Testa *et al.*, 2004).

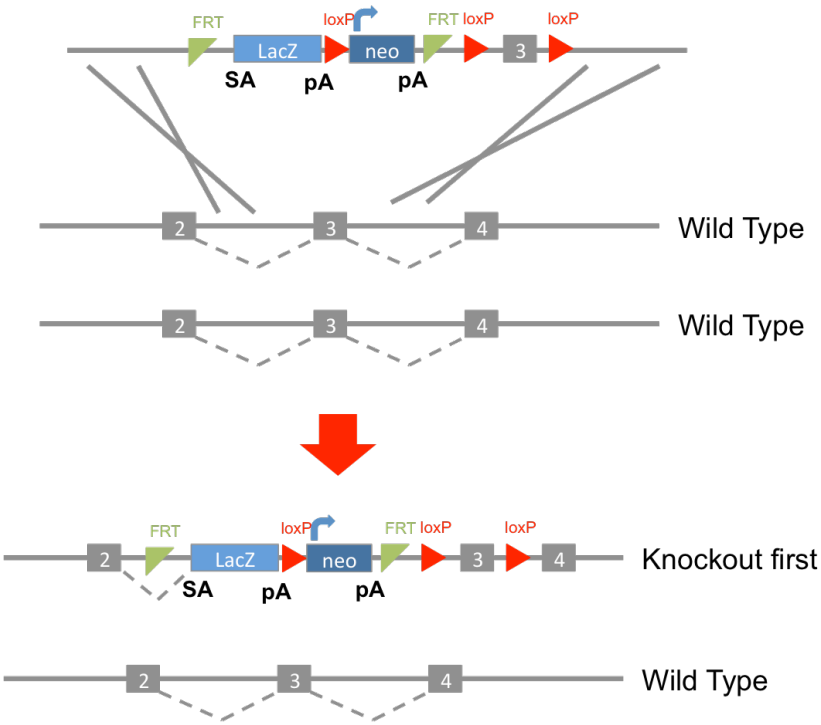

Figure 5.3. 'Knockout-first' targeting approach. Schematic illustrating knockout-first targeting. The targeting vector inserts a LacZ reporter and neomycin selectable marker flanked by FRT sites (green triangles), whilst also introducing loxP sites either side of a critical exon. SA=splice acceptor, pA=polyadenylation sequence.

Tate *et al.* have described a serial targeting strategy for the generation of homozygous conditional mutations, which takes advantage of the readily available EUCOMM/KOMP targeting vectors and targeted mESC clones (Figure 5.4) (Tate & Skarnes, 2011). The first step in this strategy consists of transiently exposing the heterozygous "knockout-first" clones

to Flp recombinase to generate a conditional allele. In the second step, the remaining wild-type allele can then be targeted using the targeting vector that was used to create the Yap knockout-first allele. In the third step subsequent targeting of a tamoxifen-responsive Cre recombinase to the *Rosa26* locus can create inducible Cre expression (Vooijs, Jonkers & Berns, 2001; Indra *et al.*, 1999). Ultimately, the addition of tamoxifen will induce loxP recombination in the conditional and knockout first alleles, resulting in gene deletion.

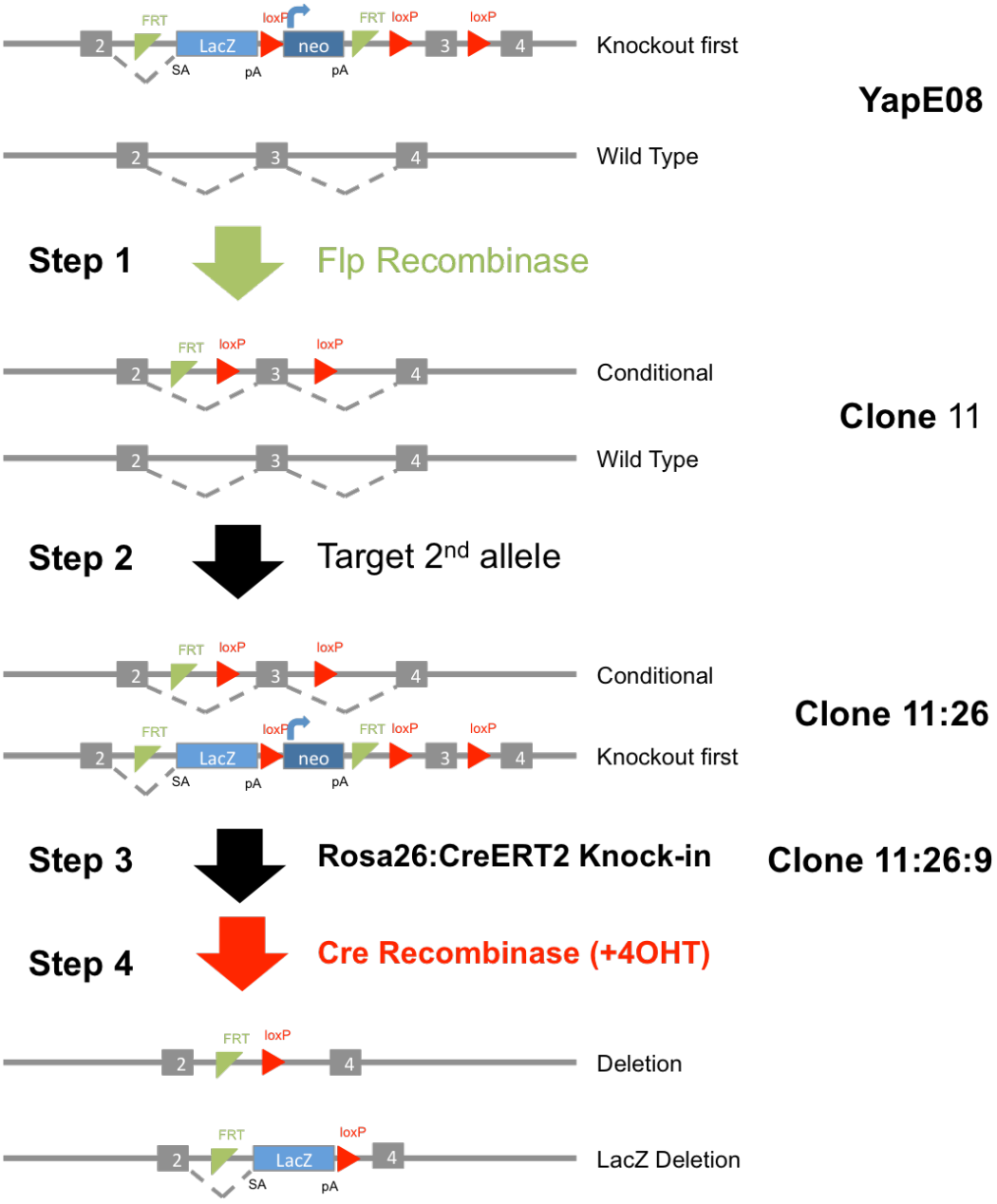

Figure 5.4. Serial targeting strategy Schematic illustrating serial targeting strategy. Step 1 involves transient expression of Flp recombinase to remove the selection cassette. Step 2 involves targeting the wild type Yap allele, using the KOMP knockout-first targeting vector. Step 3 involves targeting CreERT^2 into the *ROSA26* locus. Step 4 is addition of tamoxifen (+4OHT) to induce Cre-mediated recombination and generation of a Yap knockout. Names of Cell lines and Clones derived from each step are indicated on the right.

5.2 Serial targeting strategy

A Yap targeted knockout-first mESC clone (YapE08) was acquired from KOMP. This was generated by KOMP through targeting of JM8 cells, a mESC cell line derived from C57BL/6N mice (Pettitt *et al.*, 2009). The targeting vector inserted a knockout first trapping cassette into the

intronic region between exon 2 and exon 3 of the mouse *Yap* locus (Figure 5.5). KOMP supplied this clone with PCR confirmation of the correct targeting. The YapE08 cell line is heterozygous for Yap, shows no overt phenotype and can be cultured in standard mouse embryonic stem cell conditions with serum and LIF, with or without mouse embryonic fibroblasts. The splice acceptor in the LacZ portion of the cassette results in production of β-galactosidase driven by the endogenous Yap promoter. Histochemical staining with X-Gal confirmed that β-galactosidase is expressed in the YapE08 cell line, which implies the expression of Yap (Figure 5.5).

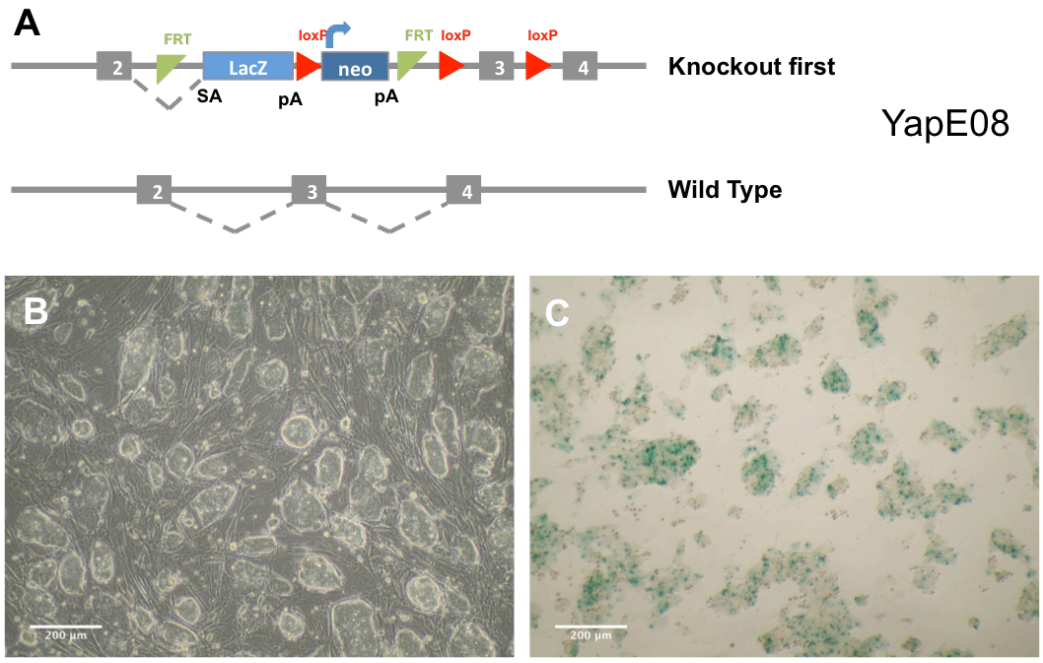

Figure 5.5. YapE08 'knockout first' targeted cell line. (**A**) Schematic illustrating the KOMP targeted knockout-first allele in YapE08. (**B**) Phase contrast image of YapE08 cells growing in culture. (**C**) X-gal staining of YapE08 cells. Scale bars 200µm.

In order to target the wild-type allele, the first step required removal of the selection cassette by transient expression of Flp recombinase. Creation of a conditional allele can be accomplished by removal of the selection cassette using Flp recombination (step 1 in Figure 5.4). The pCAGGS-FlpE-Puro plasmid (Beard *et al.*, 2006) was used to transiently express Flp recombinase in YapE08 cells. Digestion of the pCAGGS-FlpE-Puro plasmid with EcoR1 resulted in the expected band sizes of 7kb and 0.5kb,

confirming that the plasmid contained Flp recombinase (Figure 5.6). The circular plasmid was electroporated into YapE08 cells, and subsequently selected for with puromycin for 2 days to eliminate cells that did not take up the plasmid. As Flp-induced recombination of the selection cassette would also remove the LacZ reporter, subsequent clones were screened for loss of β-galactosidase by histochemical staining with X-Gal (Figure 5.7A). 21 clones were obtained following electroporation with pCAGGS-Flp-Puro and selection with puromycin. Of these 21 clones, 13 had lost expression of β-galactosidase, 5 had retained expression and 3 had failed to proliferate (Figure 5.7B). This represents 62% efficiency for Flp recombination of the selection cassette under these electroporation and selection conditions.

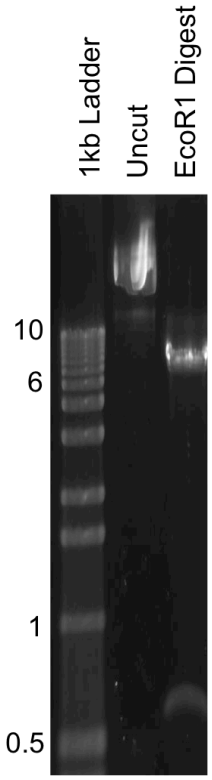

Figure 5.6. Restriction digest of pCAGGS-Flpe-Puro. pCAGGS-FlepE-Puro plasmid digest with EcoRI. Expected band sizes 7kb and 0.5kb

A

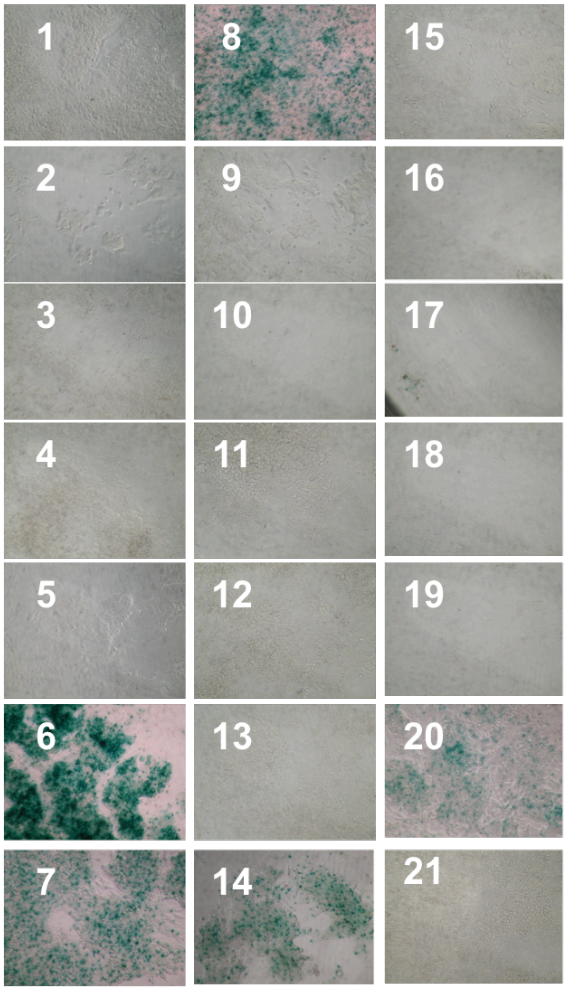

B

LacZ XGAL	Total Clones
Positive	5
Negative	13
Failed	3
	62 %

Figure 5.7. Screening for loss of LacZ in Flp-treated ES cell clones. (**A**) X-gal staining of 21 expanded clones after transient transfection of *Yap* knockout-first cells with pCAGGS-FlpE-Puro. (**B**) Table indicates proportion of cells positive or negative for X-gal stain. Failed indicates clones that did not proliferate in culture.

The presence of any remaining selective resistance gene would hinder further targeting. Flp recombination should have led to excision of the Neo selection marker, while puromycin resistance from the pCAGGS-Flp-Puro plasmid should not have been integrated. The resulting clones were therefore screened for sensitivity to puromycin and G418 (Figure 5.8). Clones were expanded in triplicate and cultured in standard culture media or in the presence of 1μg/ml puromycin or 150μg/ml G418. Of the 21 clones, only one displayed resistance to puromycin and all 21 clones were sensitive to G418. As clone 11 had lost expression of β-galactosidase, and was sensitive to both G418 and puromycin, this

indicated that Flp recombination had possibly occurred. Clone 11 was therefore selected as suitable for subsequent targeting steps.

A

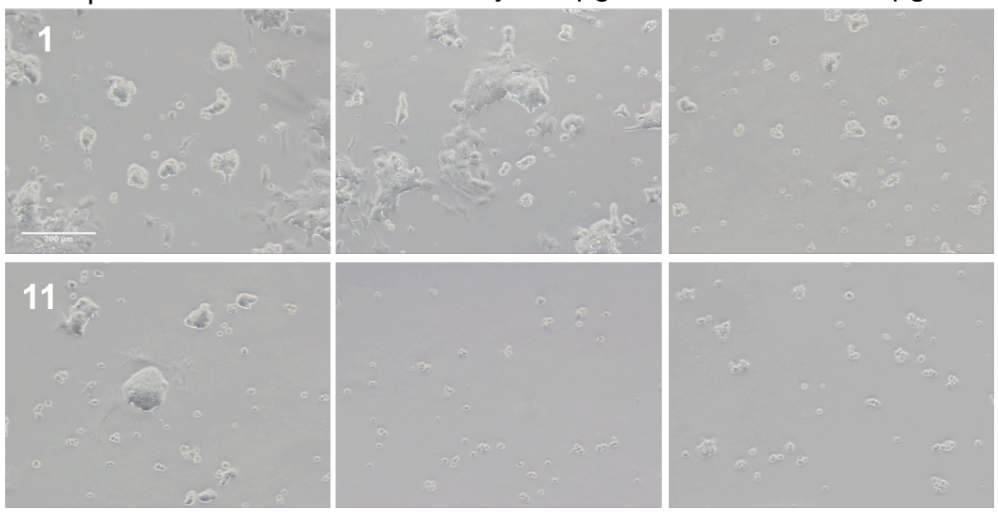

B

	Total Clones (21)
Puro Sensitive	20
G418 Sensitive	21

Figure 5.8. Screening for antibiotic resistance in Flp-treated ES cell clones. (**A**) Phase contrast images of expanded Flp treated clones, in the conditions indicated. Clone numbers 1 and 11 are shown. Note presence of cells growing in puromycin in clone 11. (**B**) Table indication Total number of clones sensitive to Puromycin and G418.

In order to target the second allele (step 2 in Figure 5.4), the Yap targeting vector used in the creation of YapE08 was acquired from KOMP (Figure 5.9A). Digestion of the Yap targeting plasmid with FspI or PvuII resulted in the expected band sizes, confirming that the plasmid contained the Yap targeting vector (Figure 5.9B). The targeting vector was linearized by a restriction digest at a unique restriction site with AsiSI (Figure 5.9C). The linearized targeting vector was electroporated into clone 11 and subsequently selected for with G418. 96 clones were derived after selection with G418.

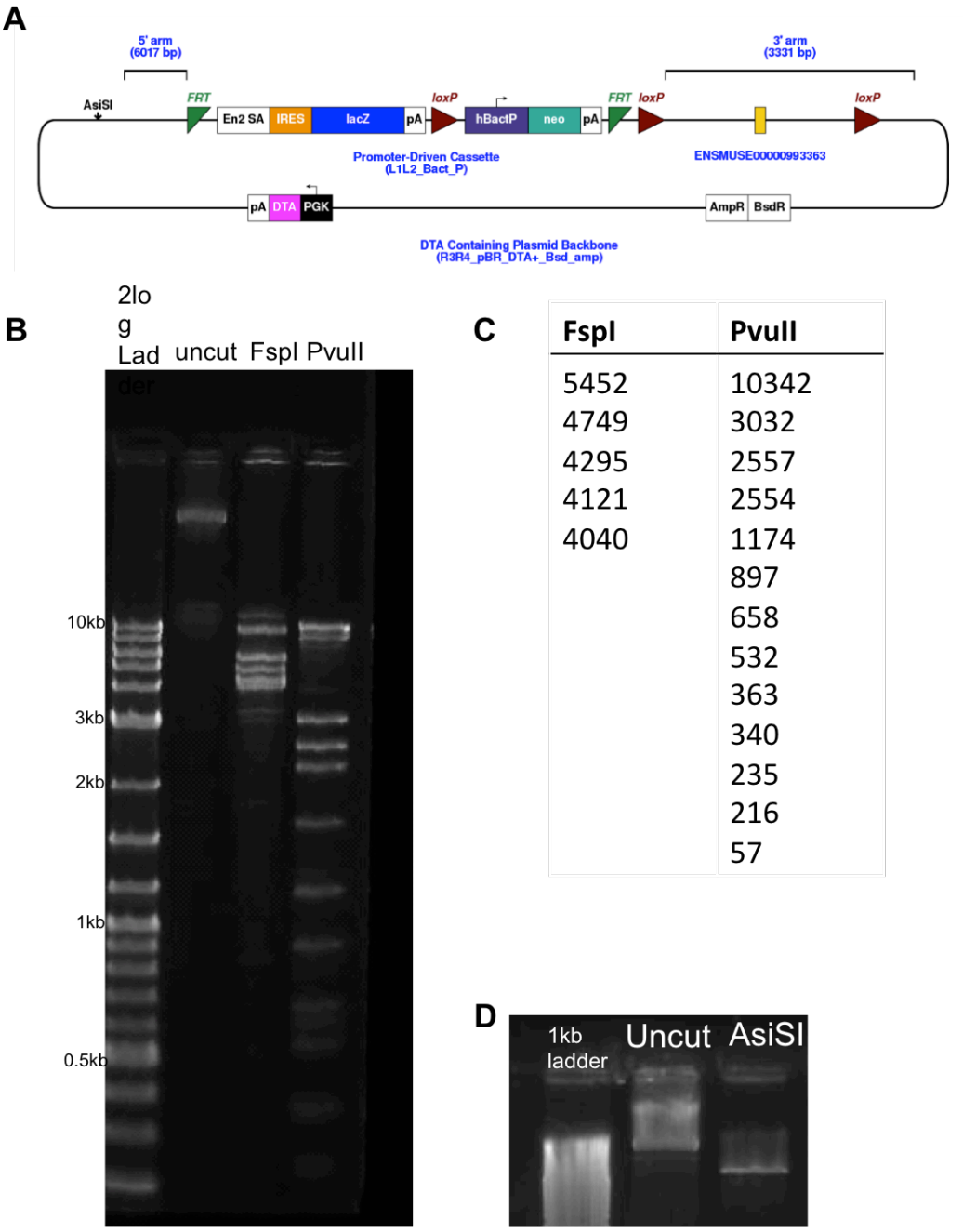

Figure 5.9. Restriction digests of the Yap targeting vector (**A**) Schematic of Yap targeting vector. (**B**) Restriction digest of Yap targeting vector with FspI or PvuII. (**C**) Expected band sizes in kb of restriction digest in A. (**D**) Linearization of Yap targeting vector with AsISI.

The 96 clones were then screened for the expression of LacZ as an indicator of the correct targeting event. As this targeting vector re-introduces the LacZ reporter into the Yap locus, and Yap is expressed in mESCs, correct targeting should result in expression of β-galactosidase from the endogenous Yap promoter. Histochemical staining of the 96

clones with X-Gal revealed 12 clones expressing β-galactosidase (Figure 5.10). This narrows down screening of these 12 clones for correct targeting.

A

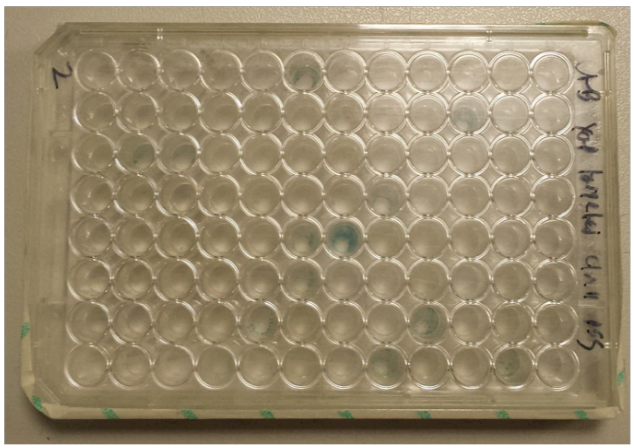

B

LacZ XGAL	Total Clones
Positive	12
Negative	68
Failed	16
	12.5%

Figure 5.10. Screening for expression of LacZ in Yap-targeted ES cell clones. (**A**) X-gal staining of 96clones in a 96-well plate. (**B**)Table indicates proportion of cells positive or negataive for X-gal. Failed indicates clones that did not proliferate in culture.

Detection of bi-allelic targeting was screened for using long-range PCR (Figure 5.11). Clones with targeted mutations in both alleles will have one conditional allele and one knockout-first allele. The presence of the knockout-first allele can be detected using *Yap* gene-specific primers in combination with vector-specific primers to the splice acceptor and neo gene (termed GF+EN2R and NF+GR respectively). This will also confirm target vector integration at the correct locus, as opposed to random vector integration (Figure 5.11). Presence of the conditional allele can be detected using primers directed to the upstream 5' *Yap* locus and the distal loxP site in the targeting vector (GF+LR) (Figure 5.11). As the knockout-first allele is approximately 5kb larger than the conditional allele, it is too large to be amplified by the primer pair GF+LR in this protocol. The 12 clones that were positive for β-galactosidase expression were screened for the presence of bi-allelic targeting using this long range PCR strategy. Clone number 11:26 was found to be positive for both the conditional allele and the knockout-first allele (Figure 5.11). Clone 11:26

was therefore selected for subsequent targeting of Cre-ER^{T2} to the *ROSA26* locus.

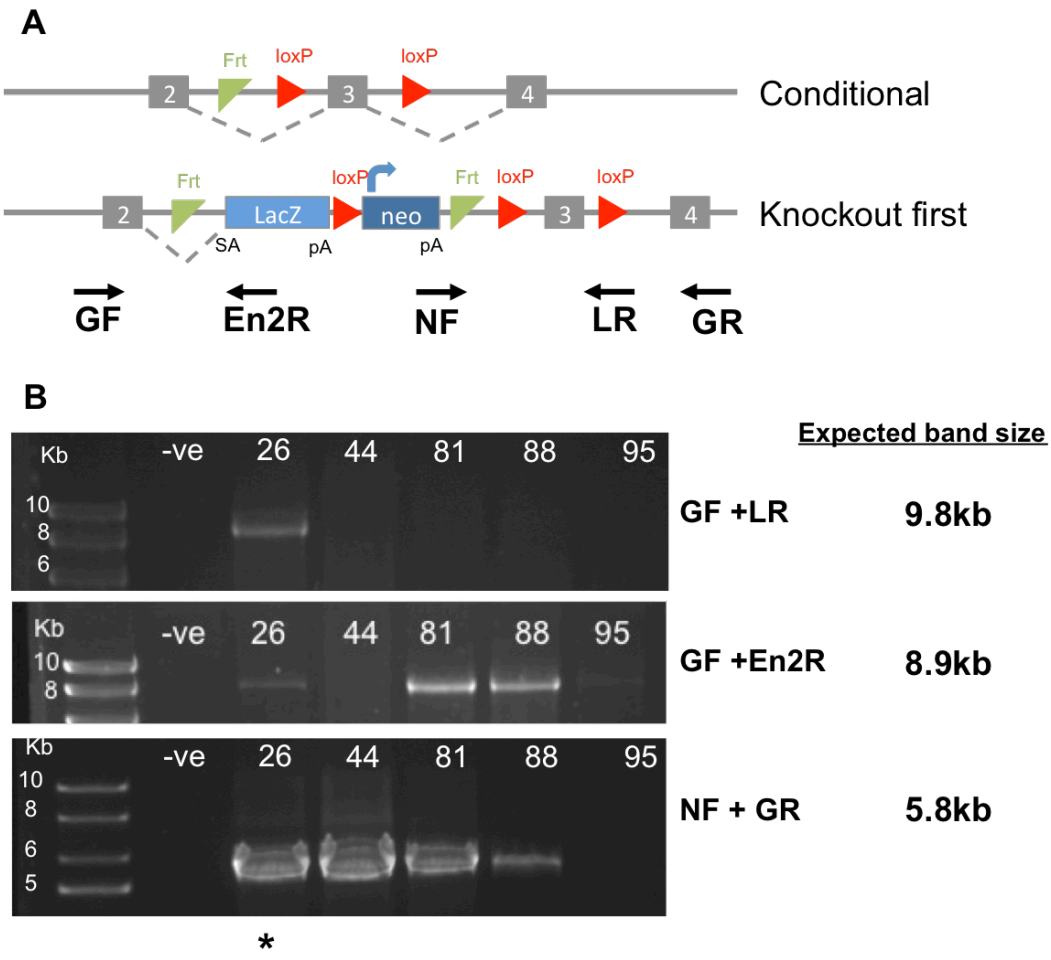

Figure 5.11. Screening for bi-allelic targeted clones by long-range PCR. (**A**) Schematic illustrating primer locations. (**B**) Long-Rage PCR of *Yap* targeted clones. Primer pairs GF+En2R and NF+GR detect presence of the targeting cassette in the knockout-first allele. Primer pair GF+LR detects presence of the conditional allele. Expected band sizes for each primer pair are shown. * indicates that clone 11:26 has expected bands for each primer pair, implying the presence of both knockout-first and conditional alleles.

Targeting of the tamoxifen responsive Cre-ER^{T2} gene to the *ROSA26* locus (step 3 in Figure 5.4) will provide a system for temporal regulation of Cre recombination. The PMB80 (Ventura *et al.*, 2007) plasmid was used to introduce Cre-ER^{T2} into the *ROSA26* locus. Digestion of the pMB80 plasmid with XBaI confirmed (Figure 5.12). The targeting vector was linearized by restriction digest at a unique restriction site with AscI. The linearized targeting vector was electroporated into clone 11:26 and

subsequently selected for with puromycin. 36 clones were obtained following selection with puromycin.

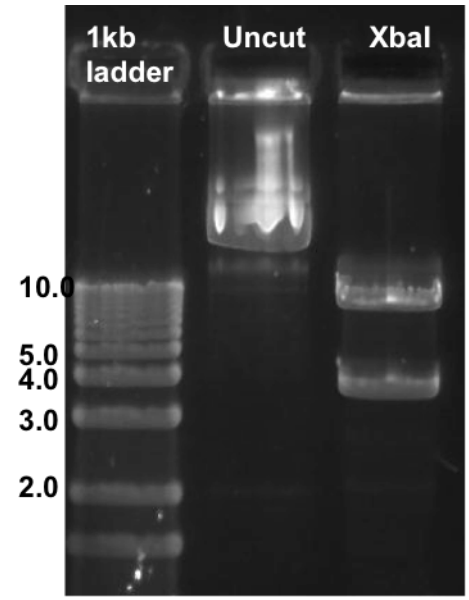

Figure 5.12. Restriction digest of pMB80 with XbaI. Restriction digest of pMB80 with XbaI, expected band sizes 10kb and 4kb.

As targeting of Cre-ER^{T2} to the *ROSA26* locus is highly efficient (Vooijs, Jonkers & Berns, 2001), the 36 clones were screened for tamoxifen responsive Cre activity. Clones were expanded in duplicate, and cultured in standard culture medium with or without tamoxifen for 24hours. Tamoxifen induced Cre recombination was screened for using PCR (Figure 5.13). Primers were designed either side of the floxed exon which would give a PCR product of 1.1kb (CritF+CritR Figure 5.13A). Cre recombination would lead to excision of the exon thus resulting in a smaller PCR product of 280bp. The presence of the smaller PCR product upon addition of tamoxifen would therefore indicate inducible Cre recombination. From the 36 clones only clone 11:26:9 was found to exhibit the shortened PCR product upon addition of tamoxifen and therefore was assumed to have inducible Cre activity (Figure 5.13B,C). As clone 11:26 contained a conditional and knockout-first allele, Cre recombination induced by tamoxifen in clone 11:26:9 should result in knockout alleles.

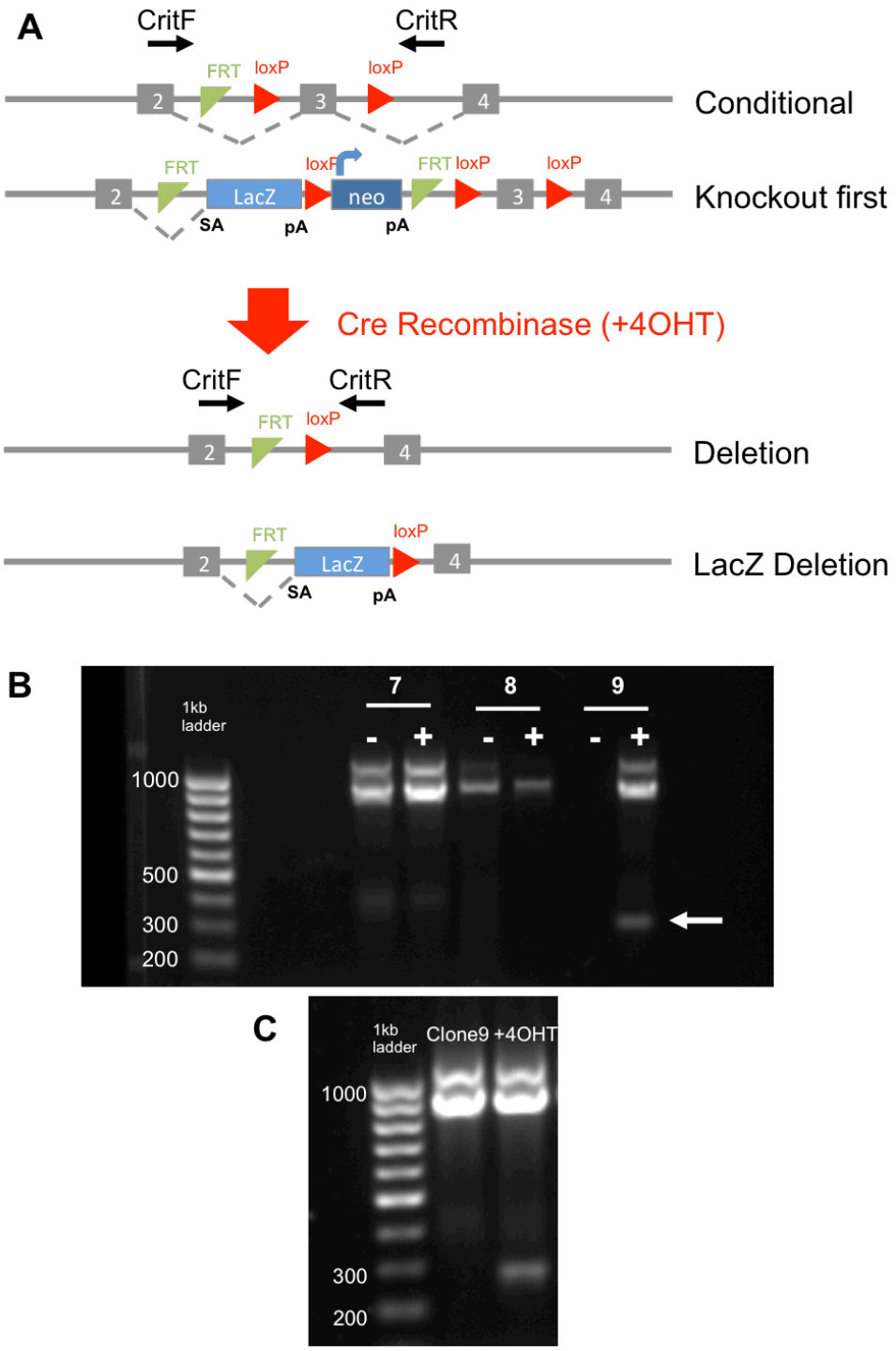

Figure 5.13. Screening for tamoxifen responsive Cre activity in ROSA26:Cre-ER^{T2} clones. (**A**) Schematic illustrating location of CritF and CritR primers. (**B**) PCR analysis of clones 11:26:7, 11:26:8 and 11:26:9 with CritF+CritR primer pair. Cells were treated with or without tamoxifen (+4OHT), indicated by + or – respectively. Expected band sizs are 1.1kb for the conditional allele and 280bp for the deletion allele. As PCR amplification failed in the –Tamoxifen control of 11:26:9, PCR analysis was repeated in (**C**) repeat PCR of clone 11:26:9

In order to check that Cre recombination was leading to loss of *Yap* exon3, a primer was designed to inside exon 3 (Ex3F, Figure 5.14A). PCR amplification using the primer pair Ex3F+CritR would result in a product of 400bp. Upon tamoxifen induced Cre recombination, this exon should be recombined out, thus no PCR product should be obtained. Clone 11:26:9 was expanded in duplicate and cultured in standard culture medium with or without tamoxifen for 24 hours. A PCR product of the expected size was amplified from cells following addition of tamoxifen (Figure 5.14B), suggesting that complete recombination of exon3 had not occurred.

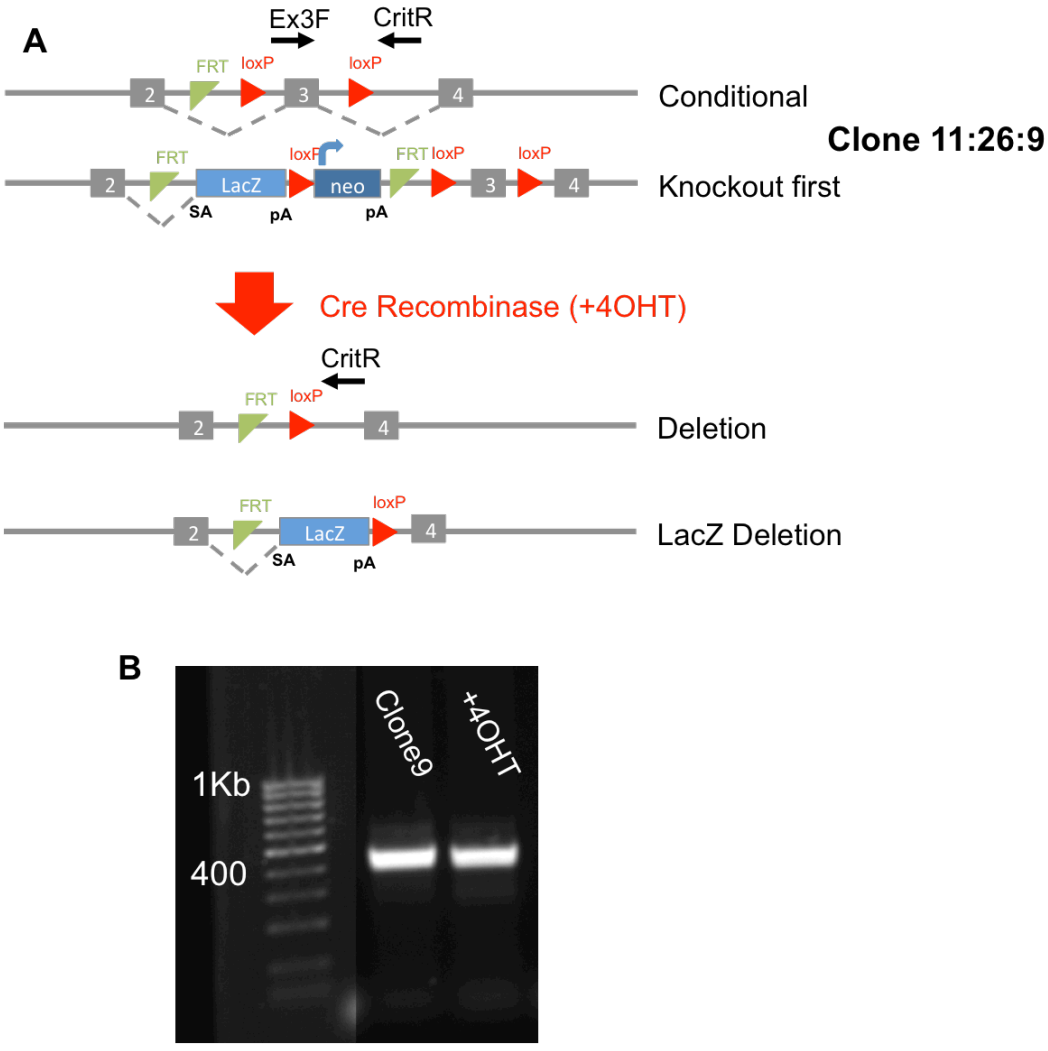

Figure 5.14. *Yap* exon 3 is not excised following addition of tamoxifen (**A**) Schematic illustrating location of Ex3F and CritR primers. Note that upon Cre-mediated recombination Ex3F primer site should be removed. (**B**) PCR analysis of clone 11:26:9 with Ex3F+CritR primer pair. Cells were treated with or without tamoxifen (+4OHT) for 24hours. Expected band size 400bp.

Deletion of *Yap* exon 3 is predicted by KOMP to result in a frame shift, leading to nonsense-mediated decay of the mRNA. RT-PCR was therefore performed to assess if there was a reduction in Yap mRNA levels following addition of tamoxifen to clone 11:26:9. Clone 11:26:9 was expanded in duplicate and cultured in standard culture medium with or without tamoxifen for 24 hours, and then RT-PCR was performed. No difference was observed in Yap mRNA levels following addition of tamoxifen (Figure 5.15A). To assess if addition of tamoxifen had any effect on Yap protein expression, Clone 11:26:9 was expanded in duplicate and cultured in standard culture medium with or without tamoxifen for 48 hours and then immunostained for Yap (Figure 5.15B). No loss of Yap protein was observed by immunofluorescence was observed following addition of tamoxifen. This suggests that addition of tamoxifen is not leading to knockout alleles of *Yap* in this clone.

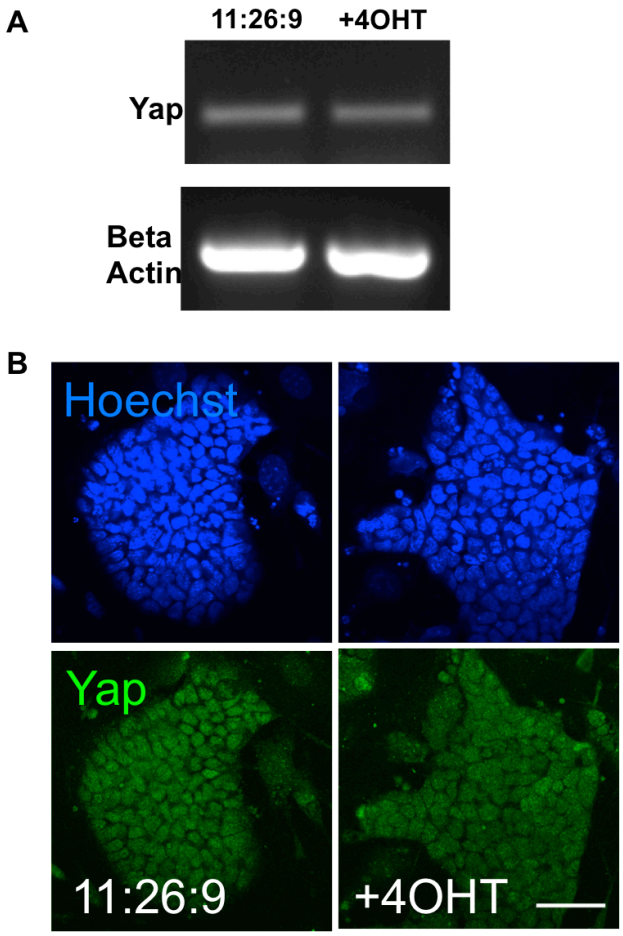

Figure 5.15. Treatment with tamoxifen does not lead to loss of Yap mRNA or Protein expression in clone 11:26:9. (**A**) Clone 11:26:9 was treated with or without tamoxifen for 24 hours and RT-PCR was performed. Beta-Actin was used as a loading control. (**B**) Representative confocal images of clone 11:26:9 stained for Hoechst (blue), Yap (green), grown in S+L (left panels) or treated with tamoxifen for 48h (right panels). Scale bar: 50μm.

In order to ascertain why clone 11:26:9 did not behave as expected upon tamoxifen treatment, a more detailed PCR analysis of clone 11:26:9 and its parental clones was undertaken. Using the CrtiF and CritR primers the expected amplified PCR product from clone 11:26:9 would be 1.1kb. However, this PCR resulted in two bands, one of the expected size of 1.1kb and another smaller 900kb band (Figure 5.16A). The same two bands were seen in clone 11:26. Clone 11 contains a conditional allele and a wild-type allele (Figure 5.4). As the CritF and CritR primer pair will also amplify the wild-type allele, two bands of sizes 1.1kb and 900kb are expected. This therefore suggests that the 900kb band is from the wild-type *Yap* allele. This was confirmed by PCR amplification of YapE08 using the CritF and CritR primer pair (Figure 5.16B). As YapE08 does not

contain a conditional allele, but does contain a wild-type allele, only one band of 900kb is expected.

As targeting of the second allele in clone 11:26 should eliminate the wild-type allele, the wild-type allele should not be present in clone 11:26:9. This suggests that clone 11:26 was clonally impure and contained a mixed population of cells: some cells with the correct targeted allele (labelled as clone 11:26, Figure 5.4) and some cells remaining from the previous step in the cloning strategy *i.e.* clone 11. This mixed population of clone 11:26 and clone 11 cells could explain the presence of the wild-type band. Indeed, addition of G418 to the culture medium led to widespread cell death in cultured clones 11:26 and 11:26:9 indicating that they did not contain the knockout-first allele, which contained the Neo selectable marker.

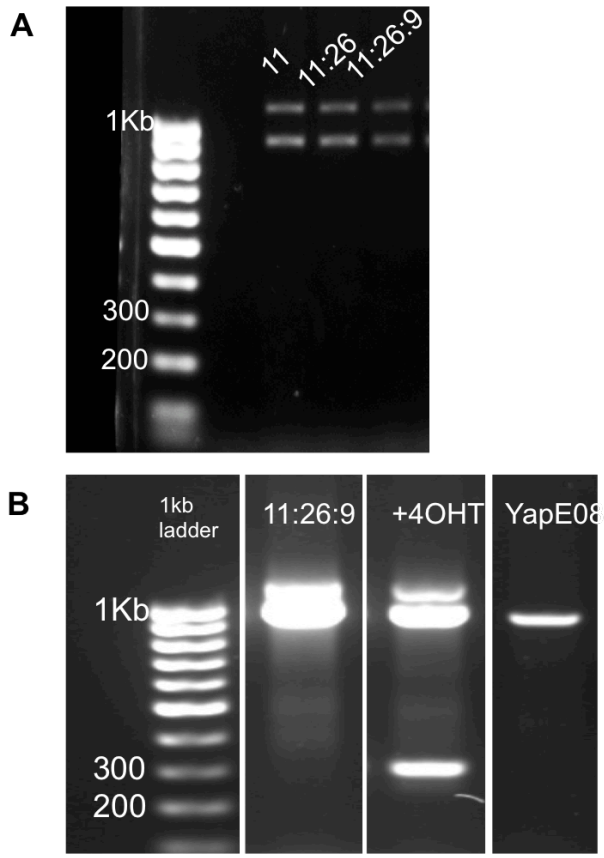

Figure 5.16. PCR analysis reveals wild-type allele in clones 11:26 and 11:26:9 (**A**) PCR analysis of clones 11, 11:26:8 and 11:26:9 with CritF+CritR primer pair. Expected band sizs are 1.1kb for the conditional allele and 900bp for the wild-type allele. (**B**) PCR analysis of clone 11:26:9 with and without tamoxifen treatment and YapE08 with CritF+CritR primer pair. Expected band sizes are 1.1kb for the conditional allele, 900bp for the wild-type allele and280bp for the deletion allele

5.3 Summary

A serial targeting strategy was implemented with the aim of creating an inducible Yap knockout mESC line. This line would then be used to assess the role of Yap in the processes of self-renewal and differentiation. While the serial targeting strategy initially appeared to be successful, further investigation revealed that resulting cell line did not induce knockout alleles of Yap and was clonally impure.

5.4 Discussion

Creation of an inducible knock out of Yap in mESCs would provide an experimental model in which to assess the role of Yap in the processes of self-renewal and differentiation. In order to achieve this, both alleles of Yap must be targeted. The serial targeting strategy as described by Tate

et al. requires multiple rounds of targeting and selection, which introduces multiple possibilities for error. PCR analysis appears to show that isolation of clone 11:26 resulted in contamination with cells carrying a wild-type allele from the previous step in the strategy. At this step, only long range PCR was used to screen for presence of conditional and knockout alleles. The primers used in this screening would not detect the presence of wild-type allele, as they were designed on parts of the targeting vector, and as these cells had survived selection, and were picked as individual colonies, clonality was assumed. However, it is possible that contamination with incorrectly targeted cells occurred during high throughput expansion of clones in 96 well plates. In hindsight, further checks should have been made in regards to the identity of clone 11:26, such as checking for resistance to G418 before proceeding with the targeting protocol.

A mixed population of cells in this case would be especially detrimental due to the phenomenon of cell competition, in which 'fitter' cells outcompete 'less fit' cells (Amoyel & Bach, 2014). The *Drosophila* homologue of Yap, Yorkie (Yki) has been shown to be involved in cell competition, such that cells with higher levels of Yki are able to outcompete wild-type cells (Ziosi *et al.*, 2010; Neto-Silva, de Beco & Johnston, 2010). More recently, Tead transcription factors have been shown to be involved in cell competition with increased Tead transcriptional activity leading to increased cell fitness in mouse embryonic fibroblasts (Mamada *et al.*, 2015). This would suggest that cells homozygous for Yap would have a competitive advantage over cells that are heterozygous. Thus, contamination of clone 11:26 with cells that are potentially homozygous for Yap (as evidenced by presence of a wild-type allele) would lead to the contaminating cells outcompeting and overrunning the culture. This could explain why clones 11:26 and 11:26:9 were so sensitive to G418.

Since beginning this work using this serial targeting strategy, which relies on random homologous recombination, numerous technologies for introducing targeted mutations have been described. Zinc finger

nucleases, Transcription Activator-Like Nucleases (TALENs) and CRISPR-Cas9 systems can be designed to induce targeted double strand breaks, which then introduce mutations through endogenous repair pathways (reviewed in Gaj, Gersbach & Barbas, 2013). Non Homologous End Joining (NHEJ) repairs double strand breaks through direct ligation. NHEJ is an error prone process, which can result in insertions or deletions at the target site, which leads to frame shift mutations, thus impairing gene function(reviewed in Gaj, Gersbach & Barbas, 2013). Alternatively, template DNA can be provided, and Homology Directed Repair (HDR) will use the template DNA to repair the double strand break thus incorporating a desired mutation(reviewed in Gaj, Gersbach & Barbas, 2013). However, despite their increased efficiency compared to homologous recombination, zinc finger nucleases and TALEN systems have been expensive (reviewed in Gaj, Gersbach & Barbas, 2013). More recently, the CRISPR-Cas9 system has emerged as a low cost, simple, high efficiency method for genome editing (reviewed in Ran *et al.*, 2013). The use of targeted double strand breaks would allow mutations to be introduced more efficiently, therefore reducing the large amount of screening as required with random homologous recombination techniques (reviewed in Ran *et al.*, 2013).

The serial targeting strategy was implemented in order to create an inducible mutant of Yap, due to potential cell death or differentiation upon knockout of Yap. However, recently it has been shown that depletion of Yap and Taz by siRNA is inconsequential for mESC propagation in 2i culture (Azzolin *et al.*, 2014). This observation suggests that Yap is not required for growth or maintenance of self-renewal in mESCs under 2i conditions. Therefore, a conditional approach may not be required for the creation of Yap knockout mESCs. The CRISPR-Cas9 system could be used as an efficient, cost effective method to create a constitutive knockout in order to study the role of Yap in differentiation.

Chapter 6: Final discussion

6.1 Summary of findings

In this work I have examined Yap in the context of differentiation and cell fate choice, focusing mainly on differentiation towards primitive endoderm (PrE). In Chapter 3: I show that upon initial differentiation of mouse embryonic stem cells (mESCs), nuclear Yap expression increases. Furthermore, in an *in vitro* model of PrE differentiation, I show that increased nuclear Yap expression is associated with differentiation towards PrE-like cells, as opposed to epiblast-like cells. Furthermore I show that the increase in nuclear Yap expression does not appear to be a result of reduced phosphorylation of Yap at S112. Subsequently I show that cytoplasmic retention of Yap using dobutamine results in decreased differentiation towards PrE.

In Chapter 4: I examine Yap in the corresponding differentiation event in the mouse pre-implantation embryo. I show that increased nuclear Yap expression is associated with increased Gata6 expression in PrE cells, during both specification and eventual sorting. As in mESCs, this increase in nuclear Yap expression did not appear to be a result of reduced phosphorylation of Yap at S112. Cytoplasmic retention of Yap in embryos using dobutamine resulted in decreased markers of both PrE and Epi fates.

Finally in Chapter 5: I attempt to create an inducible knockout of Yap, with the intention to assess the requirement of Yap in self-renewal of mESCs. Unfortunately, although the serial targeting strategy initially appeared to be successful, subsequent analysis found the resulting cell line was not inducing knockout alleles of Yap and was most likely clonally impure.

6.2 Yap in PrE cell fate specification

As increased nuclear Yap expression was associated with differentiation towards PrE both *in vitro* and *in vivo*, this may suggest that Yap is involved in the specification of PrE. As Yap is important in the previous cell fate specification of the trophectoderm (TE) (Nishioka *et al.*, 2009), this could suggest that Yap is part of a conserved mechanism for cell-fate

specification. However, whereas specification of the TE involves position-dependent inhibition of Hippo signalling, specification of PrE and Epi precursors occurs throughout the inner cell mass (ICM) apparently independent of position (Nishioka *et al.*, 2009; Chazaud *et al.*, 2006; Plusa *et al.*, 2008). Yet one of the remarkable aspects of Hippo signalling is the diverse array of upstream inputs, including cell-cell junctions, polarity, mechanical cues, cellular stress, extracellular signals and cross talk with other signalling pathways (reviewed in Yu, Zhao & Guan, 2015). Perhaps in the specification of PrE, Hippo signalling is initially regulated by another input other than polarity. One example could be Fgf signalling, which is instrumental in the this cell fate specification through up-regulation of Gata6 and down-regulation of Nanog (Chazaud *et al.*, 2006; Kang *et al.*, 2012; Yamanaka, Lanner & Rossant, 2010; Nichols *et al.*, 2009; Bessonnard *et al.*, 2014). Expression of constitutively active Ras, a downstream component of Fgf signalling, has been reported to increase nuclear Yap expression in mammalian cells (Reddy & Irvine, 2013). Furthermore siRNA knock-down of Tead4 in cells of the ICM leads to reduced expression of the Fgf receptor (Fgfr2), perhaps suggesting that Fgfr2 is a target of Yap-Tead4 co-activation (Mihajlović, Thamodaran & Bruce, 2015). Yap may therefore have a role in reinforcing PrE cell fate specification downstream of Fgf signalling, forming a positive feedback loop whereby activation of Fgf signalling may lead to increased nuclear Yap expression, resulting in increased expression of Fgfr2 (Figure 6.1).

Another potential input into the Hippo signalling pathway during the specification of PrE is LIF signalling. In mESCs, LIF binds to a heterodimeric receptor composed of glycoprotein 130 (gp130), resulting in activation of Janus associated tyrosine kinases (JAK) that phosphorylates signal transducer and activation of transcription 3 (STAT3) (reviewed in Hirai, Karian & Kikyo, 2011). LIF activation of STAT3 subsequently results in the up regulation of pluripotency markers (Hall *et al.*, 2009). However recent studies have reported a role that LIF also supports extraembryonic gene expression in mESC culture and furthermore, treatment of pre-implantation embryos with LIF results in an

increased proportion of PrE cells (Morgani *et al.*, 2013; Morgani & Brickman, 2015). Interestingly, LIF has also been shown to activate the Src family kinase Yes, resulting in a subsequent tyrosine phosphorylation of Yap in mESCs (Tamm, Bower & Anneren, 2011). This tyrosine phosphorylation of Yap leads to increased Tead2 dependent transcription (Tamm, Bower & Anneren, 2011). It is therefore possible that Yap acts downstream of LIF leading to increased extraembryonic gene expression thereby supporting speciation of PrE.

In specification of the TE, Yap co-activates Tead4 transcription of Cdx2 and Gata3, two TE specific transcription factors (Nishioka *et al.*, 2009; Ralston *et al.*, 2010). It would be interesting to investigate transcriptional targets of Yap in PrE cells to examine if Yap leads to increased expression of PrE specific factors such as Gata6. Interestingly, a recent study has shown that in embryonic pancreatic progenitor cells, Yap, Tead and Gata6 bind to enhancers of genes associated with pancreatic development, notably Hhex and Fgfr2 (Cebola *et al.*, 2015). Hhex and Fgfr2 are associated with PrE development (Thomas, Brown & Beddington, 1998; Arman *et al.*, 1998), which suggests the possibility that during differentiation, Yap acts with Gata6 to enhance transcription of endodermal associated targets.

In the specification of the TE, Hippo signalling is inhibited in outer, polarized cells, thus allowing Yap to act as a transcriptional co-activator leading to increased expression of TE specific transcription factors such as Cdx2 (Nishioka *et al.*, 2009; Hirate *et al.*, 2013). Inner, apolar, cells have increased cell-cell contacts resulting in activation of Hippo signalling, which results in cytoplasmic Yap and specification of the ICM (Nishioka *et al.*, 2009; Hirate *et al.*, 2013). Subsequently specification of PrE and Epi precursors occurs in cells of the ICM independently of positional information (Chazaud *et al.*, 2006; Plusa *et al.*, 2008). Perhaps increased stability of Yap downstream of Fgf and Lif signalling provides a mechanism for Yap to overcome Hippo mediated cytoplasmic retention, thus allowing Yap to translocate to the nucleus and support the expression of genes associated with PrE (Figure 6.1). Furthermore,

overexpression of Nanog has been reported to reduce Tead2 dependent transcriptional activity in mESCs (Tamm, Bower & Anneren, 2011), which could indicate a mechanism for Nanog to prevent Yap dependent expression of PrE associated genes in Epi precursors. This could therefore represent possible mechanisms of Hippo signalling in the specification of Pre and Epi.

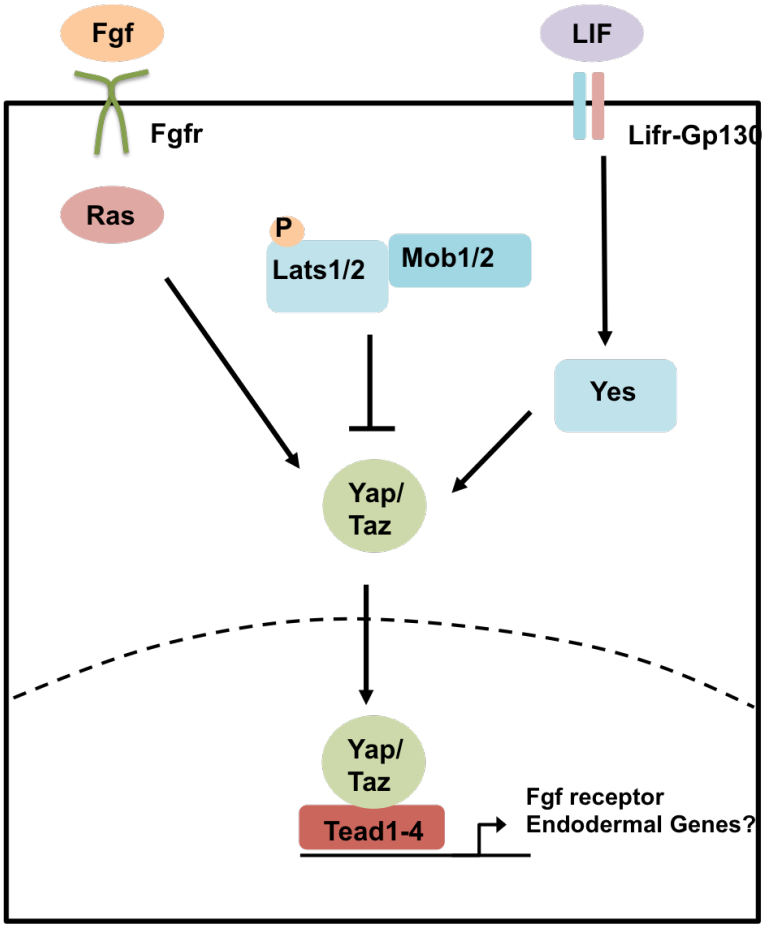

Figure 6.1. Possible regulation of Yap by Hippo, Fgf and LIF signalling pathways in specification of PrE. Hippo signalling member Lats can phosphorylate Yap resulting in cytoplasmic retention. Fgf signalling through Ras may lead to increased nuclear Yap expression, resulting in expression of Fgf receptor (Fgfr) forming a positive feedback loop. LIF signalling can activate Yes kinase, leading to phosphorylation and subsequent increased transcriptional activity of Yap.

6.3 Yap and the Hippo signalling pathway in cell fate decisions

The specification of TE and PrE, are binary fate decisions, such that a precursor cell differentiates into one of two available fates, i.e. TE or ICM,

PrE or Epi. Yap has been reported to be involved in a number of binary cell fate decisions. In zebrafish eye development, optic vesicle progenitors will differentiate into either neural retina or retinal pigment epithelium (RPE) (reviewed in Fuhrmann, Zou & Levine, 2014). Yap has been shown to be required for in this cell fate specification such that Yap mutants cannot form RPE (Miesfeld *et al.*, 2015). Furthermore, in the D*rosophila* visual system, bi-potent R8 photoreceptor neurons differentiate into one of two alternative photoreceptor subtypes, expressing either blue light sensitive Rhodopsin5 (Rh5) or green light sensitive Rhodopsin6 (Rh6). Yorkie (Yki), the *Drosophila* homolog of Yap, is reported to be central in a positive feedback network, which promotes differentiation of the Rh5 subtype (Jukam *et al.*, 2013). Yap and the Hippo pathway could therefore represent a common mechanism of integrating multiple upstream signals in specification of cell fates.

6.4 Future directions

Is Yap absolutely required for PrE cell fate specification?

I have shown that increased nuclear Yap expression is associated with PrE specification, and that inhibition of Yap with dobutamine can decrease differentiation towards PrE cell fate. However studies of Yap knockout cell lines and embryos would identify if there is an absolute requirement of Yap in PrE cell fate. Crispr genome editing could be used to create a knockout of Yap in the Gata6-inducible mESC line. If Yap is absolutely required for differentiation towards PrE, induction of Gata6 would no longer result in PrE differentiation. Furthermore analysis of markers of PrE in $Yap^{-/-}$ mouse embryos could provide insight into the requirement for Yap in specification and differentiation of the PrE.

What are the transcriptional targets of Yap in PrE differentiation?

If Yap is associated with PrE cell fate specification, how does it mediate this effect? Differentiation towards PrE could be induced by overexpression of Gata6 in mESCs and Chromatin immunoprecpitation and gene expression microarray analysis could identify transcriptional targets of Yap.

Is Yap required for self-renewal of mESCs?

Yap is believed to have a critical role in the maintenance of self-renewal and pluripotency in mESCs. Unfortunately my attempt at creating an inducible knockout of Yap using a serial targeting strategy was unsuccessful. However the CRISPR-Cas9 system represents an efficient, cost effective method to create a constitutive knockout in order to study the role of Yap in mESC self renewal and differentiation.

Is Yap stability affected by Fgf signalling in mESCs?

There is evidence that Hippo signalling can be regulated in mammalian cells by Ras-Mapk signalling, which is a downstream component of Fgf signalling. However, it is unknown if this is also the case in mESCs. This could be investigated using small molecule inhibitors of Fgf pathway components and examining their effect on Yap in mESCs. If Yap stability is increased by Fgf signalling, inhibition of Fgf signalling would result in decreased Yap expression. Conversely, addition of Fgf would result in an increase in Yap expression.

Is Yap downstream of LIF dependent expression of endodermal genes?

LIF has been shown to support expression of endodermal associated genes in mESCs. To determine if Yap is downstream of LIF in supporting endodermal gene expression, expression of endodermal genes could be examined in Yap knockout mESCs. If Yap is downstream of LIF, then endodermal gene expression would be reduced in Yap knockout mESCs, upon treatment with LIF.

References

Amoyel, M. & Bach, E.A. (2014) Cell competition: how to eliminate your neighbours. *Development*. 141 (5), pp. 988–1000.

Anneren, C. (2004) The Src Family of Tyrosine Kinases Is Important for Embryonic Stem Cell Self-renewal. *Journal of Biological Chemistry*. 279 (30), pp. 31590–31598.

Arman, E., Haffner-Krausz, R., Chen, Y., Heath, J.K. & Lonai, P. (1998) Targeted disruption of fibroblast growth factor (FGF) receptor 2 suggests a role for FGF signaling in pregastrulation mammalian development. *Proceedings of the National Academy of Sciences*. 95 (9), pp. 5082–5087.

Artus, J., Piliszek, A. & Hadjantonakis, A.-K. (2011) The primitive endoderm lineage of the mouse blastocyst: sequential transcription factor activation and regulation of differentiation by Sox17. *Developmental Biology*. 350 (2), pp. 393–404.

Avilion, A.A., Nicolis, S.K., Pevny, L.H., Perez, L., Vivian, N. & Lovell-Badge, R. (2003) Multipotent cell lineages in early mouse development depend on SOX2 function. *Genes & Development*. 17 (1), pp. 126–140.

Azzolin, L., Panciera, T., Soligo, S., Enzo, E., Bicciato, S., Dupont, S., Bresolin, S., Frasson, C., Basso, G., Guzzardo, V., Fassina, A., Cordenonsi, M. & Piccolo, S. (2014) YAP/TAZ incorporation in the β-catenin destruction complex orchestrates the Wnt response. *Cell*. 158 (1), pp. 157–170.

Bao, Y., Nakagawa, K., Yang, Z., Ikeda, M., Withanage, K., Ishigami-Yuasa, M., Okuno, Y., Hata, S., Nishina, H. & Hata, Y. (2011) A cell-based assay to screen stimulators of the Hippo pathway reveals the inhibitory effect of dobutamine on the YAP-dependent gene transcription. *Journal of Biochemistry*. 150 (2), pp. 199–208.

Basu, S., Totty, N.F., Irwin, M.S., Sudol, M. & Downward, J. (2003) Akt phosphorylates the Yes-associated protein, YAP, to induce interaction with 14-3-3 and attenuation of p73-mediated apoptosis. *Molecular Cell*. 11 (1), pp. 11–23.

Beard, C., Hochedlinger, K., Plath, K., Wutz, A. & Jaenisch, R. (2006) Efficient method to generate single-copy transgenic mice by site-specific integration in embryonic stem cells. *genesis*. 44 (1), pp. 23–28.

Beddington, R.S. & Robertson, E.J. (1989) An assessment of the developmental potential of embryonic stem cells in the midgestation mouse embryo. *Development*. 105 (4), pp. 733–737.

Bessonnard, S., De Mot, L., Gonze, D., Barriol, M., Dennis, C., Goldbeter, A., Dupont, G. & Chazaud, C. (2014) Gata6, Nanog and Erk signaling control cell fate in the inner cell mass through a tristable regulatory network. *Development*. 141 (19), pp. 3637–3648.

Burdon, T., Stracey, C., Chambers, I., Nichols, J. & Smith, A. (1999) Suppression of SHP-2 and ERK Signalling Promotes Self-Renewal of Mouse Embryonic Stem Cells. *Developmental Biology*. 210 (1), pp. 30–43.

Cai, K.Q., Capo-Chichi, C.D., Rula, M.E., Yang, D.-H. & Xu, X.-X. (2008) Dynamic GATA6 expression in primitive endoderm formation and maturation in early mouse embryogenesis Parker B Antin, Marion K Gordon, Catherine E Krull, M Angela Nieto, & Kathy Svoboda (eds.). *Developmental dynamics : an official publication of the American Association of Anatomists*. 237 (10), pp. 2820–2829.

Callus, B.A., Verhagen, A.M. & Vaux, D.L. (2006) Association of mammalian sterile twenty kinases, Mst1 and Mst2, with hSalvador via C-terminal coiled-coil domains, leads to its stabilization and phosphorylation. *The FEBS journal*. 273 (18), pp. 4264–4276.

Camargo, F.D., Gokhale, S., Johnnidis, J.B., Fu, D., Bell, G.W., Jaenisch, R. & Brummelkamp, T.R. (2007) YAP1 Increases Organ Size and Expands Undifferentiated Progenitor Cells. *Current Biology*. 17 (23), pp. 2054–2060.

Canham, M.A., Sharov, A.A., Ko, M.S.H. & Brickman, J.M. (2010) Functional Heterogeneity of Embryonic Stem Cells Revealed through Translational Amplification of an Early Endodermal Transcript Hiroshi Hamada (ed.). *PLoS Biology*. 8 (5), pp. e1000379.

Cebola, I., Rodríguez-Seguí, S.A., Cho, C.H.-H., Bessa, J., Rovira, M., Luengo, M., Chhatriwala, M., Berry, A., Ponsa-Cobas, J., Maestro, M.A., Jennings, R.E., Pasquali, L., Morán, I., Castro, N., et al. (2015) TEAD and YAP regulate the enhancer network of human embryonic pancreatic progenitors. *Nature cell biology*. 17 (5), pp. 615–626.

Chambers, I., Silva, J., Colby, D., Nichols, J., Nijmeijer, B., Robertson, M., Vrana, J., Jones, K., Grotewold, L. & Smith, A. (2007) Nanog safeguards pluripotency and mediates germline development. *Nature*. 450 (7173), pp. 1230–1234.

Chan, E.H.Y., Nousiainen, M., Chalamalasetty, R.B., Schäfer, A., Nigg, E.A. & Silljé, H.H.W. (2005) The Ste20-like kinase Mst2 activates the human large tumor suppressor kinase Lats1. *Oncogene*. 24 (12), pp. 2076–2086.

Chazaud, C., Yamanaka, Y., Pawson, T. & Rossant, J. (2006) Early lineage segregation between epiblast and primitive endoderm in mouse blastocysts through the Grb2-MAPK pathway. *Developmental Cell*. 10 (5), pp. 615–624.

Chen, D., Sun, Y., Wei, Y., Zhang, P., Rezaeian, A.H., Teruya-Feldstein, J., Gupta, S., Liang, H., Lin, H.-K., Hung, M.-C. & Ma, L. (2012) LIFR is a breast cancer metastasis suppressor upstream of the Hippo-YAP pathway and a prognostic marker. *Nature Medicine*. 18 (10), pp. 1511–1517.

Chen, Q., Zhang, N., Xie, R., Wang, W., Cai, J., Choi, K.-S., David, K.K., Huang, B., Yabuta, N., Nojima, H., Anders, R.A. & Pan, D. (2015) Homeostatic control of Hippo signaling activity revealed by an endogenous activating mutation in YAP. *Genes & Development*. 29 (12), pp. 1285–1297.

Cockburn, K., Biechele, S., Garner, J. & Rossant, J. (2013) The Hippo Pathway Member Nf2 Is Required for Inner Cell Mass Specification. *Current Biology*. 23 (13), pp. 1195–1201.

Coucouvanis, E. & Martin, G.R. (1995) Signals for death and survival: a two-step mechanism for cavitation in the vertebrate embryo. *Cell*. 83 (2), pp. 279–287.

Cretu, A., Castagnino, P. & Assoian, R. (2010) Studying the Effects of Matrix Stiffness on Cellular Function using Acrylamide-based Hydrogels. *Journal of Visualized Experiments*. (42).

Deng, H., Wang, W., Yu, J., Zheng, Y., Qing, Y. & Pan, D. (2015) Spectrin regulates Hippo signaling by modulating cortical actomyosin activity. *eLife*.

Dietrich, J.-E. & Hiiragi, T. (2007) Stochastic patterning in the mouse pre-implantation embryo. *Development*. 134 (23), pp. 4219–4231.

Dong, J., Feldmann, G., Huang, J., Wu, S., Zhang, N., Comerford, S.A., Gayyed, M.F., Anders, R.A., Maitra, A. & Pan, D. (2007) Elucidation of a Universal Size-Control Mechanism in Drosophila and Mammals. *Cell*. 130 (6), pp. 1120–1133.

Dow, L.E. & Humbert, P.O. (2007) Polarity regulators and the control of epithelial architecture, cell migration, and tumorigenesis. *International review of cytology*. 262pp. 253–302.

Dupont, S., Morsut, L., Aragona, M., Enzo, E., Giulitti, S., Cordenonsi, M., Zanconato, F., Le Digabel, J., Forcato, M., Bicciato, S., Elvassore, N. & Piccolo, S. (2011) Role of YAP/TAZ in mechanotransduction. *Nature*. 474 (7350), pp. 179–183.

Eagle, H., Levine, E.M. & Koprowski, H. (1968) Species specificity in growth regulatory effects of cellular interaction. *Nature*. 220 (5164), pp. 266–269.

Engler, A.J., Sen, S., Sweeney, H.L. & Discher, D.E. (2006) Matrix Elasticity Directs Stem Cell Lineage Specification. *Cell*. 126 (4), pp. 677–689.

Evans, M.J. & Kaufman, M.H. (1981) Establishment in culture of pluripotential cells from mouse embryos. *Nature*. 292 (5819), pp. 154–156.

Fletcher, G.C., Elbediwy, A., Khanal, I., Ribeiro, P.S., Tapon, N. & Thompson, B.J. (2015) The Spectrin cytoskeleton regulates the Hippo signalling pathway. *The EMBO journal*. 34 (7), pp. 940–954.

Frankenberg, S., Gerbe, F., Bessonnard, S., Belville, C., Pouchin, P., Bardot, O. & Chazaud, C. (2011) Primitive Endoderm Differentiates via a Three-Step Mechanism Involving Nanog and RTK Signaling. *Developmental Cell*. 21 (6), pp. 1005–1013.

Frankenberg, S., Shaw, G., Freyer, C., Pask, A.J. & Renfree, M.B. (2013) Early cell lineage specification in a marsupial: a case for diverse mechanisms among mammals. *Development*. 140 (5), pp. 965–975.

Fuhrmann, S., Zou, C. & Levine, E.M. (2014) Retinal pigment epithelium development, plasticity, and tissue homeostasis. *Experimental Eye Research*. 123pp. 141–150.

Gaj, T., Gersbach, C.A. & Barbas, C.F., III (2013) ZFN, TALEN, and CRISPR/Cas-based methods for genome engineering. *Trends in Biotechnology*. 31 (7), pp. 397–405.

Gu, H., Zou, Y.R. & Rajewsky, K. (1993) Independent control of immunoglobulin switch recombination at individual switch regions evidenced through Cre-loxP-mediated gene targeting. *Cell*. 73 (6), pp. 1155–1164.

Guo, G., Huss, M., Tong, G.Q., Wang, C., Sun, L.L., Clarke, N.D. & Robson, P. (2010) Resolution of Cell Fate Decisions Revealed by Single-Cell Gene Expression Analysis from Zygote to Blastocyst. *Developmental Cell*. 18 (4), pp. 675–685.

Hall, J., Guo, G., Wray, J., Eyres, I., Nichols, J., Grotewold, L., Morfopoulou, S., Humphreys, P., Mansfield, W., Walker, R., Tomlinson, S. & Smith, A. (2009) Oct4 and LIF/Stat3 Additively Induce KrUppel Factors to Sustain Embryonic Stem Cell Self-Renewal. *Stem Cell*. 5 (6), pp. 597–609.

Hamazaki, T., Oka, M., Yamanaka, S. & Terada, N. (2004) Aggregation of embryonic stem cells induces Nanog repression and primitive endoderm differentiation. *Journal of Cell Science*. 117 (Pt 23), pp. 5681–5686.

Hao, Y., Chun, A., Cheung, K., Rashidi, B. & Yang, X. (2007) Tumor Suppressor LATS1 Is a Negative Regulator of Oncogene YAP. *Journal of Biological Chemistry*. 283 (9), pp. 5496–5509.

Harvey, K.F., Pfleger, C.M. & Hariharan, I.K. (2003) The Drosophila Mst ortholog, hippo, restricts growth and cell proliferation and promotes apoptosis. *Cell*. 114 (4), pp. 457–467.

Hirai, H., Karian, P. & Kikyo, N. (2011) Regulation of embryonic stem cell self-renewal and pluripotency by leukaemia inhibitory factor. *Biochemical Journal*. 438 (1), pp. 11–23.

Hirate, Y., Cockburn, K., Rossant, J. & Sasaki, H. (2012) Tead4 is constitutively nuclear, while nuclear vs. cytoplasmic Yap distribution is regulated in preimplantation mouse embryos. *Proceedings of the National Academy of Sciences of the United States of America*. 109 (50), pp. E3389–E3390.

Hirate, Y., Hirahara, S., Inoue, K.-I., Suzuki, A., Alarcon, V.B., Akimoto, K., Hirai, T., Hara, T., Adachi, M., Chida, K., Ohno, S., Marikawa, Y., Nakao, K., Shimono, A., et al. (2013) Polarity-Dependent Distribution of Angiomotin Localizes Hippo Signaling in Preimplantation Embryos. *Current Biology*. 23 (13), pp. 1181–1194.

Home, P., Saha, B., Ray, S., Dutta, D., Gunewardena, S., Yoo, B., Pal, A., Vivian, J.L., Larson, M. & Petroff, M. (2012) Altered subcellular localization of transcription factor TEAD4 regulates first mammalian cell lineage commitment. *Proceedings of the National Academy of Sciences of the United States of America*. 109 (19), pp. 7362–7367.

Hong, X., Nguyen, H.T., Chen, Q., Zhang, R., Hagman, Z., Voorhoeve, P.M. & Cohen, S.M. (2014) Opposing activities of the Ras and Hippo pathways converge on regulation of YAP protein turnover. *The EMBO journal*. 33 (21), pp. 2447–2457.

Hooper, M., Hardy, K., Handyside, A., Hunter, S. & Monk, M. (1987) HPRT-deficient (Lesch-Nyhan) mouse embryos derived from germline colonization by cultured cells. *Nature*. 326 (6110), pp. 292–295.

Huang, J., Wu, S., Barrera, J., Matthews, K. & Pan, D. (2005) The Hippo signaling pathway coordinately regulates cell proliferation and apoptosis by inactivating Yorkie, the Drosophila Homolog of YAP. *Cell*. 122 (3), pp. 421–434.

Indra, A.K., Warot, X., Brocard, J., Bornert, J.M., Xiao, J.H., Chambon, P. & Metzger, D. (1999) Temporally-controlled site-specific mutagenesis in the basal layer of the epidermis: comparison of the recombinase activity of the tamoxifen-inducible Cre-ER(T) and Cre-ER(T2) recombinases. *Nucleic Acids Research*. 27 (22), pp. 4324–4327.

Jukam, D., Xie, B., Rister, J., Terrell, D., Charlton-Perkins, M., Pistillo, D., Gebelein, B., Desplan, C. & Cook, T. (2013) Opposite feedbacks in the Hippo pathway for growth control and neural fate. *Science (New York, N.Y.)*. 342 (6155), pp. 1238016.

Justice, R.W., Zilian, O., Woods, D.F., Noll, M. & Bryant, P.J. (1995) The Drosophila tumor suppressor gene warts encodes a homolog of human myotonic dystrophy kinase and is required for the control of cell shape and proliferation. *Genes & Development*. 9 (5), pp. 534–546.

Kang, M., Piliszek, A., Artus, J. & Hadjantonakis, A.K. (2012) FGF4 is required for lineage restriction and salt-and-pepper distribution of primitive endoderm factors but not their initial expression in the mouse. *Development*. 140 (2), pp. 267–279.

Kim, N.-G., Koh, E., Chen, X. & Gumbiner, B.M. (2011) E-cadherin mediates contact inhibition of proliferation through Hippo signaling-pathway components. *Proceedings of the National Academy of Sciences of the United States of America*. 108 (29), pp. 11930–11935.

Kwon, G.S., Viotti, M. & Hadjantonakis, A.-K. (2008) The Endoderm of the Mouse Embryo Arises by Dynamic Widespread Intercalation of Embryonic and Extraembryonic Lineages. *Developmental Cell*. 15 (4), pp. 509–520.

Lai, Z.-C., Wei, X., Shimizu, T., Ramos, E., Rohrbaugh, M., Nikolaidis, N., Ho, L.-L. & Li, Y. (2005) Control of cell proliferation and apoptosis by mob as tumor suppressor, mats. *Cell*. 120 (5), pp. 675–685.

Le Bin, G.C., Muñoz Descalzo, S., Kurowski, A., Leitch, H., Lou, X., Mansfield, W., Etienne-Dumeau, C., Grabole, N., Mulas, C., Niwa, H., Hadjantonakis, A.-K. & Nichols, J. (2014) Oct4 is required for lineage priming in the developing inner cell mass of the mouse blastocyst. *Development*. 141 (5), pp. 1001–1010.

Lefebvre, L., Dionne, N., Karaskova, J., Squire, J.A. & Nagy, A. (2001) Selection for transgene homozygosity in embryonic stem cells results in extensive loss of heterozygosity. *Nature genetics*. 27 (3), pp. 257–258.

Lei, Q.Y., Zhang, H., Zhao, B., Zha, Z.Y., Bai, F., Pei, X.H., Zhao, S., Xiong, Y. & Guan, K.-L. (2008) TAZ Promotes Cell Proliferation and Epithelial-Mesenchymal Transition and Is Inhibited by the Hippo Pathway. *Molecular and Cellular Biology*. 28 (7), pp. 2426–2436.

Levy, D., Adamovich, Y., Reuven, N. & Shaul, Y. (2008) Yap1 phosphorylation by c-Abl is a critical step in selective activation of proapoptotic genes in response to DNA damage. *Molecular Cell*. 29 (3), pp. 350–361.

Li, S. & Yurchenco, P.D. (2006) Matrix assembly, cell polarization, and cell survival: analysis of peri-implantation development with cultured embryonic stem cells. *Methods in molecular biology (Clifton, N.J.)*. 329pp. 113–125.

Li, Z., Zhao, B., Wang, P., Chen, F., Dong, Z., Yang, H., Guan, K.-L. & Xu, Y. (2010) Structural insights into the YAP and TEAD complex. *Genes & Development*. 24 (3), pp. 235–240.

Lian, I., Kim, J., Okazawa, H., Zhao, J., Zhao, B., Yu, J., Chinnaiyan, A., Israel, M.A., Goldstein, L.S.B., Abujarour, R., Ding, S. & Guan, K.-L. (2010) The role of YAP transcription coactivator in regulating stem cell self-renewal and differentiation. *Genes & Development*. 24 (11), pp. 1106–1118.

Liu-Chittenden, Y., Huang, B., Shim, J.S., Chen, Q., Lee, S.J., Anders, R.A., Liu, J.O. & Pan, D. (2012) Genetic and pharmacological disruption of the TEAD-YAP complex suppresses the oncogenic activity of YAP. *Genes & Development*. 26 (12), pp. 1300–1305.

Lorthongpanich, C., Messerschmidt, D.M., Chan, S.W., Hong, W., Knowles, B.B. & Solter, D. (2013) Temporal reduction of LATS kinases in the early preimplantation embryo prevents ICM lineage differentiation. *Genes & Development*. 27 (13), pp. 1441–1446.

Lou, X., Kang, M., Xenopoulos, P., Muñoz Descalzo, S. & Hadjantonakis, A.-K. (2014) A Rapid and Efficient 2D/3D Nuclear Segmentation Method for Analysis of Early Mouse Embryo and Stem Cell Image Data. *Stem Cell Reports*. 2 (3), pp. 382–397.

Mahoney, J.E., Mori, M., Szymaniak, A.D., Varelas, X. & Cardoso, W.V. (2014) The hippo pathway effector Yap controls patterning and differentiation of airway epithelial progenitors. *Developmental Cell*. 30 (2), pp. 137–150.

Mamada, H., Sato, T., Ota, M. & Sasaki, H. (2015) Cell competition in mouse NIH3T3 embryonic fibroblasts is controlled by the activity of Tead family proteins and Myc. *Journal of Cell Science*. 128 (4), pp. 790–803.

Martin, G.R. (1981) Isolation of a pluripotent cell line from early mouse embryos cultured in medium conditioned by teratocarcinoma stem cells. *Proceedings of the National Academy of Sciences*. 78 (12), pp. 7634–7638.

Matsuda, T., Nakamura, T., Nakao, K., Arai, T., Katsuki, M., Heike, T. & Yokota, T. (1999) STAT3 activation is sufficient to maintain an undifferentiated state of mouse embryonic stem cells. *The EMBO journal*. 18 (15), pp. 4261–4269.

McClatchey, A.I., Saotome, I., Ramesh, V., Gusella, J.F. & Jacks, T. (1997) The Nf2 tumor suppressor gene product is essential for extraembryonic development immediately prior to gastrulation. *Genes & Development*. 11 (10), pp. 1253–1265.

Miesfeld, J.B., Gestri, G., Clark, B.S., Flinn, M.A., Poole, R.J., Bader, J.R., Besharse, J.C., Wilson, S.W. & Link, B.A. (2015) Yap and Taz regulate retinal pigment epithelial cell fate. *Development*. pp. 1–30.

Mihajlović, A.I., Thamodaran, V. & Bruce, A.W. (2015) The first two cell-fate decisions of preimplantation mouse embryo development are not functionally independent. *Scientific Reports*. 5pp. 15034–16.

Miller, E., Yang, J., DeRan, M., Wu, C., Su, A.I., Bonamy, G.M.C., Liu, J., Peters, E.C. & Wu, X. (2012) Identification of serum-derived sphingosine-1-phosphate as a small molecule regulator of YAP. *Chemistry & Biology*. 19 (8), pp. 955–962.

Mitsui, K., Tokuzawa, Y., Itoh, H., Segawa, K., Murakami, M., Takahashi, K., Maruyama, M., Maeda, M. & Yamanaka, S. (2003) The homeoprotein Nanog is required for maintenance of pluripotency in mouse epiblast and ES cells. *Cell*. 113 (5), pp. 631–642.

Mohler, P.J., Kreda, S.M., Boucher, R.C., Sudol, M., Stutts, M.J. & Milgram, S.L. (1999) Yes-associated protein 65 localizes p62c-Yes to the apical compartment of airway epithelia by association with EBP50. *The Journal of Cell Biology*. 147 (4), pp. 879–890.

Molls, M., Zamboglou, N. & Streffer, C. (1983) A comparison of the cell kinetics of pre-implantation mouse embryos from two different mouse strains. *Cell and tissue kinetics*. 16 (3), pp. 277–283.

Morgani, S.M. & Brickman, J.M. (2015) LIF supports primitive endoderm expansion during pre-implantation development. *Development*. pp. 1–33.

Morgani, S.M., Canham, M.A., Nichols, J., Sharov, A.A., Migueles, R.P., Ko, M.S.H. & Brickman, J.M. (2013) Totipotent Embryonic Stem Cells Arise in Ground-State Culture Conditions. *CellReports*. 3 (6), pp. 1945–1957.

Morin-Kensicki, E.M., Boone, B.N., Howell, M., Stonebraker, J.R., Teed, J., Alb, J.G., Magnuson, T.R., O'Neal, W. & Milgram, S.L. (2006) Defects in yolk sac vasculogenesis, chorioallantoic fusion, and embryonic axis elongation in mice with targeted disruption of Yap65. *Molecular and Cellular Biology*. 26 (1), pp. 77–87.

Moroishi, T., Park, H.W., Qin, B., Chen, Q., Meng, Z., Plouffe, S.W., Taniguchi, K., Yu, F.-X., Karin, M., Pan, D. & Guan, K.-L. (2015) A YAP/TAZ-induced feedback mechanism regulates Hippo pathway homeostasis. *Genes & Development*. 29 (12), pp. 1271–1284.

Mortensen, R.M., Conner, D.A., Chao, S., Geisterfer-Lowrance, A.A. & Seidman, J.G. (1992) Production of homozygous mutant ES cells with a single targeting construct. *Molecular and Cellular Biology*. 12 (5), pp. 2391–2395.

Mountford, P., Zevnik, B., Düwel, A., Nichols, J., Li, M., Dani, C., Robertson, M., Chambers, I. & Smith, A. (1994) Dicistronic targeting constructs: reporters and modifiers of mammalian gene expression. *Proceedings of the National Academy of Sciences*. 91 (10), pp. 4303–4307.

Muñoz Descalzo, S., RuÉ, P., Garcia-Ojalvo, J. & Martinez Arias, A. (2012) Correlations Between the Levels of Oct4 and Nanog as a Signature for Naïve Pluripotency in Mouse Embryonic Stem Cells. *STEM CELLS*. 30 (12), pp. 2683–2691.

Neto-Silva, R.M., de Beco, S. & Johnston, L.A. (2010) Evidence for a growth-stabilizing regulatory feedback mechanism between Myc and Yorkie, the Drosophila homolog of Yap. *Developmental Cell*. 19 (4), pp. 507–520.

Niakan, K.K., Ji, H., Maehr, R., Vokes, S.A., Rodolfa, K.T., Sherwood, R.I., Yamaki, M., Dimos, J.T., Chen, A.E., Melton, D.A., McMahon, A.P. & Eggan, K. (2010) Sox17 promotes differentiation in mouse embryonic stem cells by directly regulating extraembryonic gene expression and indirectly antagonizing self-renewal. *Genes & Development*. 24 (3), pp. 312–326.

Nichols, J., Silva, J., Roode, M. & Smith, A. (2009) Suppression of Erk signalling promotes ground state pluripotency in the mouse embryo. *Development*. 136 (19), pp. 3215–3222.

Nichols, J., Zevnik, B., Anastassiadis, K., Niwa, H., Klewe-Nebenius, D., Chambers, I., Schöler, H. & Smith, A. (1998) Formation of pluripotent stem cells in the mammalian embryo depends on the POU transcription factor Oct4. *Cell*. 95 (3), pp. 379–391.

Nishioka, N., Inoue, K.-I., Adachi, K., Kiyonari, H., Ota, M., Ralston, A., Yabuta, N., Hirahara, S., Stephenson, R.O., Ogonuki, N., Makita, R., Kurihara, H., Morin-Kensicki, E.M., Nojima, H., et al. (2009) The Hippo Signaling Pathway Components Lats and Yap Pattern Tead4 Activity to Distinguish Mouse Trophectoderm from Inner Cell Mass. *Developmental Cell*. 16 (3), pp. 398–410.

Nishioka, N., Yamamoto, S., Kiyonari, H., Sato, H., Sawada, A., Ota, M., Nakao, K. & Sasaki, H. (2008) Tead4 is required for specification of trophectoderm in pre-implantation mouse embryos. *Mechanisms of Development*. 125 (3-4), pp. 270–283.

Niwa, H., Burdon, T., Chambers, I. & Smith, A. (1998) Self-renewal of pluripotent embryonic stem cells is mediated via activation of STAT3. *Genes & Development*. 12 (13), pp. 2048–2060.

Niwa, H., Miyazaki, J. & Smith, A.G. (2000) Quantitative expression of Oct-3/4 defines differentiation, dedifferentiation or self-renewal of ES cells. *Nature genetics*. 24 (4), pp. 372–376.

Niwa, H., Toyooka, Y., Shimosato, D., Strumpf, D., Takahashi, K., Yagi, R. & Rossant, J. (2005) Interaction between Oct3/4 and Cdx2 determines trophectoderm differentiation. *Cell*. 123 (5), pp. 917–929.

Oka, T. & Sudol, M. (2009) Nuclear localization and pro-apoptotic signaling of YAP2 require intact PDZ-binding motif. *Genes to Cells*. 14 (5), pp. 607–615.

Overholtzer, M., Zhang, J., Smolen, G.A., Muir, B., Li, W., Sgroi, D.C., Deng, C.-X., Brugge, J.S. & Haber, D.A. (2006) Transforming properties of YAP, a candidate oncogene on the chromosome 11q22 amplicon. *Proceedings of the National Academy of Sciences*. 103 (33), pp. 12405–12410.

Pettitt, S.J., Liang, Q., Rairdan, X.Y., Moran, J.L., Prosser, H.M., Beier, D.R., Lloyd, K.C., Bradley, A. & Skarnes, W.C. (2009) Agouti C57BL/6N embryonic stem cells for mouse genetic resources. *Nature methods*. 6 (7), pp. 493–495.

Piccolo, S., Dupont, S. & Cordenonsi, M. (2014) The Biology of YAP/TAZ: Hippo Signaling and Beyond. *Physiological reviews*. 94 (4), pp. 1287–1312.

Plusa, B., Piliszek, A., Frankenberg, S., Artus, J. & Hadjantonakis, A.K. (2008) Distinct sequential cell behaviours direct primitive endoderm formation in the mouse blastocyst. *Development*. 135 (18), pp. 3081–3091.

Praskova, M., Xia, F. & Avruch, J. (2008) MOBKL1A/MOBKL1B phosphorylation by MST1 and MST2 inhibits cell proliferation. *Current Biology*. 18 (5), pp. 311–321.

Radzisheuskaya, A., Chia, G.L.B., Santos, dos, R.L., Theunissen, T.W., Castro, L.F.C., Nichols, J. & Silva, J.C.R. (2013) A defined Oct4 level governs cell state transitions of pluripotency entry and differentiation into all embryonic lineages. *Nature cell biology*. 15 (6), pp. 579–590.

Ralston, A. & Rossant, J. (2008) Cdx2 acts downstream of cell polarization to cell-autonomously promote trophectoderm fate in the early mouse embryo. *Developmental Biology*. 313 (2), pp. 614–629.

Ralston, A., Cox, B.J., Nishioka, N., Sasaki, H., Chea, E., Rugg-Gunn, P., Guo, G., Robson, P., Draper, J.S. & Rossant, J. (2010) Gata3 regulates trophoblast development downstream of Tead4 and in parallel to Cdx2. *Development*. 137 (3), pp. 395–403.

Ramalho-Santos, M., Yoon, S., Matsuzaki, Y., Mulligan, R.C. & Melton, D.A. (2002) ' Stemness': transcriptional profiling of embryonic and adult stem cells. *Science (New York, N.Y.)*. 298 (5593), pp. 597–600.

Ran, F.A., Hsu, P.D., Wright, J., Agarwala, V., Scott, D.A. & Zhang, F. (2013) Genome engineering using the CRISPR-Cas9 system. *Nature Protocols*. 8 (11), pp. 2281–2308.

Rayon, T., Menchero, S., Nieto, A., Xenopoulos, P., Crespo, M., Cockburn, K., Cañon, S., Sasaki, H., Hadjantonakis, A.-K., la Pompa, de, J.L., Rossant, J. & Manzanares, M. (2014) Notch and hippo converge on cdx2 to specify the trophectoderm lineage in the mouse blastocyst. *Developmental Cell*. 30 (4), pp. 410–422.

Reddy, B.V.V.G. & Irvine, K.D. (2013) Regulation of Hippo Signaling by EGFR-MAPK Signaling through Ajuba Family Proteins. *Developmental Cell*. 24 (5), pp. 459–471.

Riele, te, H., Maandag, E.R., Clarke, A., Hooper, M. & Berns, A. (1990) Consecutive inactivation of both alleles of the pim-1 proto-oncogene by homologous recombination in embryonic stem cells. *Nature*. 348 (6302), pp. 649–651.

Ringwald, M., Iyer, V., Mason, J.C., Stone, K.R., Tadepally, H.D., Kadin, J.A., Bult, C.J., Eppig, J.T., Oakley, D.J., Briois, S., Stupka, E., Maselli, V., Smedley, D., Liu, S., et al. (2010) The IKMC web portal: a central point of entry to data and resources from the International Knockout Mouse Consortium. *Nucleic Acids Research*. 39 (Database), pp. D849–D855.

Roh, M.H. (2003) The Crumbs3-Pals1 complex participates in the establishment of polarity in mammalian epithelial cells. *Journal of Cell Science*. 116 (14), pp. 2895–2906.

Rossant, J. (1975) Investigation of the determinative state of the mouse inner cell mass. II. The fate of isolated inner cell masses transferred to the oviduct. *Journal of embryology and experimental morphology*. 33 (4), pp. 991–1001.

Saha, B., Home, P. & Paul, S. (2012) Reply to Sasaki et al.: TEAD4 is predominantly cytoplasmic in the inner cell mass of mouse blastocysts. *Proceedings of the National Academy of Sciences of the United States of America*. 109 (50), pp. E3391–E3392.

Saiz, N., Grabarek, J.B., Sabherwal, N., Papalopulu, N. & Plusa, B. (2013) Atypical protein kinase C couples cell sorting with primitive endoderm maturation in the mouse blastocyst. *Development*. 140 (21), pp. 4311–4322.

Sansores-Garcia, L., Bossuyt, W., Wada, K.-I., Yonemura, S., Tao, C., Sasaki, H. & Halder, G. (2011) Modulating F-actin organization induces organ growth by affecting the Hippo pathway. *The EMBO journal*. 30 (12), pp. 2325–2335.

Sauer, B. & Henderson, N. (1988) Site-specific DNA recombination in mammalian cells by the Cre recombinase of bacteriophage P1. *Proceedings of the National Academy of Sciences*. 85 (14), pp. 5166–5170.

Schlegelmilch, K., Mohseni, M., Kirak, O., Pruszak, J., Rodriguez, J.R., Zhou, D., Kreger, B.T., Vasioukhin, V., Avruch, J., Brummelkamp, T.R. & Camargo, F.D. (2011) Yap1 Acts Downstream of alpha-Catenin to Control Epidermal Proliferation. *Cell*. 144 (5), pp. 782–795.

Schöler, H.R., Hatzopoulos, A.K., Balling, R., Suzuki, N. & Gruss, P. (1989) A family of octamer-specific proteins present during mouse embryogenesis: evidence for germline-specific expression of an Oct factor. *The EMBO journal*. 8 (9), pp. 2543–2550.

Schrode, N., Xenopoulos, P., Piliszek, A., Frankenberg, S., Plusa, B. & Hadjantonakis, A.-K. (2013) Anatomy of a blastocyst: Cell behaviors driving cell fate choice and morphogenesis in the early mouse embryo. *genesis*. 51 (4), pp. 219–233.

Schröter, C., RuÉ, P., Mackenzie, J.P. & Martinez Arias, A. (2015) FGF/MAPK signaling sets the switching threshold of a bistable circuit controlling cell fate decisions in embryonic stem cells. *Development*. 142 (24), pp. 4205–4216.

Smith, A.G., Heath, J.K., Donaldson, D.D., Wong, G.G., Moreau, J., Stahl, M. & Rogers, D. (1988) Inhibition of pluripotential embryonic stem cell differentiation by purified polypeptides. *Nature*. 336 (6200), pp. 688–690.

Steinhardt, A.A., Gayyed, M.F., Klein, A.P., Dong, J., Maitra, A., Pan, D., Montgomery, E.A. & Anders, R.A. (2008) Expression of Yes-associated protein in common solid tumors. *Human pathology*. 39 (11), pp. 1582–1589.

Strano, S. (2001) Physical Interaction with Yes-associated Protein Enhances p73 Transcriptional Activity. *Journal of Biological Chemistry*. 276 (18), pp. 15164–15173.

Strumpf, D., Mao, C.-A., Yamanaka, Y., Ralston, A., Chawengsaksophak, K., Beck, F. & Rossant, J. (2005) Cdx2 is required for correct cell fate specification and differentiation of trophectoderm in the mouse blastocyst. *Development*. 132 (9), pp. 2093–2102.

Sudol, M. (1994) Yes-associated protein (YAP65) is a proline-rich phosphoprotein that binds to the SH3 domain of the Yes proto-oncogene product. *Oncogene*. 9 (8), pp. 2145–2152.

Sudol, M., Bork, P., Einbond, A., Kastury, K., Druck, T., Negrini, M., Huebner, K. & Lehman, D. (1995a) Characterization of the mammalian YAP (Yes-associated protein) gene and its role in defining a novel protein module, the WW domain. *The Journal of biological chemistry*. 270 (24), pp. 14733–14741.

Sudol, M., Chen, H.I., Bougeret, C., Einbond, A. & Bork, P. (1995b) Characterization of a novel protein-binding module--the WW domain. *FEBS letters*. 369 (1), pp. 67–71.

Tamm, C., Bower, N. & Anneren, C. (2011) Regulation of mouse embryonic stem cell self-renewal by a Yes-YAP-TEAD2 signaling pathway downstream of LIF. *Journal of Cell Science*. 124 (7), pp. 1136–1144.

Tapon, N., Harvey, K.F., Bell, D.W., Wahrer, D.C.R., Schiripo, T.A., Haber, D.A. & Hariharan, I.K. (2002) salvador Promotes both cell cycle exit and apoptosis in Drosophila and is mutated in human cancer cell lines. *Cell*. 110 (4), pp. 467–478.

Tate, P.H. & Skarnes, W.C. (2011) Bi-allelic gene targeting in mouse embryonic stem cells. *Methods*. 53 (4), pp. 331–338.

Testa, G., Schaft, J., van der Hoeven, F., Glaser, S., Anastassiadis, K., Zhang, Y., Hermann, T., Stremmel, W. & Stewart, A.F. (2004) A reliable lacZ expression reporter cassette for multipurpose, knockout-first alleles. *genesis*. 38 (3), pp. 151–158.

Thomas, K.R. & Capecchi, M.R. (1987) Site-directed mutagenesis by gene targeting in mouse embryo-derived stem cells. *Cell*. 51 (3), pp. 503–512.

Thomas, P. & Beddington, R. (1996) Anterior primitive endoderm may be responsible for patterning the anterior neural plate in the mouse embryo. *Current Biology*. 6 (11), pp. 1487–1496.

Thomas, P.Q., Brown, A. & Beddington, R.S. (1998) Hex: a homeobox gene revealing peri-implantation asymmetry in the mouse embryo and an early transient marker of endothelial cell precursors. *Development*. 125 (1), pp. 85–94.

Varelas, X., Samavarchi-Tehrani, P., Narimatsu, M., Weiss, A., Cockburn, K., Larsen, B.G., Rossant, J. & Wrana, J.L. (2010) The Crumbs Complex Couples Cell Density Sensing to Hippo-Dependent Control of the TGF-β-SMAD Pathway. *Developmental Cell*. 19 (6), pp. 831–844.

Varlet, I., Collignon, J. & Robertson, E.J. (1997) nodal expression in the primitive endoderm is required for specification of the anterior axis during mouse gastrulation. *Development*. 124 (5), pp. 1033–1044.

Ventura, A., Kirsch, D.G., McLaughlin, M.E., Tuveson, D.A., Grimm, J., Lintault, L., Newman, J., Reczek, E.E., Weissleder, R. & Jacks, T. (2007) Restoration of p53 function leads to tumour regression in vivo. *Nature*. 445 (7128), pp. 661–665.

Vooijs, M., Jonkers, J. & Berns, A. (2001) A highly efficient ligand-regulated Cre recombinase mouse line shows that LoxP recombination is position dependent. *EMBO reports*. 2 (4), pp. 292–297.

Wada, K.-I., Itoga, K., Okano, T., Yonemura, S. & Sasaki, H. (2011) Hippo pathway regulation by cell morphology and stress fibers. *Development*. 138 (18), pp. 3907–3914.

Wamaitha, S.E., del Valle, I., Cho, L.T.Y., Wei, Y., Fogarty, N.M.E., Blakeley, P., Sherwood, R.I., Ji, H. & Niakan, K.K. (2015) Gata6 potently initiates reprograming of pluripotent and differentiated cells to extraembryonic endoderm stem cells. *Genes & Development*. 29 (12), pp. 1239–1255.

Wei, X., Shimizu, T. & Lai, Z.-C. (2007) Mob as tumor suppressor is activated by Hippo kinase for growth inhibition in Drosophila. *The EMBO journal*. 26 (7), pp. 1772–1781.

Wettschureck, N. & Offermanns, S. (2005) Mammalian G proteins and their cell type specific functions. *Physiological reviews*. 85 (4), pp. 1159–1204.

Williams, R.L., Hilton, D.J., Pease, S., Willson, T.A., Stewart, C.L., Gearing, D.P., Wagner, E.F., Metcalf, D., Nicola, N.A. & Gough, N.M. (1988) Myeloid leukaemia inhibitory factor maintains the developmental potential of embryonic stem cells. *Nature*. 336 (6200), pp. 684–687.

Wu, S., Huang, J., Dong, J. & Pan, D. (2003) hippo encodes a Ste-20 family protein kinase that restricts cell proliferation and promotes apoptosis in conjunction with salvador and warts. *Cell*. 114 (4), pp. 445–456.

Xenopoulos, P., Kang, M., Puliafito, A., Di Talia, S. & Hadjantonakis, A.-K. (2015) Heterogeneities in Nanog Expression Drive Stable Commitment to Pluripotency in the Mouse Blastocyst. *CellReports*. pp. 1–14.

Xu, T., Wang, W., Zhang, S., Stewart, R.A. & Yu, W. (1995) Identifying tumor suppressors in genetic mosaics: the Drosophila lats gene encodes a putative protein kinase. *Development*. 121 (4), pp. 1053–1063.

Yagi, R., Chen, L.F., Shigesada, K., Murakami, Y. & Ito, Y. (1999) A WW domain-containing yes-associated protein (YAP) is a novel transcriptional co-activator. *The EMBO journal*. 18 (9), pp. 2551–2562.

Yagi, R., Kohn, M.J., Karavanova, I., Kaneko, K.J., Vullhorst, D., DePamphilis, M.L. & Buonanno, A. (2007) Transcription factor TEAD4 specifies the trophectoderm lineage at the beginning of mammalian development. *Development*. 134 (21), pp. 3827–3836.

Yamanaka, Y., Lanner, F. & Rossant, J. (2010) FGF signal-dependent segregation of primitive endoderm and epiblast in the mouse blastocyst. *Development*. 137 (5), pp. 715–724.

Ye, F. & Zhang, M. (2013) Structures and target recognition modes of PDZ domains: recurring themes and emerging pictures. *Biochemical Journal*. 455 (1), pp. 1–14.

Yu, F.-X., Zhao, B. & Guan, K.-L. (2015) Hippo Pathway in Organ Size Control, Tissue Homeostasis, and Cancer. *Cell*. 163 (4), pp. 811–828.

Yu, F.-X., Zhao, B., Panupinthu, N., Jewell, J.L., Lian, I., Wang, L.H., Zhao, J., Yuan, H., Tumaneng, K., Li, H., Fu, X.-D., Mills, G.B. & Guan, K.-L. (2012) Regulation of the Hippo-YAP pathway by G-protein-coupled receptor signaling. *Cell*. 150 (4), pp. 780–791.

Zender, L., Spector, M.S., Xue, W., Flemming, P., Cordon-Cardo, C., Silke, J., Fan, S.-T., Luk, J.M., Wigler, M., Hannon, G.J., Mu, D., Lucito, R., Powers, S. & Lowe, S.W. (2006) Identification and validation of oncogenes in liver cancer using an integrative oncogenomic approach. *Cell*. 125 (7), pp. 1253–1267.

Zhang, L., Ren, F., Zhang, Q., Chen, Y., Wang, B. & Jiang, J. (2008) The TEAD/TEF family of transcription factor Scalloped mediates Hippo signaling in organ size control. *Developmental Cell*. 14 (3), pp. 377–387.

Zhao, B., Li, L., Lu, Q., Wang, L.H., Liu, C.-Y., Lei, Q. & Guan, K.-L. (2011) Angiomotin is a novel Hippo pathway component that inhibits YAP oncoprotein. *Genes & Development*. 25 (1), pp. 51–63.

Zhao, B., Li, L., Tumaneng, K., Wang, C.Y. & Guan, K.-L. (2010) A coordinated phosphorylation by Lats and CK1 regulates YAP stability through SCF -TRCP. *Genes & Development*. 24 (1), pp. 72–85.

Zhao, B., Wei, X., Li, W., Udan, R.S., Yang, Q., Kim, J., Xie, J., Ikenoue, T., Yu, J., Li, L., Zheng, P., Ye, K., Chinnaiyan, A., Halder, G., et al. (2007) Inactivation of YAP oncoprotein by the Hippo pathway is involved in cell contact inhibition and tissue growth control. *Genes & Development*. 21 (21), pp. 2747–2761.

Zhao, B., Ye, X., Yu, J., Li, L., Li, W., Li, S., Lin, J.D., Wang, C.Y., Chinnaiyan, A.M., Lai, Z.C. & Guan, K.-L. (2008) TEAD mediates YAP-dependent gene induction and growth control. *Genes & Development*. 22 (14), pp. 1962–1971.

Ziosi, M., Baena-López, L.A., Grifoni, D., Froldi, F., Pession, A., Garoia, F., Trotta, V., Bellosta, P., Cavicchi, S. & Pession, A. (2010) dMyc functions downstream of Yorkie to promote the supercompetitive behavior of hippo pathway mutant cells. Gregory S Barsh (ed.). *PLoS Genetics*. 6 (9), pp. e1001140.